

**Aus dem
Zentrum für Physiologie
Institut für Herz- und Kreislaufphysiologie
der Heinrich-Heine-Universität Düsseldorf
Director: Prof. Dr. Jürgen Schrader**

**Mapping of coronary endothelial cell membrane proteome and
comparative proteomic analysis of regulatory T cells in CD73
knockout mice**

Inaugural-Dissertation

**zur
Erlangung des Doktorgrades der
Mathematisch-Naturwissenschaftlichen Fakultät
der Heinrich-Heine-Universität Düsseldorf**

**vorgelegt von
Selvam Arjunan
aus
Avalurpettai, Indien
Düsseldorf
2008**

Gedruckt mit der Genehmigung der Mathematisch-Naturwissenschaftlichen
Fakultät
der Heinrich-Heine-Universität Düsseldorf
Berichtersteller: Prof. Dr. Jürgen Schrader
Prof. Dr. William Martin
Tag der mündlichen Prüfung: 16.01.2009

**TO MY PARENTS
TO MY WIFE**

ACKNOWLEDGEMENTS

I would like to thank my supervisor Prof. Dr. Jürgen Schrader for giving me the opportunity for the conductance and completion of this work. With out his careful guidance this work would not have been possible.

I thank Prof. Dr. William Martin for making it possible for me to present this thesis.

I would also like to thank Dr. Michael Reinartz, Dr. Stefanie Gödecke, for invaluable discussions and criticisms, which helped me on to thinking independently and acquiring the skills that I needed to perform experimentation successfully.

I want to thank Dr. Barbara Emde and Dr. Klaus Zanger (Institute of Anatomy II, Heinrich-Heine-University, Düsseldorf) to carry out electron microscopic experiment of this work. I would like to extend my gratitude to Annamária Simon for the valuable suggestions for MS analysis.

Most importantly, I extend my gratitude to all my friends and colleagues of our institute. Thanks for the lively working atmosphere that you have created and for the care you have always shown to me. I am very thankful to all the people who kindly provided valuable chemicals and reagents to accomplish this work.

And I thank my parents, wife and relatives for the constant support they have provided throughout my studies.

Contents

Abbreviations	1
1. Introduction	
1.1. Endothelium.....	3
1.1.1. Structural heterogeneity of the endothelium.....	4
1.1.2. Functions of endothelium.....	5
1.1.3. Phenotypic heterogeneity of the endothelium.....	6
1.1.4. Mapping of membrane proteins.....	9
1.2. Ecto 5' Nucleotidase (CD73)	
1.2.1. The extra cellular adenosine nucleotide cascade and role of CD73.....	12
1.2.2. Physiological responses coordinated by CD73.....	13
1.2.3. Studies revealing the importance of CD73 in CD73 deficient mice.....	17
1.3. MS analysis of proteins	
1.3.1. High performance liquid chromatography.....	20
1.3.2. Multidimensional separation techniques.....	21
1.3.3. Detectors for HPLC.....	22
1.3.4. Electro spray ionization.....	22
1.3.5. Quantitative proteomic profiling.....	24
1.3.6. DATA Analysis.....	26

1.4. Objectives..... 27

2. Materials and methods

2.1. Materials: Chemicals and source..... 28

2.2. Methods..... 30

2.2.1. Physiological experiments..... 30

2.2.1.1. In situ perfusion of colloidal silica by Langendorff perfusion system..... 30

2.2.2. Biochemical techniques

2.2.2.1. Protein estimation..... 32

2.2.2.2. SDS-PAGE electrophoresis..... 32

2.2.2.3. Immunohistochemistry..... 34

2.2.3. Electron microscopy..... 35

2.2.4. Cell culture

2.2.4.1. Vascular endothelial cells isolation from mouse aorta..... 36

2.2.4.2. Vascular endothelial cells isolation from mouse lungs..... 38

2.2.4.3. FACS analysis..... 39

2.2.5. Regulatory T cells

2.2.5.1. Isolation of CD4⁺ CD25⁺ regulatory T cells from mouse spleen..... 41

2.2.5.2. FACS-protocol for FOXP3 cells with membrane disintegration..... 43

2.2.6. Mass spectrometry

2.2.6.1. Preparation of fused silica capillary column.....	44
2.2.6.2. Peptide separation.....	45
2.2.6.3. Stable isotope dimethyl labeling.....	46
2.2.6.4. 2D-LC for peptide separation.....	48
2.2.6.5. Protein identification.....	48
2.2.7. Statistical analysis.....	49

3. Results

3.1. Proteomic analysis of endothelial cell membrane

3.1.1. Selective labelling of mouse heart EC membrane by colloidal silica	50
3.1.2. Endothelial cell membrane analysis by western blot.....	51
3.1.3. Protein identification by LC-MS.....	54

3.2. Culturing of endothelial cells from various tissue in the mouse

3.2.1. Mouse aortic endothelial cell.....	57
3.2.2. Mouse lung endothelial cell.....	65
3.2.3. Expression of CD73 in mouse kidney and spleen by IHC.....	69

3.3. Proteomic study of regulatory T cells

3.3.1. Analysis of CD73 expression on regulatory T cell by FACS analysis.....	73
3.3.2. Proteomic study of regulatory T cells in control Vs CD73 knockouts.....	75

4. Discussion

4.1. Proteomic analysis of EC membranes under <i>in vivo</i> conditions.....	86
4.2. Functional role of endothelial CD73 (ecto- 5'-nucleotidase).....	88
4.3. Limitations of proteomic analysis of endothelial cells.....	90
4.4. Functional role of CD73 in regulatory T cells (T reg).....	92
4.5. Differentially expressed proteins in T reg cells lacking CD73.....	94

5. Summary	98
-------------------------	----

6. References	101
----------------------------	-----

7. Curriculum vitae	120
----------------------------------	-----

8. Declaration	121
-----------------------------	-----

Abbreviations

5-LO	5-lipoxygenase
aa	Amino acid(s)
ABC	ATP-binding cassette
AdoR	Adenosine receptors
ALK1	Activin-receptor-like kinase 1
Amp	Ampicillin
bEND	Brain endothelial cells
BUN	Blood urea nitrogen
CLP	Coactosin-like protein
C-terminal	Carboxy terminal
DANCE	Developing arteries and neural crest EGF-like
DMEM	Dulbecco's modified Eagle's medium
DMSO	Dimethylsulfoxide
DLL4	Delta-like 4
DTT	Dithiothreitol
ECs	Endothelial cells
ECL	Enhanced chemoluminescence
EDRF	Endothelium-derived relaxing factor
EDTA	Ethylenediamine tetraacetic acid
ESI	Electrospray ionization
EPAS 1	Endothelial PAS domain protein 1
EPCR	Endothelial protein C receptor
FACS	Fluorescence-activated cell sorting
FCS	Fetal calf serum
FITC	Fluorescein-isothiocyanate
FOXP3	Forkhead box P3
FT-ICR	Fourier transform-ion cyclotron resonance
GAPDH	Glyceraldehyde-3-phosphate dehydrogenase
GPI	Glycosylphosphatidylinositol
HEPES	N-(2-hydroxyethyl)piperazine-N'-(2-ethanesulfonic acid)
HFBA	Heptafluorobutyric acid
HIF1	Hypoxia-inducible factor-1
HPLC	High performance liquid chromatography
HSPs	Heat shock proteins
IAA	Iodoacetic acid
ICAM 1	Inter-Cellular Adhesion Molecule 1
IFN- γ	Interferon- γ
IHC	Immunohistochemistry
IP	Ischemic preconditioning
kDa	Kilodalton
KH buffer	Krebs-henseleit buffer
LAMP 1	Lysosomal-associated membrane protein 1
LPS	Lipopolysaccharides
MAECs	Mouse aortic endothelial cells
MLECs	Mouse lung endothelial cells

MS	Mass spectrometry
MES	2-(N-morpholino)ethanesulfonic acid
MVECGM	Microvascular endothelial cell growth medium
MudPIT	Multidimensional protein identification technology
NDS	Neutrophil-derived secretagogue
NF- κ B	Nuclear factor κ B
NP-40	Nonidet P-40
NRP1	Neuropilin 1
N-terminal	Amino terminal
OD	Optical density
PAGE	Polyacrylamide gel electrophoresis
PAI	Plasminogen activator inhibitor
PBS	Phosphate-buffered saline
PECAM -1	Platelet endothelial cell adhesion molecule-1
PMSF	Phenylmethylsulfonylfluoride
PMN	Polymorphonuclear
PS	Phosphatidylserine
PVDF	Polyvinylidene difluoride
PTA	Phosphotungstic acid
rpm	Rounds per minute
RLMVEC- P	Rat Lung Micro Vascular Endothelial Cells - P
RT	Room temperature
SCX	strong cation exchange
SDS	Sodium dodecyl sulfate
SILAC	Stable isotope labeling technology
TE	Tris / EDTA
TEM	Transmission electron microscope
TFPI	Tissue factor pathway inhibitor
TRP	Transient receptor potential
TPA	Tissue-type plasminogen activator
T reg	Regulatory T cells
TNF α	Tumor necrosis factor alpha
UAc	Uranyl acetate
UPS	Ubiquitin-proteasome system
UV	Ultraviolet light
VCAM-1	Vascular cell adhesion molecule 1
VLA4	Very late antigen – 4
vWF	von Willebrand Factor

1. Introduction

1.1. Endothelium

The vascular endothelium is the inner layer of the circulatory system its primary function being the maintenance of vessel wall permeability (Figure 1). In 1628, after the first description of blood circulation by William Harvey, a study by Malphigi, described the physical separation between blood and tissues, which led to the concept of a network of vessels. In the 1800s von Reckinghausen described that the vessels are lined by the cells and these cells are called endothelium in 1896 in experiments carried out by Starling. An electron microscopic study of the vessel wall by Palade (1953), revealed the presence of characteristic organelles, including plasmalemmal vesicles (caveolae) and Weibel-Palade bodies. In addition they also revealed for the first time the existence of structural heterogeneity of the endothelium.

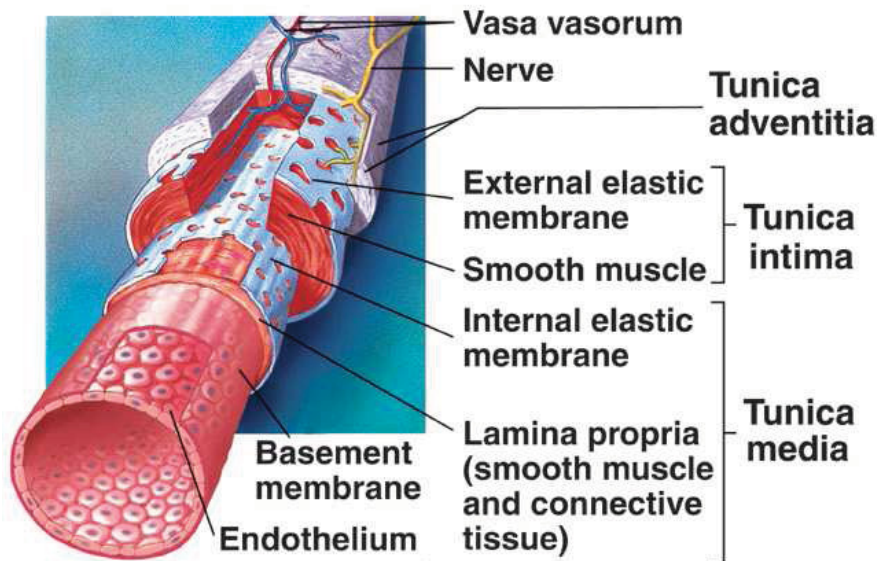


Fig 1: Structure of the blood vessels wall: The inner layer of a blood vessel consists of squamous epithelial cells known as the endothelium. At the base of the epithelial layer is a thin layer of spongy connective tissue that secretes a layer of elastic collagen. This stretchy layer forms the "basement membrane". The surrounding layer of smooth muscle is quite thick in arteries. Adjacent to the muscle layer is (internal elastic membrane) a spongy layer of connective tissues that produces elastic collagen fibers. Together these two layers are known as the tunica intermedia. Surrounding the tunica intermedia is a layer of connective tissues that produces both elastic collagen fibers and more rigid collagen fibers. This layer is called the tunica externa. [This figure was taken from [www.rci.rutgers.edu /Blood-Vessels.html](http://www.rci.rutgers.edu/Blood-Vessels.html)].

1.1.1. Structural heterogeneity of the endothelium

Three different types of endothelium are known; it is continuous, fenestrated or discontinuous (Figure 2). Continuous endothelium is the one in which the ECs are tightly connected to one another and surrounded by a continuous basement membrane. The ECs which exhibit holes or fenestrae are called fenestrated endothelium. The third type of endothelium, discontinuous endothelium, is characterized by the presence of fenestrated, open gaps, and a poorly formed underlying basement membrane.

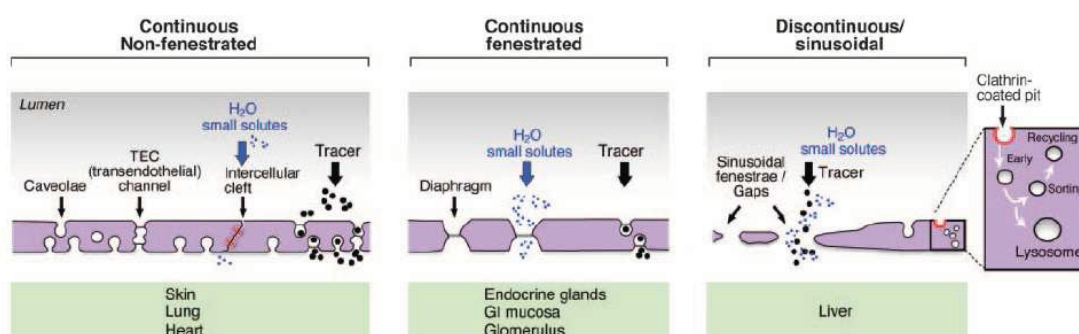


Fig 2: Endothelium and permeability: Capillaries mediate constitutive transfer of solutes and fluids between blood and underlying tissue. In continuous nonfenestrated endothelium, water and small solutes pass between ECs, whereas larger solutes pass through ECs either via transendothelial channels or transcytosis, the latter process being mediated primarily by caveolae. Compared with their nonfenestrated counterpart, continuous fenestrated endothelium demonstrates greater permeability to water and small solutes but similar reflection coefficients to albumin and larger macromolecules. Discontinuous endothelium is characterized by fenestrae, gaps, and poorly organized basement membrane [This figure is taken from (Aird 158-73)].

Nonfenestrated continuous endothelium is found in arteries, veins, and capillaries of the brain, skin, heart and lung. Continuous endothelium may be fenestrated or non-fenestrated. Fenestrated continuous endotheliums are localized in capillaries of exocrine and endocrine glands, gastric, and intestinal mucosa, choroids plexus, glomeruli, and a subpopulation of renal tubules where an increased filtration or increased transendothelial transport occurs. Discontinuous endothelium is found in certain sinusoidal vascular beds, most notably the liver (Aird 158-73).

1.1.2. Functions of endothelium

The endothelial cells (ECs), which form a physiologically important interface between the circulating blood and the underlying cells inside the tissue by lining all blood vessels, are a dynamic and metabolically very active cell population. Thus, the EC as an interface between blood and tissues selectively allows the flow of nutrients, biological molecules and even blood cells. Endothelial cells also play an important role in many other physiological functions like, including the control of vasomotor tone, blood cell trafficking, permeability, proliferation, and innate and adaptive immunity [for review see (Aird 174-90;Aird 158-73)].

The endothelium regulates the barrier function by the redistribution of surface adhesive structures like occludin, cadherins in tight and adherent junctions respectively, presence or absence of fenestrae and /or differential activity of the transcytotic machinery. Under pathophysiological conditions, loss of this barrier can lead to edema. Depending on the type of stimuli, the increase in vascular permeability also varies.

Another common function of the endothelium is to maintain blood in a fluid state and to promote limited clot formation when there is a breach in the integrity of the vascular wall. On the anticoagulant side, ECs express tissue factor pathway inhibitor (TFPI), heparan, thrombomodulin, endothelial protein C receptor (EPCR), tissue-type plasminogen activator (t-PA), ecto-ADPase, prostacyclin and additionally it regulates the formation of nitric oxide. On the procoagulant side, ECs synthesize tissue factor, plasminogen activator inhibitor (PAI)-1, von willebrand factor (vWF), and protease activated receptors. Importantly, endothelial-derived anticoagulant and procoagulant molecules are unevenly distributed throughout the vasculature (Aird S28-S34;Aird 1392-406)

The endothelium participates in regulation of vascular tone. It has been demonstrated that the relaxation of vascular smooth muscle cells in response to acetylcholine is dependent on the integrity of the endothelium. Endothelium-derived relaxing factor (EDRF) or NO generation by endothelial cells is constitutive but may be enhanced by a wide variety of compounds like acetylcholine, angiotension II, bradykinin, etc. In addition, NO release is regulated by shear stress. NO is not only released following stimulation but also plays an important role in the maintenance of basal vascular tone.

The endothelium also generates PGI₂ (Moncada et al. 663-65), which relaxes the underlying smooth muscle cells through activation of adenylate cyclase and subsequent generation of cAMP. ECs constitutively release PGI₂ which appears to be involved in the regulation of resting vascular tone, in addition to NO. Under some pathophysiological conditions, endothelium derived vasoconstrictive factors like endothelin (ET) can be released and contributes to a paradoxical vasoconstrictive effect. Endothelin, an endothelium-derived 21 amino acids vasoconstricting peptide, consists of three structurally related peptides, ET-1, ET-2 and ET-3 (Kedzierski and Yanagisawa 851-76). It has been noted that many factors that stimulate ET synthesis, for eg., thrombin, angiotensin II, also causes the release of the vasodilator PGI₂ and/or NO, which oppose the vasoconstricting action of ET. Thus, the overall response is likely to be complex due to the interaction of many vasoactive pathways.

Endothelial cells coordinate the recruitment of inflammatory cells to sites of tissue injury or infection and produce/ release cytokines and growth factors serving as communication signals to leukocytes. In addition, endothelial cells respond to inflammatory stimuli like lipopolysaccharides (LPS) or cytokines (Klein et al. 204-12). Finally, a series of cell adhesion molecules expressed on leukocytes and on endothelial cells mediate leukocyte attachment on and migration across endothelium in a stepwise process. The different sequential steps involved in neoangiogenesis include the release of proteases from activated endothelial cells with subsequent degradation of the basement membrane, migration of endothelial cells into the interstitial space, endothelial cell proliferation and differentiation into mature blood vessels. These processes are mediated by angiogenic inducers like growth factors, chemokines, angiogenic enzymes, endothelial specific receptors and adhesion molecules (Carmeliet 389-95; Carmeliet and Jain 249-57).

1.1.3. Phenotypic heterogeneity of the endothelium: representative vascular beds

Endothelial cells (ECs) form the inner lining of blood vessels and lymphatics. Each vascular bed has unique structural and functional properties, and an understanding of these properties holds important clues to site-specific diagnostics and therapeutics. Although arteries and veins both function as conduits and are lined by continuous nonfenestrated endothelium, they differ in fundamental ways (Figure 3). Arteries have thick walls, and they pulsate. Veins have thin walls and do not pulsate. Veins have valves; arteries do not. Endothelial junctions in arteries

are tighter compared with those in veins. Arteries carry well oxygenated blood, whereas veins contain deoxygenated blood. An exception is the pulmonary circulation, where the oxygenation status is reversed. Compared with arteries, large veins have a greater capacity to mediate an inflammatory response. Discrete regions of the arterial tree, including branch points and large curvatures, are exposed to disturbed flow. These areas are primed for activation and serve as “hot spots” for inflammation, coagulation, and atherosclerosis (Lupu et al. 1161-72;Hajra et al. 9052-57)

Arteries and veins express unique molecular markers. Genes that are preferentially expressed in arterial ECs include ephrinB2, Delta-like 4 (Dl14), activin-receptor-like kinase 1 (Alk1), endothelial PAS domain protein 1 (EPAS1), Hey1 and Hey2, neuropilin 1 (NRP1), and decidual protein induced by progesterone (Depp). Venous EC-specific genes include EphB4, neuropilin 2 (NRP2), and COUP-TFII. A recent study demonstrated that class III β -tubulin is expressed in ECs at the tip of venous valves, but not in the vein.

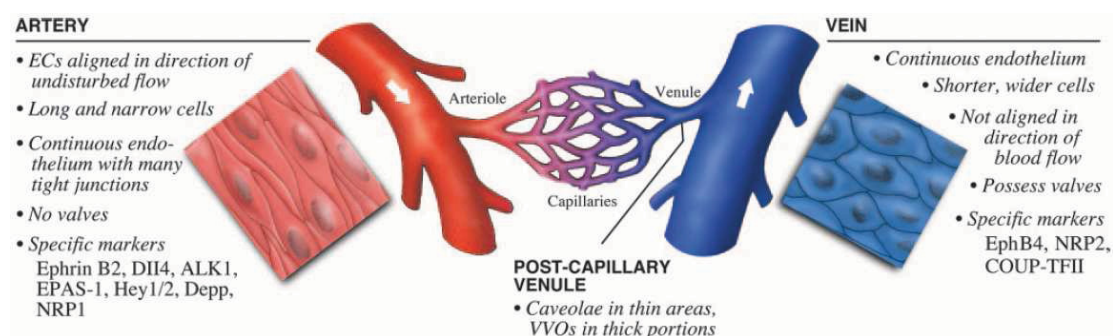


Fig 3: ECs in arteries, veins, and capillaries: Shown are selected phenotypic differences between ECs in arteries, veins, postcapillary venules, and capillaries. ALK1 indicates activin-receptor-like kinase 1; Depp, decidual protein induced by progesterone; Dll4, delta-like4; EPAS-1, endothelial PAS domain protein 1; NRP1, neuropilin 1; TE, transendothelial; VVOs, vesiculo-vacuolar organelles [This figure is taken from (Aird 174-90)].

Endothelial cells are heterogeneous with respect to their cell surface glycoproteins and lectin binding patterns (Porter, Palade, and Milici 85-95;Ponder and Wilkinson 535-41;Schnitzer, Shen, and Palade 241-51;Belloni and Nicolson 398-410;Fatehi et al. 30-39), protein expression and mRNA expression (Fatehi et al. 30-39;Belloni and Nicolson 398-410). With few exceptions, virtually all endothelial cell-specific genes are differentially or unevenly expressed throughout the vascular tree and are given below in Table 1.

Table 1: List of markers expressed on different vascular endothelium [from (Aird S221-S230)]

Markers	Vascular endothelium
Lung endothelial cell adhesion molecule-1	Lung (Elble et al. 27853-61)
Endothelial-specific molecule-1	Lung, gastrointestinal tract, kidney (Lassalle et al. 20458-64;Bechard et al. 417-25)
DANCE (developing arteries and neural crest EGF-like)	Lung, kidney, and spleen (Jean et al. L75-L82)
Membrane dipeptidase	Predominantly in lung and kidney (Rajotte and Ruoslahti 11593-98)
γ -Glutamyl leukotrienase	Microvascular endothelium expect in lungs where it is expressed in small and large vessels (Han et al. 481-90)
von Willebrand factor	Veins > arteries, not present in sinusoidal endothelial cells (Turner et al. 569-75;Yamamoto et al. 2791-801;Aird S28-S34)
Tissue-type plasminogen activator	Highest levels in the brain (Yamamoto and Loskutoff 2440-51); in the lung, present in bronchial, but not pulmonary circulation (Levin, Santell, and Osborn 139-48)
Tissue factor pathway inhibitor	Microvascular endothelium (Osterud, Bajaj, and Bajaj 873-75)
Endothelial cell protein C receptor	Large vessel endothelium (Esmon S48-S51;Laszik et al. 3633-40)
Thrombomodulin	Absent in brain (Ishii et al. 362-65)
Endothelial nitric oxide synthase	Arteries > veins (Ishii et al. 362-65;Andries, Brutsaert, and Sys 195-203;Pollock et al. C1379-C1387)
Receptor protein tyrosine phosphatase μ	Arteries > veins (Bianchi et al. 329-38)
Vascular cell adhesion molecule-1	Heart > mesentery, brain, and small intestine (Henninger et al. 1825-32)
P-selectin	Highest in lung, lowest in muscle and brain (Eppihimer et al. 560-69)
E-selectin	Absent (with possible exception of mouse heart) (Eppihimer et al. 560-69;Drake et al. 1458-70;Bevilacqua et al. 9238-42)
Multidrug-resistant P-glycoprotein	Blood-brain barrier (Cordon-Cardo et al. 695-98)
Ephrin-B2	Arteries (Wang, Chen, and Anderson 741-53)
Eph-B4	Veins (Wang, Chen, and Anderson 741-53)
Early growth response gene-1	Large vessels brain, heart capillaries (Tsai et al. 1870-72)
CD36	Low in brain (Greenwalt, Scheck, and Rhinehart-Jones 1382-88)

Thus endothelial cells derived from different organs and from within different vascular beds within these organs, display morphological, biochemical and antigenic heterogeneity. This fact has highlighted the need for methods to study endothelial cell membrane proteins from variety of tissues under *in vivo* and *in vitro* conditions.

1.1.4. Mapping of membrane proteins

The vascular endothelium is critically important for human and mammalian physiology and pathology, but at present, the information needed to understand its function at the cellular and molecular level is still limiting. A wide range of assays has been used to uncover and map endothelial cell heterogeneity. Scanning electron microscopy has provided some of the earliest and most compelling descriptions of phenotypic diversity among endothelial cells (DeFouw 645-54;Smith et al. 925-27). Immunohistochemistry and *in situ* hybridization studies have been used to map the expression of a protein or mRNA species to unique sites of the vascular tree (Turner et al. 569-75;Page et al. 673-83). Whole tissue extracts or purified endothelial cells have been used to generate antibodies that recognize site specific epitopes in the vasculature (Ghandour et al. 165-70;Streeter et al. 41-46). The injection of labeled antibodies into mice has provided a another perspective of vascular heterogeneity at the level of cell adhesion molecule expression (Eppihimer et al. 560-69;Eppihimer et al. 560-69;Henninger et al. 1825-32).

Recently, innovative proteomic and genomic approaches have been applied to the study of vascular diversity. For example, antibody and subfractionated protocols have been used to generate monoclonal antibodies that specifically target the caveolae in the microcirculation of the lung (Eppihimer et al. 560-69;McIntosh et al. 1996-2001). Other groups have used phage-display peptide libraries to select for peptides that home to specific vascular beds *in vivo* (Arap et al. 121-27;Pasqualini and Ruoslahti 364-66;Rajotte et al. 430-37). Although there are technical challenges in studying transcriptional profiles in the context of an appropriate microenvironment, DNA microarrays have recently been used to map cell subtype-specific gene expression in different populations of endothelial cells (Gerritsen et al. 13-20;Kim et al. 83-93).

Unfortunately, not all endothelia are amenable to growth in culture and those that can be cultured exhibit both structural and biochemical drift (Stolz and Jacobson 169-82;Madri and Williams 153-65). The microenvironment of the tissue surrounding the blood vessels clearly influences EC phenotype little molecular information is available regarding vascular endothelium as it exists in native tissue. This is in large part because of technical limitations in molecular profiling of a cell type that represents such a small percentage of the cells in the tissue. Past approaches have analyzed endothelial cells isolated from tissue by enzymatic

digestion and sorting of the released single cells using EC markers (Au 1822-26; Au 1822-26; Obermeyer et al. 167-78). Although the study of isolated and even cultured ECs *in vitro* has yielded much functional and molecular information, both enzymatic and mechanical tissue disassembly and growth in culture contribute to phenotypic changes that result in morphological alterations as well as loss of native function and protein expression (Madri and Williams 153-65).

Although expected to be substantial, the molecular differences between ECs *in vivo* and *in vitro* are unknown. Comparative proteomic analysis of EC surface membranes isolated from rat lung versus cultured RLMVEC revealed striking differences. Only 51% of the integral membrane proteins and plasma membrane associated proteins identified were expressed in common between silica coated endothelial cell plasma membrane and cultured rat lung microvascular endothelial cells (RLMVEC). Interestingly, 65 of 73 (89%) total known EC marker proteins were detected in silica coated endothelial cell plasma membrane versus only 32 (43.8%) in RLMVEC. 41 markers, such as ACE (Angiotensin converting enzyme) and ECE (endothelin converting enzyme) were detected in silica coated endothelial cell plasma membrane but not in RLMVEC. Overall, more than 180 (41%) proteins were detected in silica coated endothelial cell plasma membrane under *in vivo* condition but not at all in RLMVEC under *in vitro* condition (Durr et al. 985-92). The author conclude that, one approach that holds promise is that the direct mapping of endothelial cell surface proteins under *in vivo* conditions.

Ideally, the direct isolation of native unmodified endothelial cells from an organ with a differentiated microvascular bed would considerably advance our understanding of the biochemistry and function of this important mediator of blood - tissue interactions, but this is technically impossible at present. In previous studies the exposed (free) surface of cultured endothelial cells was coated with a layer of cationized silica particles followed by a polyanion cross linker (Stolz and Jacobson 39-51). This method was modified (Density of colloidal silica 2.55g/cm³) and allowed to isolation of the silica coated membrane by density gradient centrifugation from endothelial homogenates. In another approach the endothelial luminal plasmalemma of the vascular bed of a given organ was coated with colloidal silica by perfusion, and coated plasmalemma fragments are isolated from the homogenate by nycodenz density gradients centrifugation (Figure 4). The result obtained are documented on the microvascular of the rat lung (Jacobson et al. 296-306; Schnitzer et al. 1759-63).

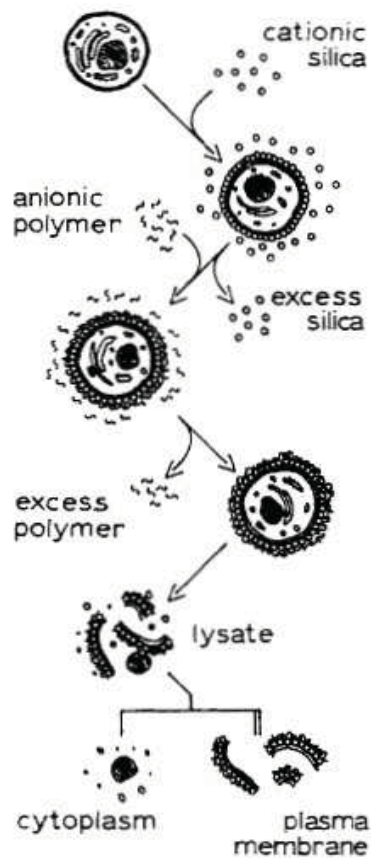


Fig 4: Membrane isolation procedure using cationic silica: Freshly harvested washed cells are combined with cationic colloidal silica. These particles bind to the anionic cell surface by ionic attractions. An anionic polymer is added to cross-link the silica beads into a dense pellicle and to neutralize the exposed surfaces of the silica beads. At this point, bead attachment and polyanion overcoating can be repeated several times if a thicker pellicle is desired. Once coating is completed, the cells are lysed for membrane preparation [This figure is taken from (Chaney and Jacobson 10062-72)].

The present study applied a modified method to enrich vascular endothelium from the mouse heart. This method is based on the binding of positive charged colloidal silica to the surface of endothelial cell membranes by in situ perfusion of isolated hearts by Langendorff perfusion system. The coated plasmalemma fragments were then isolated by two different homogenisation method followed by centrifugation in nycodenz density gradients and the analysis of its composition by mass spectrometry (see result section).

1.2. Ecto 5' Nucleotidase (CD73)

1.2.1. The extra cellular adenosine nucleotide cascade and role of CD73

The formation of extracellular adenosine from ATP is accomplished primarily through CD39 (ATP-diphosphohydrolase) and CD73 (ecto-5'-nucleotidase) (Figure 5). CD73, a glycosylphosphatidylinositol-linked (GPI) membrane protein found on the surface of a variety of cell types and it was first described in heart and skeletal muscle about 70 years ago (Reis, 1934).

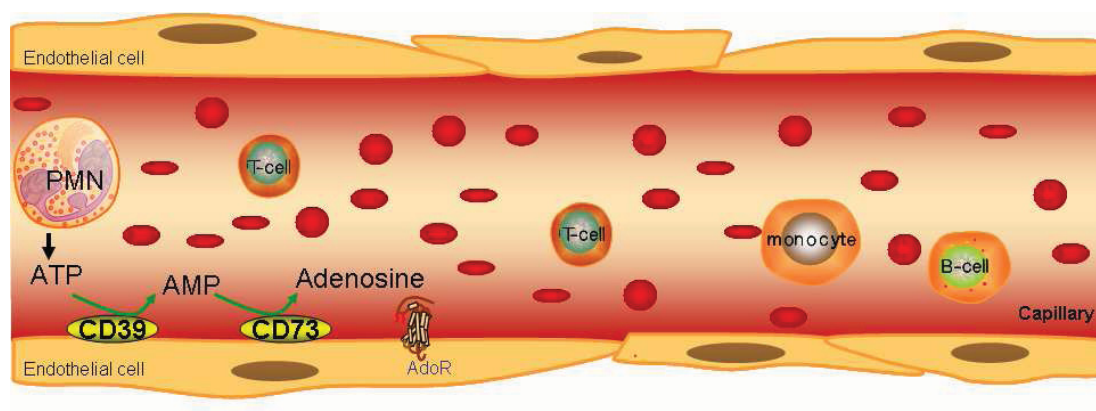


Fig 5: Cascade of CD39 and CD73 to produce adenosine at the surface of endothelial cells

Adenosine which when formed by this pathway can activate one of four types of G-protein coupled, seven transmembrane spanning adenosine receptors (AdoR) A1, A2A, A2B, and A3, each of which operates via different intracellular signaling mechanisms and exhibits distinct patterns of tissue distribution. Adenosine receptors are expressed on a wide variety of cells, and many cell types have been shown to express more than one isoform of the receptor. Likewise, activation of surface AdoR has been shown to regulate diverse physiologic endpoints. In human neutrophils, adenosine A1 and A2 receptor occupancy mediate opposing roles for adenosine in inflammation: A1 activation plays a role in proinflammatory, whereas the A2 receptor plays an anti-inflammatory role. A2 receptor activation inhibits the neutrophil oxidative burst, whereas the A3 receptor inhibits neutrophil degranulation and may play an important role in inflammation by inhibiting eosinophil migration (Bouma et al. 5400-08).

1.2.2. Physiological responses coordinated by CD73

A number of purine nucleotide metabolites, including adenosine, have been shown to influence epithelial electrogenic chloride secretion in lung and intestine (Gamba 423-93). Examining biological properties of soluble mediators derived from activated inflammatory cells (e.g. neutrophils and eosinophils) identified a small protease-resistant fraction termed neutrophil-derived secretagogue (NDS), which when incubated on epithelia, activated electrogenic chloride secretion and fluid transport. A biophysical analysis of NDS led to the identification of this molecule to be AMP (Madara et al. 2320-25).

Studies have shown that the CD73 is implicated in the control of tissue barrier function. Successful transmigration of leukocytes, particularly polymorphonuclear (PMN, neutrophil) leukocytes across the vascular endothelium is accomplished by temporary self-deformation with localized widening of the inter-junctional spaces (Ley 1105-06; Madara et al. 2320-25), a process with the potential to disturb endothelial and epithelial barrier function. A study by Lennon et al., (Lennon et al. 1433-43) revealed that the prominent signaling pathway for closing interendothelial gaps during neutrophil transmigration involved adenosine-stimulated 'resealing' of the barrier. The study also examined interactions of leukocytes at cell-cell junctions; it was shown that inhibition of CD73 using either APCP (alpha, beta-methylene adenosine-5'-diphosphate) or anti-CD73 monoclonal antibody 1E9 inhibited the resealing of endothelial and epithelial barriers by as much as 85%, suggesting the necessity for extracellular nucleotide metabolism in this barrier function.

A study by Yegutkin G et al., has demonstrated that endothelial shear stress induces the release of surface proteins capable of ATP and AMP phosphohydrolysis. The source of this activity was the cell surface, and presumably represents soluble forms of CD73 and CD39. This study also revealed that shear stress induces the release of endogenous ATP. It is not clear how exactly neutrophils and/or endothelial cells release ATP, although several mechanisms have been proposed, including direct transport through ATP-binding cassette (ABC) proteins, transport through connexin hemichannels, as well as vesicular release (Yegutkin, Bodin, and Burnstock 921-26). Clearly, CD73 lies central to the regulation of tissue barriers.

Studies in mouse models of intestinal permeability revealed that oral delivery the CD73 inhibitor APCP (α , β -methylene ADP) increases movement of inert tracers, such as FITC-labeled dextran, across the intestinal epithelium. To investigate changes in vascular permeability in CD73^{-/-} mice, Evan's blue dye was used, which binds tightly to plasma albumin. Quantification of formamide-extractable Evan's blue from individual tissues can then be interpreted as a function of vascular leak (Takano et al. 819-26). In general, hypoxia increases vascular permeability two- to four-fold over normoxic conditions, depending on the tissue being studied. Pharmacologic interventions have suggested that CD73 is protective under such circumstances, and most studies have suggested a protective role for adenosine A2 receptors in maintaining barrier function (Weissmuller, Eltzschig, and Colgan 229-39). All together, these studies define CD73 as a gatekeeper for the fine tuning of epithelial and endothelial permeability.

During hypoxia generation of extracellular adenosine has been widely implicated as an adaptive response to hypoxia. In humans, ambient hypoxia (SpO₂ = 80% over 20 min) induced plasma adenosine concentration to increase from 21 to 51 nM in the presence of dipyridamole, an inhibitor of adenosine reuptake (Saito et al. 1014-18). Similarly, when measuring adenine nucleotide concentrations in isolated, perfused skeletal muscles of anesthetized dogs, normobaric hypoxia was associated with increases of adenosine in the venous blood, but not of AMP, ADP or ATP (Mo and Ballard 593-603). A possible role for adenosine during hypoxia may include vasodilation. It is unclear, however, whether this adenosine is formed intracellularly or extracellularly by the action of CD73.

A number of studies have suggested that CD73 contributes to the protective effects of adenine nucleotide released during hypoxia and ischemia. Recently, hypoxia has been shown to upregulate CD73 expression in different cell types including a rapid and prolonged induction of CD73 in epithelia (Semenza et al. 123-30). Given the long lasting and robust hypoxia response observed, hypoxia-inducible factor-1 (HIF-1) was identified as a regulator of oxygen homeostasis, which facilitates both oxygen delivery and adaptation to oxygen deprivation (Semenza et al. 123-30).

During stress or when subjected to injurious stimuli, it is known that the cells of the cardiovascular system generate and release adenosine in increasing quantities (Zernecke et al. 2120-27). This increased adenosine can modulate cellular function and phenotype by interacting with surface receptors in myocardial, vascular, fibroblast, and inflammatory cells. Increased CD73 activity in ischemic preconditioning (IP) has been attributed to a variety of acute activation pathways and CD73 which is transcriptionally regulated by HIF-1. Because CD73 is induced during ischemia and hypoxia (Eltzschig et al. 783-96), it is thought to be primarily responsible for adenosine production under these circumstances. Using CD73^{-/-} mice the relative importance of CD73 in cardiac tissue was recently explored by using the isolated perfused heart. In addition, histochemical analysis revealed CD73 to be the predominant AMPase associated with the vascular endothelium of large conduit vessels such as the aorta, carotid, and coronary artery with no measurable contribution by alkaline phosphatase (Koszalka et al. 814-21).

Recent studies have focused on targeting adenosine receptors to limit tissue injury in a variety of diseases using either native adenosine or pharmacological agonism/antagonism with receptor-selective analogs. A study by Rosengren et al., (Rosengren, Arfors, and Proctor 345-57) using the nonselective adenosine receptor antagonist 8-phenyl-theophylline demonstrated enhanced inflammation in the hamster cheek pouch, thereby suggesting tonic regulation of neutrophil receptors to endogenous adenosine sources.

Transcriptional pathways mediated by HIF-1 may serve as barrier-protective elements during inflammatory hypoxia. Mice engineered to conditionally delete intestinal epithelial HIF-1 exhibit more severe clinical symptoms of colitis, while conditional increases in epithelial HIF-1 are protective (Semenza et al. 123-30). Furthermore, colons with constitutive activation of HIF-1 displayed increased expression levels of HIF-1 regulated barrier protective genes (multidrug resistance gene-1, intestinal trefoil factor, CD73), attenuating the loss of barrier function during colitis in vivo. During active phases of colitis, CD73 mRNA was increased ~ 4 fold in wild-type animals. Parallel analyses in animals expressing constitutively active HIF-1 revealed a nearly 18-fold increase in CD73 mRNA. Such findings confirm previous observations of HIF-1 dependent regulation of CD73 expression, and define an inflammatory metabolic loop involving of hypoxia, a condition termed 'inflammatory hypoxia' (Karhausen et al. 1098-106).

CD73 mediates the suppression of inflammation most likely through regulatory T cells (Figure 6). Deaglio et al., (Deaglio et al. 1257-65) showed that the expression of CD39/ENTPD1 in concert with CD73/ecto-5'-nucleotidase distinguishes CD4⁺/CD25⁺/Foxp3⁺ T reg cells from other T cells. These ectoenzymes generate pericellular adenosine from extra cellular nucleotides. The coordinated expression of CD39/CD73 on T reg cells and the adenosine A2A receptor on activated T effector cells generates immunosuppressive loops, indicating roles in the inhibitory function of T reg cells.

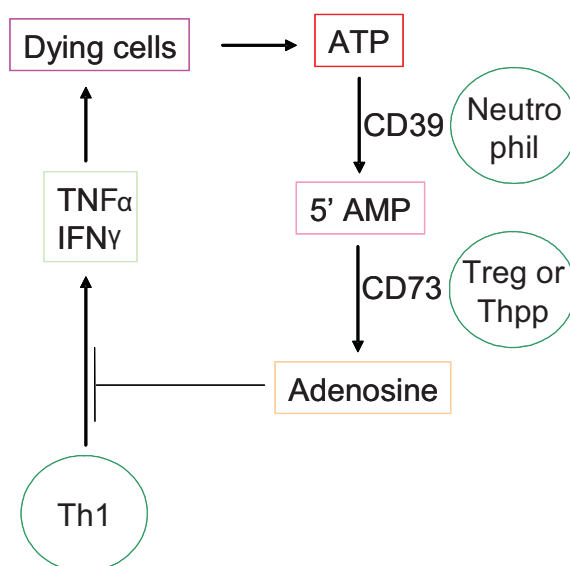


Fig 6: CD73-mediated suppression of inflammation: ATP released during inflammation from dying cells or activated neutrophils is converted by CD39 to 5-AMP. The resulting 5-AMP is dephosphorylated by CD73 expressed on the surface of Thpp or Treg cells to adenosine. Adenosine suppresses the production of IFN- γ and TNF α - by effector CD4 T cells, including Th1 cells, thus limiting inflammation [This figure is taken from (Kobie et al. 6780-86)].

Consequently, T reg cells from CD39-null mice showed impaired suppressive properties in vitro and fail to block allograft rejection in vivo. These findings suggested that CD39 and CD73 are surface markers of T reg cells that play a specific biochemical signature characterized by adenosine generation that has functional relevance for cellular immunoregulation.

1.2.3. Studies revealing the importance of extracellularly formed adenosine in CD73 deficient mice

CD73-generated adenosine plays an important role in the local hemodynamic control of glomerular filtration pressure and filtration rates in the kidney as shown by Castrop et al., who compared tubuloglomerular feedback in the kidneys of CD73^{-/-} and wild type mice (Castrop et al. 634-42). Interestingly, kidney function of CD73 deficient mice was found to be normal with respect to renal blood flow, renal vascular resistance, and stimulation of renin secretion by furosemide, plasma osmolarity, and plasma concentrations of Na⁺, Cl⁻, BUN (Blood Urea Nitrogen), creatinine, uric acid, and total protein. However, in response to saturating increases in tubular perfusion flow, CD73^{-/-} animals demonstrated significantly decreased reductions in stop flow pressure and superficial nephron glomerular filtration rates compared to wild type animals.

Although wild type mice showed relatively constant tubuloglomerular feedback responses during prolonged perfusion of the loop of Henle, the residual feedback response was nearly lost in CD73^{-/-} mice. Observed deficiencies in tubuloglomerular feedback responses were due to decreased concentrations of extracellular adenosine, rather than any defects in adenosine receptor activation. It was concluded that CD73 serves as an important means of communication between the macula densa and the underlying smooth muscle cells (Castrop et al. 634-42).

Thompson et al., (Thompson et al. 1395-405) has recently shown that vascular leak syndromes associated with hypoxia are significantly accentuated in mice lacking CD73. In an attempt to define the role of CD73 in vascular permeability, they used the hypoxia model and compared wild-type and CD73^{-/-} mice administered either vehicle or the 5'-nucleotidase inhibitor APCP. These studies revealed a profound increase of hypoxia-induced vascular leak in different organs (lung, heart, intestine, kidneys) in response to CD73 inhibition or genetic deficiency. Pulmonary leak was particularly obvious in these mice. Indeed, lung vascular leak was highly influenced by exogenous administration of APCP in wild type animals, and the vascular leak phenotype was most prominent in the lungs of CD73^{-/-} mice. Vascular leak was confirmed by assessment of lung wet: dry ratios, with a nearly 70% increase in lung water content of CD73^{-/-} compared to wild type mice.

Nucleotides and nucleotide metabolism have been widely implicated in platelet function (Di Virgilio et al. 587-600). CD73-deficient animals have revealed some insight with regard to the role of CD73-generated adenosine in platelet thrombosis *in vivo* (Koszalka et al. 814-21). Initial studies of ADP-stimulated platelet aggregation *ex vivo* have not revealed significant differences between wild-type and CD73-deficient animals, suggesting that platelet function is intrinsically normal in CD73 gene targeted mice. However, bleeding time after tail tip resection and vessel occlusion induced by free radical injury were significantly reduced in the Cd73-deficient animals, suggesting a degree of platelet dysfunction. Other studies have indicated that platelet cAMP is reduced in CD73-deficient mice, suggesting that plasma adenosine levels regulate basal platelet cAMP, and that decreases in circulating adenosine in CD73-deficient animals contribute to such changes. Additional studies of platelet function and clotting will be necessary to define the contribution of CD73 to these pathways.

1.3. MS analysis of proteins

Mass spectrometry is emerging as an important tool in biochemical research which is capable of analyzing small and large molecules. Analytical chemists have added fresh inputs to bioresearch with new mass spectrometry ionization techniques suitable for proteins and peptides, namely electrospray ionization (ESI) by Fenn and co-workers (Whitehouse et al. 675-79). A mass spectrometer is an analytical device that determines the molecular weight of biological compounds by separating molecular ions according to their mass-to-charge ratio (m/z). Mass spectrometer has seven major components: a sample inlet, an ion source, a mass analyzer, a detector, a vacuum system, an instrumental control system and a data system which is shown in figure 7.

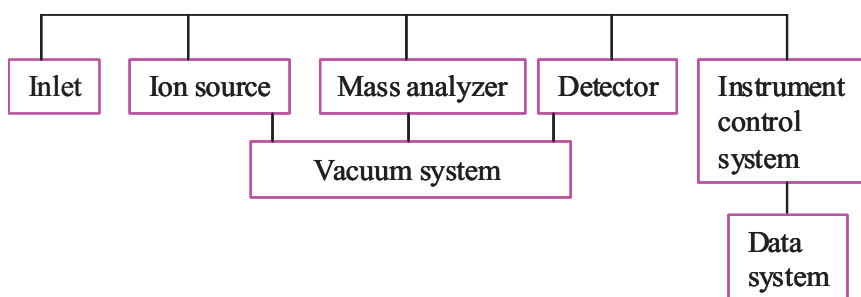


Fig 7: The basic components of a mass spectrometer

The sample inlet is the interface between the sample and mass spectrometer. A sample at atmospheric pressure must be introduced into the MS such that the vacuum within remains relatively unchanged. Sample can be introduced in several ways, the most common with a direct insertion probe or by through a capillary column. The sample can then be heated to facilitate thermal desorption or undergo any number of high energy desorption process used to achieve evaporation and ionization. Electrospray ionization (ESI) is used to produce gaseous ionized molecule from a liquid solution. This is done by creating a fine spray of highly charged droplet in the presence of a strong electric field (4000 V). Either dry gas, heat or both are applied to the droplet before they enter the MS, thus causing the evaporation from the surface which leads to decrease the size of the droplet. Then the ions begin to leave the droplet through what is known as a “Taylor cone”. The ions are directed into an orifice through electrostatic lenses leading to the mass analyzer.

Mass analyzers scan or select ions over a particular m/z range. The mass analyzer contributes to the accuracy, range and sensitivity of an instrument. Six common type of mass analyzer used in MS are quadrupole, magnetic sector, time-of-flight, time-of-flight reflectron, quadrupole ion trap and fourier transform-ion cyclotron resonance (FT-ICR). The nature of the mass analyzer determines several characteristic of the overall experiment, and the two most important are m/z resolution and the m/z range of ions that can be measured.



Fig 8: Finnigan LTQ ion trap mass spectrometer (Thermo Finnigan) and HPLC-Ultimate™ 3000 (DIONEX) used in the present study

The ion detectors allows a MS to generate a signal (current) from incident ions, by generating secondary electrons, which are further amplified or by inducing a current generated by a moving charge. The electron multiplier and scintillation counter are most commonly used, to converting the kinetic energy of incident ions into secondary electrons. An electron multiplier is made up of a series of dynodes maintained at ever increasing potentials. Ions strike the dynode surface, resulting in the emission of electrons. These secondary electrons are then attracted to the next dynode where more secondary electrons are generated, ultimately resulting in a cascade of electrons. Typical amplification or current gain of an electron multiplier is 10^6 .

A vacuum is necessary to permit ions to reach the detector without colliding with other gaseous molecules. Such a collision would reduce the resolution and sensitivity of the instrument by increasing the kinetic energy distribution of the ion, thus inducing fragmentation, or prevention the ions from reaching the detector. Coupling any sample source to a MS requires that the sample at atmospheric pressure (760 Torr) be transferred into a region of high vacuum ($\sim 10^{-6}$ Torr). Maintaining a high vacuum is crucial to obtaining high quality spectra. The primary advantage of mass spectrometric sequencing include the high sensitivity, the rapid speed of the analyses, the large amount of information generated in each experiment, and the ability to characterize post-translational modifications. Figure 8 depicts the mass spectrometer including the nanoflow HPLC unit used in the present study

1.3.1. HPLC (High performance liquid chromatography)

Instrumentation for HPLC research in proteomics does not differ from conventional HPLC instrumentation. Pumping systems, separation columns and detectors used for proteomics research are also used for conventional analysis. The difference, however, is the magnitude of the flow rate and therefore of the columns. Samples for proteomic analysis are available in high amounts; however, the analytes are present in minute concentrations. Therefore, pumping systems were developed for providing flow rates in the nl/min range. There are commercially available HPLC systems both with and without flow splitting. Briefly, in systems using flow splitting, a high pump flow rate of approx. 200–300 $\mu\text{l}/\text{min}$ is split into the column flow rate of approx. 100–300 nl/min and the rest is directed into the waste.

Chromatographic systems without flow splitting use syringe pumps to deliver the mobile phase to the column. Both approaches, split flow and nonsplit flow, have, both can be successfully applied for sample analysis.

1.3.2. Multidimensional separation techniques

One-dimensional HPLC has been proved to be reproducible and effective for peptide and protein separation. However, it is restricted due to sample complexity after digestion, since the number of peptides needed to be separated reaches hundreds or thousands and this exceeds the peak capacity of most 1D-HPLC columns. To improve resolution, multidimensional separation techniques have been introduced and the use of this approach has improved rapidly. In the multidimensional separation approach, ion exchange chromatography is usually the first step preceding the nano RP-HPLC. But in specific applications, such as analysis of glycopeptides or phosphopeptides, other techniques are used, such as titanium columns or the IMAC enrichment of phosphopeptides.

In 2001, Wolters DA et al., (Wolters, Washburn, and Yates, III 5683-90) introduced the multidimensional separation for complex peptide samples by using a strong cation exchange (SCX) column for the separation of peptides in the first dimension. This approach, termed as Multidimensional Protein Identification Technology (MudPIT), involves a single biphasic column packed with SCX (ionic interaction) stationary phase, and C18 RP (hydrophobic interaction). The on-line 2-D nano HPLC-MS/MS system has been successfully established for analysis of complex mixtures of trypsin digested proteins. A SCX column serves as the first dimension, with which peptides are separated according to their electric charge state and charge distribution. In the second dimension, a RP separation according to hydrophobicity in nano mode is performed. The system described is fully automated and the risk of sample loss is low. The majority of the peptides that do not bind to the SCX column will be trapped on the RP trap column. This enables the trapping of almost all peptides from a digested protein sample and increases the amount of information. Peptides elute in more than one fraction from the SCX column when using salt injections and they are multiply detected in different fractions. This problem will be addressed in future work by using a linear gradient for the separation on the first dimension (the SCX column). Injection of only 25 fmol sample and its detection and identification with very good MASCOT scores shows that the system can also be used for low sample quantities and concentrations. These results show that this method can

indeed be used for analysis of complex biological samples (Mitulovic et al. 2545-57; Mitulovic and Mechtler 249-60). In contrast to the online methods, the 'off-line' methods separate the peptides by fraction collection and subsequent desalting and HPLC-MS/MS analysis. Wagner et al., (Wagner et al. 293-305; Wagner et al. 809-20) reported the 'off-line' 2D HPLC with a linear salt gradient applied instead of a stepwise salt injection approach, which increased the amount of recovered peptides by a factor of five.

1.3.3. Detectors for HPLC

All detector types used for conventional HPLC are applicable for proteomics analysis, but one cannot differentiate by UV spectra alone whether two or more peptides are co-eluting. While the UV detector is mainly used for quality-controlling of the separation (void volume, impurities, base line and gradient stability) and for tracing fractions when the sample is being fractionated, the mass spectrometer is the workhorse detector for proteomics. Electrospray detector used for both characterization and quantitation of separated analytes. Additionally, new and fast separation media like those in monolithic columns and ultra-performance chromatography need detectors that can respond quickly due to reduced peak width during very fast separations.

1.3.4. Electro spray ionization

The design and operation of electrospray ion sources used in current mass spectrometers is based on designs first described by Fenn and co workers in 1985 (Whitehouse et al. 675-79). In electrospray ionization (ESI) of the peptide, an acidic, aqueous solution that contains the peptides is sprayed through a small diameter needle. A high, positive voltage is applied to this needle to produce a Taylor cone from which droplets of the solution are sputtered. Protons from the acidic conditions give the droplets a positive charge, causing them to move from the needle towards the negatively charged instrument. During the course of this movement, evaporation reduces the size of the droplet into a population of smaller, charged droplets. This evaporation process can be aided by a flow of gas typically nitrogen and heat. The evaporation and droplet splitting cycle repeats until the small size and charging of the droplet desorbs protonated peptides into the gas phase, where they can be directed into the mass spectrometry by appropriate electric fields.

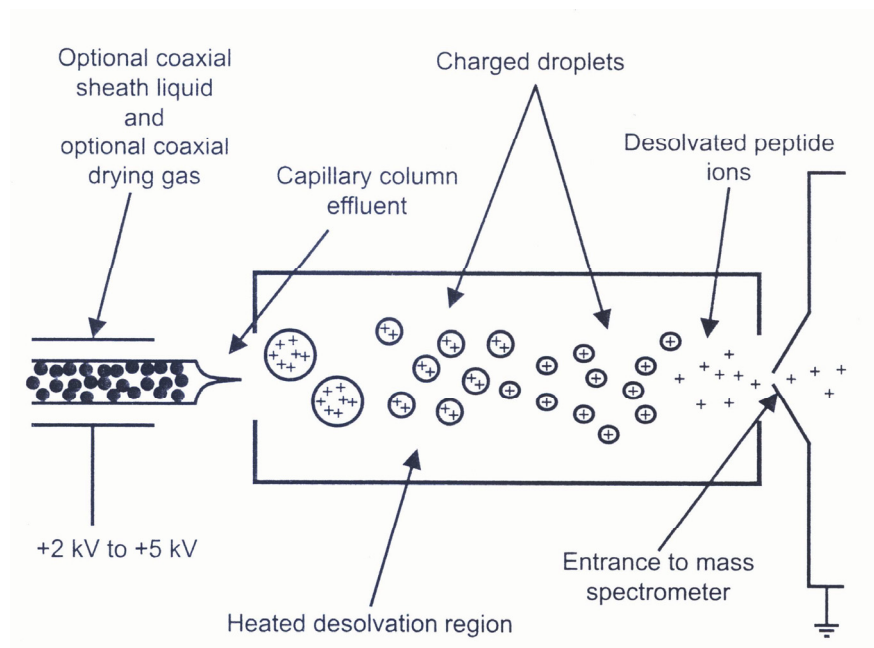


Fig 9: The processes associated with ESI: Charged droplets that are sputtered from a Taylor cone are reduced in size through a dissolved process that ultimately produces the ions that enter the mass spectrometer. The design and operation of ESI sources used in current MS is based on designs first described by Fenn and co-workers in 1985. [This figure is taken from the book “Protein sequencing and identification using tandem mass spectrometry” by Michael Kinter and Nicholas E. Sherman].

One characteristic of electrospray ionization is that the acidic conditions used to produce the positively charged droplet tend to protonate all available basic side in analyte molecules. In peptides, the primary basic sites are the N-terminal amine moiety and basic side groups of lysine, arginine and histidine residues. As a result, multiply protonated peptide ions are observed whenever a lysine, arginine or histidine residue is present in a peptide because one proton associated with the N-terminal amine and additional protons associated with each additional basic residue.

Doubly charged peptides tend to be predominant in tryptic digest of proteins because of the proteolytic specificity of trypsin, which cleaves amide bonds at the C-terminal side of each lysine and arginine residue so that, the peptide produced have only two basic sites, the N-terminal and the side chain of the C-terminal lysine or arginine residue. Ionization takes place by protonation of those two sites. Electrospray ionization is conducive to the formation of multiply charged molecules (Figure 9). This is an important feature since the mass

spectrometer measures the m/z , making it possible to observe very large molecules with an instrument having a relatively small mass range.

1.3.5. Quantitative proteomic profiling

Proteomics has emerged as a field for studying global gene expression profiles at the protein level. In general, proteomics involves the identification of protein components and the measurement of protein abundance in biological systems such as cultured cells or tissue samples. While most of the initial efforts in proteomics have focused on protein identification, recent mass spectrometry (MS)-based technology developments have provided useful platforms for the study of quantitative changes in protein components within the cell (Anderson and Anderson 1853-61; Blackstock and Weir 121-27). Quantitative analysis of global protein levels, termed 'quantitative proteomics', is important for the system-based understanding of the molecular function of each protein component and is expected to provide insights into molecular mechanisms of various biological processes and systems.

In addition to the initial identification of phenotypic expression and protein characterization, a key parameter in proteomics analysis, is the ability to quantitate proteins of interest (Gygi et al. 994-99). Quantitation is a vital tool towards an understanding of transcriptional, translational and post-translational effects that affect protein production and function. In recent years quantitative proteomics by mass spectrometry has mainly focused on the differential quantitative determination of protein expression and not on absolute measurements, as many proteomic applications to drug target discovery or to track signaling events are concerned with relative rather than absolute abundances of proteins (Mann 954-55).

In mass spectrometry the amount of analyte in the sample does not correlate directly with the ion-current intensity of its mass spectrometric signal. Additional techniques have to be implemented to enable differential quantitation of proteins with mass spectrometry. In proteomics almost all of these additional methods involve the labeling of peptides with stable isotopes by either biosynthetic or chemical methods which is given below in the figure 10. Peptides can then not only be identified, but isotope labeling also allows the measurement of differential amounts of the same peptide.

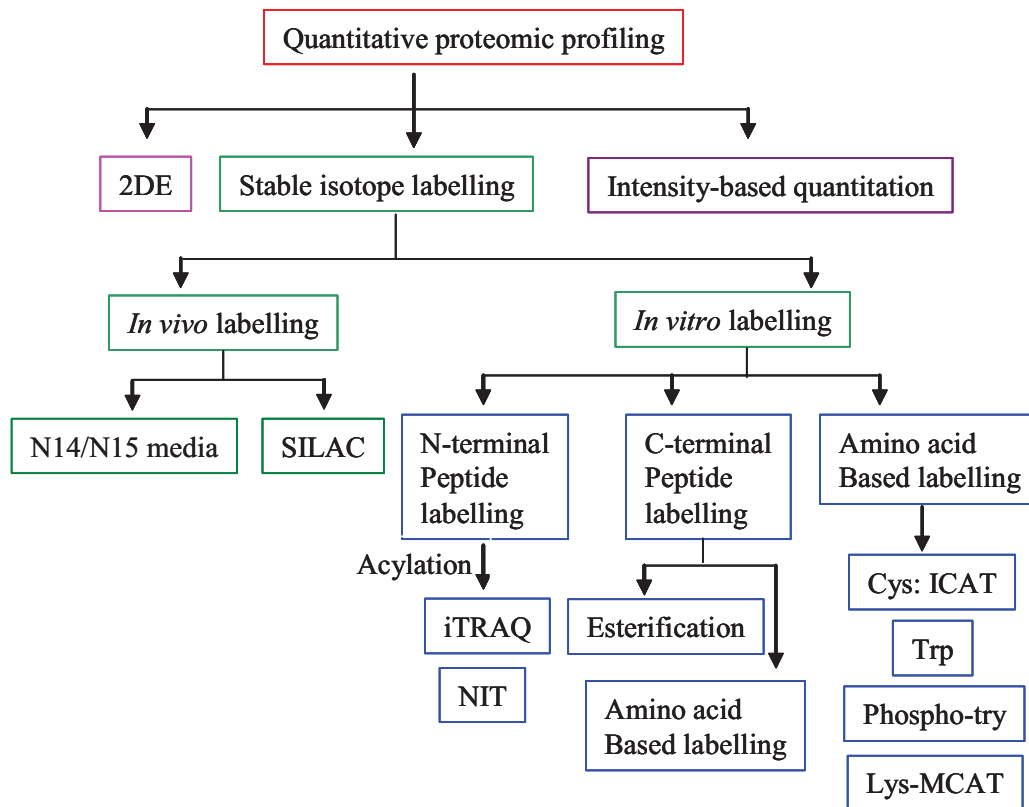


Fig 10: Strategies for quantitative proteomic profiling: 2DE, two-dimensional gel electrophoresis; SILAC, stable isotope labeling with amino acids in cell culture; iTRAQ, isobaric tags for relative and absolute quantitation; ICAT, isotope-coded affinity tags; NIT, N-terminal isotope encoded tagging; MCAT, mass-coded abundance tagging and also Cys, Cysteine; Trp, tryptophan; Tyr, tyrosine; Lys, lysine.

The *in vivo* stable isotope labeling technology (SILAC or N14/N15 media) provides a consistent and accurate method for measuring protein abundance (Ong et al. 376-86; Ong, Kratchmarova, and Mann 173-81; Ong, Foster, and Mann 124-30; Ong, Mittler, and Mann 119-26). Recent study by Marcus Kruger et al., (Kruger et al. 353-64) showing that mice can feed with stable isotope labeled amino acid to enables *in vivo* SILAC animals. The SILAC-mouse approach is a versatile tool by which to quantitatively compare proteomes from knockout mice and thereby determine protein functions under complex *in vivo* conditions. The *in vitro* labeling technology, including the commercially available ICAT and iTRAQ methods, can be used on all kinds of biological samples.

The ICAT method, which focuses on cysteine-containing peptides only, has been successfully applied to the global quantitation of many proteomes (Smolka et al. 25-31; Han et al. 946-51). The recently introduced iTRAQ method (Shadforth et al. 145; Zieske 1501-08), which can be

used to label all peptides at their N-termini, and dimethyl multiplexed labeling is a novel, stable-isotope labeling strategy for quantitative proteomics that uses a simple reagent, formaldehyde, to globally label the N-terminus and ϵ -amino group of Lys through reductive amination (Hsu et al. 6843-52; Hsu et al. 101-08; Hsu, Huang, and Chen 3652-60). Because of the enormous sample complexity of the whole proteome, a current practical and efficient method of quantitative proteomic profiling is to simplify biological samples by separating them into several subsets (sub-proteomes) using various fractionation methods. Comprehensive analyses of these biologically interesting sub-proteomes, and integration of these datasets by computational approaches, will ultimately lead to a more thorough molecular understanding of complex biological systems.

1.3.6. DATA Analysis

The first algorithm/program to identify proteins by matching MS-MS data to database sequence is SEQUEST, which was introduced by John Yates and Jimmy Eng in 1995 (Yates, III et al. 1426-36). SEQUEST provides a relatively rapid assignment of MS-MS spectra to specific peptide sequences in database. This allows fast reduction of large volumes of LC-MS-MS data in proteomic analysis. The MS-Tag program (<http://prospector.ucsf.edu>) was originally developed for analysis of PSD spectra obtained in MALDI-TOF analysis of peptides, but it has been modified to accommodate MS-MS data from different types of instruments. The user can enter a list of m/z values from the MS-MS spectrum to be analyzed. MS-Tag is particularly well-suited to the analysis of MALDI-TOF PSD spectra, which contains immonium ions (low m/z fragments indicating the presence of individual amino acids).

The Mascot program (<http://www.matrixscience.com>) uses the probability based MOWSE algorithm, precursor m/z information, and MS-MS fragment ion data to identify proteins from databases. Mascot is actually a cluster of programs that can be used for peptide mass fingerprinting as well as analysis of MS-MS data. A similar utility, PepFrag is available at (<http://prowl.rockefeller.edu/PROWL/pepfragch.html>). The Peptide Search program uses the peptide mass maps or (partial) amino acid sequences to identify the proteins by using mass spectrometric data (<http://www.narrador.embl-heidelberg.de/GroupPages/Homepage.html>).

1.4. Objectives

Recent studies implied that the CD73 (ecto-5'-nucleotidase), an ecto enzyme catalyzing the formation of adenosine from AMP plays an important role in many physiological and pathophysiological functions (Deussen et al. H692-H700; Shryock and Belardinelli 2-10). Adenosine is functionally relevant in modulating vascular tone, (Yegutkin, Bodin, and Burnstock 921-26), endothelial permeability (Weissmuller, Eltzschig, and Colgan 229-39), vasodilation during hypoxia (Mo and Ballard 593-603), suppression of cytokines production (Kobie et al. 6780-86; Deaglio et al. 1257-65) and in limiting inflammatory and prothrombotic responses by attenuating leukocyte adhesion and platelet function. (Koszalka et al. 814-21; Thompson et al. 1395-405).

Furthermore it has been recently shown that regulatory T cells are equipped with an active adenine nucleotide cascade involving CD73 (Kobie et al. 6780-86). CD73 derived adenosine may be involved in T cell mediated immunosuppression (Deaglio et al. 1257-65; Resta and Thompson 131-39). No information is available, whether lack of CD73 causes adaptive changes in membrane protein composition which secondarily might relate to the observed phenotype.

The aim of the present study was to analyze with MS-based techniques the membrane protein composition in endothelial cells and regulatory T-cells under control conditions and in the absence of CD73. Measurement of the differential protein expression is expected to answer the question whether lack of CD73 causes secondary changes in the composition of membrane proteins of endothelial cells and regulatory T-cells. To this end the membrane protein composition on endothelial cells was determined using the colloidal silica beads method with MS based techniques. Stable isotope dimethyl labeling method was employed to investigate the quantitative and differential proteome analysis in regulatory T cells isolated from control and CD73 knockouts.

2. Materials and methods

2.1. Materials: Chemicals and source

Table 2: List of chemicals and source

Substances	Suppliers
50µm and 30µm nytex net	BD Biosciences
Acrylamide	Carl Roth GmbH
Aluminium chlorohydroxide complex (chlorhydrol)	Reheis Chemical Company
Ammoniumperoxodisulfate (APS)	Carl Roth GmbH
Ampicillin	Carl Roth GmbH
Bovine serum albumin (BSA)	Sigma
Bromophenol blue	Carl Roth GmbH
Cacodylate	Fluka
Coomassie Brilliant Blue R-250	Carl Roth GmbH
Dimethylsulfoxide (DMSO)	Sigma
Dithiothreitol (DTT)	Sigma
Ethanol	Carl Roth GmbH
Ethylendiamine tetra acetic acid (EDTA)	Carl Roth GmbH
Ethylene glycol-bis-(beta - aminoethyl ether) N, N, N', N'-tetra acetic acid (EGTA)	Carl Roth GmbH
Fetal calf serum	Life Technologies GmbH
Formaldehyde	Carl Roth GmbH
Glucose	Carl Roth GmbH
Glutaraldehyde	Serva
N-[2-hydroxyethyl] piperazine - N'- [2-ethanesulfonic acid] (HEPES)	Carl Roth GmbH
Magnesium chloride	Carl Roth GmbH
Magnesium sulphate	Merk
MES	Fluka
Methanol	Carl Roth GmbH
Nalco 1060 colloidal silica	Ondeo Nalco Company
N, N', N' -Tertamethylethylenediamine (TEMED)	Carl Roth GmbH
Non-fat dry milk powder	Applichem
Nonidet P-40 (NP-40)	Calbiochem
OsO ₄	Carl Roth GmbH
Nycodenz	Sigma
Paraformaldehyde	Merk
Penicillin/Streptomycin	Life Technologies GmbH
Phenylmethylsulfonyl fluoride (PMSF)	Sigma
Polyacrylic acid sodium salt	Fluka
Ponceau-S	Sigma
Potassium chloride	Merk
Protease inhibitor cocktail (25x)	Sigma
PTA	Fluka
Sodium bi carbonate	Merk

Sodium chloride	Merk
Sodium dodecylsulfate (SDS)	Carl Roth GmbH
Sucrose	Carl Roth GmbH
SPURR resign-kit	Plano
Tris-(hydroxymethyl)-amino-methane (Tris)	Carl Roth GmbH
Triton X-100	Carl Roth GmbH
Trypsin	PAA Laboratories
Tween-20	Carl Roth GmbH
Uranyl acetate	Fluka

2.2. Methods

2.2.1. Physiological experiments

2.2.1.1. In situ perfusion of colloidal silica by Langendorff perfusion system

In order to selectively purify luminal EC membrane proteins from the mouse heart under *in vivo* conditions and analyze its composition with mass spectrometry, I have attempted to label endothelial cells of coronary vessels within the heart; with the cationic colloidal silica method as described by Oh. P et al.1998. For rat lung but with a slight modification, this is based on the binding of positive charged colloidal silica to the surface of endothelial cell membranes by in situ perfusion of colloidal silica by Langendorff perfusion system.

The heart was rapidly excised; the aorta was cannulated and perfused with Krebs-Henseleit buffer (NaCL: 116 mM, KCL: 4.63 mM, MgSO₄7H₂O: 1.1 mM, KH₂PO₄: 1.18 mM, NaHCO₃: 24.9 mM, Glucose H₂O: 8.32 mM, Pyruvate: 2 mM, CaCL₂: 2, 52 mM, pH 7.4) to wash out the blood completely (2 ml/min for 5 min (pH 7.4) at 37° C). Thereafter, the heart was perfused with MES-buffered saline (125 mM NaCL + 20 mM MES at pH 6.2) at 0.7 ml/min for 1.5 min, followed by perfusion with positively charged 1% colloidal silica (pH 6.2) at 0.5 ml/min for 1.5 min to coat the endothelial cell surface in the coronary vasculature. Cationic colloidal silica was prepared by modification of a previously published method (Schnitzer et al. 1759-63). Unbound colloidal silica was washed out with MBS buffer at 0.7 ml/min for 1.5 min. To cross-link and shield the positive charges on the membrane bound colloidal silica, 1% sodium polyacrylate (pH 6.2) in MBS was then perfused at 0.5 ml/min for 1.5 min. After one further wash with MBS at 0.7 ml/min for 1.5 min, the heart was perfused with fixing solution 1 [25 mM HEPES + 0.25 M Sucrose at pH 7.4 containing protease inhibitors (Protease inhibitor cocktail: (leupeptin (10 µg/ml), pepstatin A (10 µg/ml), O-phenanthroline (10 µg/ml), 4-(2-aminoethyl) benzenesulfonyl fluoride (10 µg/ml), and transepoxy succinyl-L-leucinamido (4 guanidono) butane (50 µg/ml))] at 0.5 ml/min for 2 min. The final perfusion step was done with fixing solution 2 (2) at 0.5 ml/min for 3 min. The pH of the fixing solution 2 (25 mM HEPES + 0.25 M Sucrose + 1 mM EDTA at pH 8.0 containing protease inhibitors) was finally adjusted to 8.0 in order to avoid binding of intracellular contaminating material to the membrane fraction during homogenization and the addition of EDTA was introduced to trap divalent cations.

For homogenisation, the hearts were minced with a razor blade in a plastic dish at 4°C and then placed in 2.5 ml lysis buffer (25 mM HEPES + 250 mM Sucrose + 1 mM EDTA + Protease inhibitor cocktail, pH 8.0). Homogenisation was alternatively carried out in two different ways for method comparison. The teflon pestle method (Potters; B.Braun; Teflon piston for glass container) used 8 or 16 up and down strokes at 1500 rpm. The ultra turrax blade method (Ultra Turrax IKA T18 basic) used low and high speed for 1 min at level 3 (14,000 rpm) and 1 min at level 5 (22,000 rpm). The homogenized samples were filtered through a 50 µm and thereafter a 30 µm (nylon monofilament net).

Fractionation was done by nycodenz gradient centrifugation, the filtered homogenate was diluted with an equal volume of 1.02 g/ml nycodenz and layered onto a 70% - 55% nycodenz gradient (formed by placing 2.0 ml of 70%, 1.5 ml of 65%, 60% and 1 ml of 55% nycodenz in a 12 ml Sorvall centrifuge tube). The tube was topped with HEPES/Sucrose containing protease inhibitors and centrifuged at 15,000 rpm for 30 min at 4°C in a swinging bucket rotor (TH-641, Sorvall). After centrifugation, the supernatant was removed and the silica membrane pellet was resuspended in 1 ml MBS. Again, an equal volume of 1.02 g/ml nycodenz was added to the sample and a second centrifugation step was performed at 30,000 rpm for 60 min, 4°C (TH-641, Sorvall) using a 80%-60% nycodenz gradient (1.5 ml of 80%, 700 µl of 75%, 70%, 65% and 60% nycodenz). The first and second nycodenz gradients composition is given below in table 3.

Table 3: Nycodenz gradient composition

Nycodenz gradients	102% Nycodenz	60% Sucrose	250mM HEPES	1M KCL	ddH2O
70% Nycodenz in HEPES/Sucrose	7 ml	1 ml	1 ml	200µl	0.8 ml
65% Nycodenz in HEPES/Sucrose	6.5 ml	1 ml	1 ml	200µl	1.3 ml
60% Nycodenz in HEPES/Sucrose	6 ml	1 ml	1 ml	200µl	1.8 ml
55% Nycodenz in HEPES/Sucrose	5.5 ml	1 ml	1 ml	200µl	2.3 ml
80% Nycodenz	8 ml	-	-	200µl	1.8 ml
75% Nycodenz	7.5 ml	-	-	200µl	2.3 ml
70% Nycodenz	7 ml	-	-	200µl	2.8 ml
65% Nycodenz	6.5 ml	-	-	200µl	3.3 ml
60% Nycodenz	6 ml	-	-	200µl	3.8 ml

The silica membrane pellet was washed in 1 ml MBS buffer in a microfuge tube at 14000 x g for 30 min. Then the silica beads were removed from derivatized EC membrane by resuspending and sonicating the pellets (Bransonic 220 Sonifier) in a small volume of 2% sodium dodecyl sulfate (SDS) in 50 mM Tris (pH 7.4) followed by heating of the suspension at 100° C for 5 minutes. Silica was separated from solubilized proteins by centrifugation at 14,000 x g for 15 minutes.

2.2.2. Biochemical techniques

2.2.2.1. Protein estimation

To determine the protein concentration, the micro BCA assay (Pierce) was used. Its for the colorimetric detection and quantitation of total protein, combines reduction of Cu^{2+} to Cu^{1+} by protein in an alkaline medium (the biuret reaction) using a unique reagent containing bicinchoninic acid and results in purple-colored reaction. This water-soluble complex exhibits a strong absorbance at 562 nm that is nearly linear with increasing protein concentrations over a broad working range (20-2,000 $\mu\text{g/ml}$).

2.2.2.2. SDS-PAGE electrophoresis

Based on the molecular weight of protein, the percentage of the acrylamide gel was decided. As shown in the table 4, the composition of solution for various percentages of the polyacrylamide gels is given below in table 4. The acrylamide stock solution contained acrylamide: bisacrylamide in a ratio of 29:1.

Table 4: Composition of solution for SDS-PAGE

	40% Acrylamide	0.5 M Tris-HCl	H2O	10% SDS	TEMED	10% APS
Stacking gel						
4%	0.375 ml	0.380 ml	2.185	30 μl	3 μl	30 μl
Separation gel						
8%	2.0 ml	2.5 ml	5.3 ml	100 μl	8 μl	100 μl
10%	2.5 ml	2.5 ml	4.7 ml	100 μl	8 μl	100 μl
12%	3.0ml	2.5 ml	4.3 ml	100 μl	8 μl	100 μl
16%	4.0 ml	2.5 ml	3.3 ml	100 μl	8 μl	100 μl

Before electrophoresis, equal amounts of protein were mixed with sample buffer (250 mM Tris-HCl pH 6.8, 40 % (v / v), glycerol, 8.2% (w / v) SDS, 400 µg/ml bromophenol blue, 4% (v / v) β-mercaptoethanol) and denatured at 95°C for 5 min. Samples were shortly centrifuged and loaded on the SDS-gel. After loading, gels were electrophoresed in 25 mM Tris, 250 mM glycine, 0.1% SDS electrophoresis buffer at constant voltage (50 V) in order to stack the samples. When the samples had entered the separating gel, it was run at 100 V until the dye front reached the bottom. Gels were carefully removed from the plates and equilibrated in wet blot transfer buffer (39 mM glycine, 48 mM Tris base, 0.037% SDS and 20% methanol). A polyvinylidene difluoride (PVDF) membrane, cut to the size of the gel, was activated in methanol for a few seconds and equilibrated in the transfer buffer. The gel was sandwiched between the PVDF membrane and Whatman blotting paper, which were equilibrated with the transfer buffer. Care was taken to avoid air pockets between membrane and gel. The sandwiched gel was placed in special transfer module provided by the manufacturer (Biorad, Munich, Germany). The tank was filled with transfer buffer and electro-blotted at constant current (50 mA) overnight. After complete transfer, the membranes were blocked in 5% non-fat milk powder prepared in TBST buffer (10 mM Tris-HCl, pH 7.5, 150 mM NaCl and 0.05% Tween 20) for 2 h at room temperature. The membrane was then washed with TBST buffer for 5 min and incubated with the primary antibody against the protein of interest overnight. Blots probed with primary antibody were washed in TBST three times at 5 min interval. Then, the membranes were incubated with their respective HRP conjugated antibodies for 1 h at room temperature. Blots were extensively washed with TBST buffer to remove unbound antibodies. ECL solution (Amersham Bioscience, Buckinghamshire, UK) was used to activate the conjugates for chemiluminescence. The blots were immediately exposed to photosensitive films (Amersham Bioscience) and developed. Antibodies used were directed against the marker proteins, which are given below in the table 5.

Table 5: List of antibodies and suppliers

	Antibody	Description	Supplier
1	Beta-COP	Polyclonal rabbit	Calbiochem
2	Caveolin 1	Polyclonal rabbit	Transduction Laboratories Bax
3	Cytochrome C	Monoclonal mouse	BD Biosciences / Pharmingen
4	Myoglobin	Polyclonal goat	Santa Cruz Biotechnology, Inc.
5	Ran	Monoclonal mouse	BD Biosciences / Pharmingen
6	LAMP 1	Monoclonal rat	BD Biosciences / Pharmingen
7	p58K	Monoclonal mouse	Sigma Aldrich
8	ERp72	Polyclonal rabbit	Calbiochem
9	EEA1	Monoclonal mouse	BD Biosciences / Pharmingen

Secondary antibodies, anti-mouse IgG and anti-rabbit IgG coupled to horseradish peroxidase were purchased from Promega (Mannheim, Germany). Anti-goat IgG coupled to horse radish peroxidase was purchased from Molecular Probes (Karlsruhe, Germany). Anti-rat IgG coupled to horse radish peroxidase was purchased from calbiochem (San Diego, CA). Primary and secondary antibody dilutions are listed below in the table 6.

Table 6: List of primary and secondary antibody dilutions

Name of the Proteins	Marker	1°Ab (Mono/poly)	2°Ab	1°Ab Dilutions	2°Ab Dilutions
Ran (25kDa)	Nuclear	Mouse mono	Anti mouse	1:5000	1:5000
Caveolin 1 (22kDa)	EC membrane	Rabbit poly	Anti Rabbit	1:2000	1:5000
p58K (58kDa)	Golgi	Mouse mono	Anti mouse	1:5000	1:5000
Beta-COP (110kDa)	Golgi	Rabbit poly	Anti Rabbit	1:2000	1:5000
ERp72 (72kDa)	ER	Rabbit poly	Anti Rabbit	1:1000	1:5000
Lamp1 (40kDa)	Lysosome	Rat mono	Anti rat	1:2000	1:1000
EEA1 (180kDa)	ER	Mouse mono	Anti mouse	1:2500	1:5000
Cyto C (15kDa)	Mitochondria	Mouse mono	Anti mouse	1:2000	1:5000

2.2.2.3. Immunohistochemistry

In order to reveal the expression of CD73 on murine tissues like mouse brain, liver, spleen and kidney an immunohistochemical staining procedure was applied by using CD73-rhodamine labelled antibody and vWF-FITC labelled antibody. Those expressions of specific markers on the specific regions of the individual tissue sections were visualised by fluorescent microscopy.

Tissue sections were fixed with paraformaldehyde (PFA) and the tissue sections were washed by using PBS for three time followed by blocking with 10% (normal) goat serum in PBS with 0.2% saponin for 1 hr at room temperature (RT). The primary antibody (CD73- rhodamine labelled antibody and vWF-FITC labelled antibody) was diluted in the ratio of 1:50 in PBS/Saponin with 2% NGS (Normal goat serum) was added into the tissue sections and incubated for overnight at 4° C. Primary antibody was washed out with PBS/Saponin for three times each steps for 10 min. Tissue sections were incubated with secondary antibody anti-rat-IgG rhodamine conjugated and goat-anti rabbit-FITC conjugated antibody with the dilution of 1:400 in PBS/Saponin with 2% NGS and incubated at RT for 2 hrs in the dark. Tissue sections were washed with PBS/Saponin three times and finally the sections were washed

with PBS without detergent. The excess of buffer was dried and the chambers were covered with chamber slide by using slow fade antifade reagent. The fluorescent labelling of the antibodies were visualised by using fluorescent microscopy.

2.2.3. Electron microscopy

To reveal the specific labelling of cationic colloidal silica (20 nm) on to the surface of endothelial cell membrane in macro and micro vessels of isolated mouse heart, transmission electron microscopy was used.

The perfused heart was flushed with MEM buffer (20 mM MES pH 6.8, 0.1 mM EGTA, 0.5 mM MgCl₂). Then the heart was fixed by perfusion with 1% PFA (Paraformaldehyde) containing 1.25% glutaraldehyde in 0.1 M cacodylate buffer, pH 7.4 (with and without 5% sucrose) and afterwards incubated overnight at 4°C. Next the heart was immersed in the same buffer, trimmed to small blocks of ~1 mm³. After two further washing steps, post fixed for 2h at 4° C in 2% OsO₄ in 0.1 M cacodylate buffer. Dehydration of specimen was performed in acetone, simultaneously stained in block in 1% PTA (Phosphotungstic acid) and 0.5% uranyl acetate (UAc) and followed by embedding in SPURR-resin kit. Thin sections were cut on a reichert ultra microtome and stained in uranyl acetate and lead citrate and micro graphed with a transmission electron microscope (TEM, HITACHI-H600).

2.2.4. Cell culture

Mouse aortic and lung cells were isolated by the collagenase enzymatic digestion method. Vascular endothelial cells were specifically labeled and separated from the total cells by endothelial specific marker proteins coupled to dynal beads. For isolation of mouse aortic endothelial cells cleavable CD31 labeled dynal beads were used and for the isolation of mouse lung endothelial cells CD102 labeled dynal beads were used. bEND and 293 cell lines were cultured and used for positive and negative controls, respectively. Vascular endothelial cells isolated from mouse aorta and mouse lung were cultured in individual growth medium as listed in the table 7 below.

Each medium was supplemented with 10% heat-inactivated fetal calf serum (FCS), 100 units of penicillin/ml, and 0.1mg streptomycin/ml (PAA Laboratories, Linz, Austria). Cells were grown at 37°C in a humidified 5% CO₂ atmosphere. Isolated EC were tested for their long-term viability by sequential passaging until arrest of growth. Total numbers of passages were determined for each culture.

Table 7: List of cells and medium

Cells	Medium
Mouse aortic endothelial cells (MAECs)	Basal medium: Dulbecco's Modified Eagle's Medium Culture medium: Microvascular endothelial cell growth medium
Mouse lung endothelial cells (MLECs)	Culture medium: Dulbecco's Modified Eagle's Medium and F12 medium
bEND (Brain endothelial cells)	Culture medium: Dulbecco's Modified Eagle's Medium (Positive control)
293 cells (Human Embryonic Kidney cells)	Culture medium: Dulbecco's Modified Eagle's Medium (Negative control)

2.2.4.1. Vascular endothelial cells isolation from mouse aorta

Mice (28 to 35 days old: n = 4) was anesthetized with urethane plus heparin and sprayed with 70 % ethanol to avoid the contamination of skin fur of animal. Then the anterior abdomen was cut and opened with sterilized instruments and to washout the blood from aorta made a small cut on thoracic aorta and immediately, a 10 ml of HBSS was infused through right ventricle. The washed aorta (free of blood) was removed from the animal and placed in the fresh basal medium containing (~ 4-5 ml) falcon tube. (Base medium: DMEM containing 25 mM HEPES, 20% FCS, 100 U/100 mg/ml Penicillin and streptomycin, and 2 mM L -glutamine).

In the laminar flow hood, the aorta was placed in the fresh DMEM medium containing 60 mm culture plate (5 ml) to remove the fat and connective tissue, which surrounds the aorta. The cleaned aorta was then transferred into another fresh base medium containing 60 mm culture plate (5 ml) and opened longitudinally with a scissor. The opened vessels were placed for 45 min in prewarmed (37°C) collagenase solution (2 ml for 4 aortas), which contained: collagenase 2: 4 mg/ml, 125 U /ml collagenase type XI, 60 U/ml hyaluronidase type 1-s , 450 U/ml collagenase type 1 and 60 U/ml DNase 1), vortexed in-between every 5 mins). After incubation, collagenase was diluted with large volume of DMEM medium to stop the enzyme action and transferred into another falcon tube and stored at 4° C.

The aorta was then removed and transferred into another 60 mm culture plate with 500 μ l base medium and the endothelial-side of the aorta was scraped once with the plastic scrubber. The scrapped mouse aortic cells were collected by centrifugation and the pellets were resuspended in microvascular endothelial cell culture medium (Provitro, GmbH) supplemented with heparin, endothelial cell growth stimulant, nonessential amino acid and sodium pyruvate. Then the resuspended cells were transferred into an appropriate tissue culture vessel, previously coated with 1% gelatine.

Mouse aortic cells were washed with S-EDTA (2x) and trypsinised (0.25% trypsin- 0.02% EDTA) for 10 min and, 10% FCS was added and diluted with 10 ml of medium to stop the enzyme action. Then the cells were spun down for 8 min at 1000 rpm. After removal of the medium, cells were resuspended in the culture medium and then counted by haemocytometer. Total cells were aliquot into another 1% gelatin coated culture plate before positive selection. Rat anti mouse CD-31 antibody (Clone MEC 13.3) was added to the mouse aortic cells according to the following concentration: 1 million cells / 1 μ g antibody/ ml of MVECG medium were used. Cells with antibody were incubated in the cold room (at 4°C) for 20 min with gentle tilting and rotation. After the incubation, the mixture was diluted with PBS buffer (PBS + 0.1% BSA and 2 mM EDTA, pH 7.4), followed by centrifugation at 1000 rpm for 10 min at 4°C. Unbound antibodies were removed and then the pellet was dissolved in 1 ml of PBS buffer and 1 mg of dynal beads (Concentration: 4×10^8 beads / ml in PBS, pH 7.4) were added to the cells (1 μ g of Ab/ mg of beads).

Cells with dynal beads were incubated in the cold room (at 4°C) for 15 min with gentle tilting and rotation to prevent dynabeads from settling. After incubation, 1 ml of PBS buffer was added to limit trapping of unbound cells. Then the tube was placed in a magnet for 3 min, to permit cell-bound and unbound magnetic beads to be pulled to the side of the tube. Gently, without moving the tube, the supernatant was aspirated. Then the tube was removed from the magnet and the beads/cells pelleted on the side of the tube were resuspended in 1 ml of PBS buffer for further wash.

Cells-bound to beads were gently washed for 4 times using the following procedure: Cells were resuspended in 1 ml of PBS buffer. Placed it in a magnetic separator for 2.5 min; the supernatant was aspirated carefully. The cell pellet was washed repeatedly for 4 times (or more) until the supernatant appeared clear. After the last wash, beads/cell pellets were

resuspended in releasing buffer (DynaL Invitrogen AS, Oslo, Norway) and pipetted up and down for 5-10 times and incubated at 4°C for 10 min with gentle tilting and rotation in cold room. Then the tube was placed in a magnet for 3 min, so that the cell-bound and unbound magnetic beads will be pulled to the magnet side of the tube. Gently, without moving the tube, the supernatant was aspirated. The tube was removed from the magnet and the beads pelleted on the side of the tube was resuspended in 1 ml of PBS buffer for further wash.

Positively selected aortic vascular endothelial cells were gently washed once again 4 times as mentioned in the above procedure. Population of endothelial cells were resuspended in culture medium, and the cells were counted and seeded in to the 1% gelatine coated culture plate. Cells were cultured in a standard 5% CO₂ incubator. After an overnight incubation, the non-adherent cells were removed. The adherent cells were washed twice with HBSS and 3 ml of fresh complete medium was added and re-fed every alternative day with 3 ml of fresh complete medium. The purity of mouse aortic endothelial cell was analysed by FACS analysis.

2.2.4.2. Vascular endothelial cells isolation from mouse lungs

In order to isolate mouse lung endothelial cells we have applied a method which was previously published (Kuhlencordt et al. C1195-C1202). The animals (6 weeks old) were killed by cervical dislocation and lungs were collected in ice-cold Dulbecco's modified Eagle's medium (DMEM). Peripheral lung tissue was minced and digested for 1 h at 37°C in 0.1% collagenase-A (10 mg/10 ml) using 50 ml tube in DMEM medium. The tissue digests were triturated through a blunt 14-gauge needle with a 20 cc syringe for 12 x up and down and filtered through a 100 µm mesh. Cells were pelleted at 300g at 4°C for 5 min and resuspended in culture medium (37° C) and then plated in 0.1% gelatin-coated T75 flasks. After 24 h, cells were washed with sterile PBS until appears clean and cultured for 2–3 days in culture medium (20% FCS, 39% DMEM, 39% F12 medium, ECGS (50 µg/ml), 2mM L-Glutamine, Heparin 100 µg/ml, Penicillin/streptomycin 100 U).

Magnetic beads (Sheep anti rat IgG - 5µg / 4 x 10⁶ beads, Dynabeads M-450) were coated with Rat anti mouse CD102 (Clone MEC 13.3) antibody (5µg). The beads and antibody was incubated over night in 0.5 ml PBS/ 2% FCS on a tube roller. The beads were washed 3 x with changes of PBS/ 2%FCS in the magnetic field and after final wash, beads were resuspended in PBS / 2% FCS and stored at 4°C.

In order to separate mouse lung vascular endothelial cells (MLECs), 3 ml of culture medium (DMEM/F12 medium) was added to the cell culture bottle (T75 flask) and closed tightly and placed at 4°C for 5 min. Then 500 µl of beads were added to T75 flask and incubated for 1 hr at 4°C (every 6 min, flask was shaken for beads distribution). After incubation cells were washed with 10ml of S-EDTA (2x) and 2 ml of warm Trypsin/EDTA was added to detach the cells. Finally, cells were placed at 37°C and checked after 5 min to know whether the cells have detached. Added enough serum containing media to bring the volume in the T75 flask to 5 ml and layered this over 4 ml of serum containing media in a 15 ml falcon tube. Cells were resuspended in 0.8 ml of PBS/ 2%FCS buffer and placed in the magnetic field for 5 min (3 washes; each wash 5 min) to make positive selection of vascular endothelial cells.

The beaded cells were resuspended in culture medium (DMEM/F12 medium) and seeded in the T75 flask. The cells were reseeded on the next day and every second day thereafter. In order to make 2nd positive selection of MLECs followed the same protocol of 1st positive selection of MLECs as mentioned above. The cells were reseeded on the next day and every second day thereafter. MLECS purity was analysed by FACS by using endothelial cell specific marker proteins.

2.2.4.3. FACS analysis

FACS analysis was used to find the initial enrichment of vascular endothelial cells isolated from mouse aorta and lung after separation of magnetic beads method and the purity of the cells during the culture. bEND and 293 cell lines were cultured and used for positive and negative controls respectively. In case of CD4⁺ CD25⁺ regulatory T cells were isolated from the mouse spleen by using CD4⁺ CD25⁺ regulatory T cells isolation kit, those cells were isolated and directly the enrichment and purity was analysed by FACS analysis. The list of

markers used for the purity analysis of individual cells isolated from the different source were mentioned in the table 8 as given below.

Table 8: List of cells and markers for FACS analysis

Cells	Markers used for the FACS analysis
Mouse aortic endothelial cells (MAECs)	PE labelled CD31, FITC labelled CD102 and PE labelled CD73
Mouse lung endothelial cells (MLECs)	PE labelled CD31, FITC labelled CD102 and PE labelled CD73
bEND (Brain endothelial cells)	PE labelled CD31, FITC labelled CD102 (Positive control)
293 cells (Human Embryonic Kidney cells)	Negative control
CD4+ CD25+ regulatory T cells (T-reg cells)	FITC labelled CD4, PE labelled CD25, FITC labelled CD73 and FITC labelled FOXP3

Cultured vascular endothelial cells isolated from mouse aorta and lung cells were washed with S-EDTA (2x) and trypsinised (0.25% trypsin- 0.02% EDTA) for 10 min and then to stop the enzyme action, 10% FCS was added and diluted with 10 ml of medium. Then the cells were spun down for 8 min at 1000 rpm. Followed by removal of the medium, the cells were resuspended in PBS buffer (PBS/ 10%FCS/ 2 mM EDTA) and used for FACS analysis.

Cells were stored in PBS buffer and diluted to a concentration of 2×10^5 /vial and washed with PBS buffer in FACS tube by centrifugation at 12000 rpm. The supernatant was aspirated, resuspended in 50 μ l of PBS buffer, and the cells were stored in all steps on crashed ice. The primary antibody was diluted to a concentration of about 1 μ g/ml and 5-10 μ l/vial (2×10^5 cells) in PBS buffer was used. Incubated for 30 min on crashed ice and diluted afterwards with 3 ml of PBS buffer. Diluted afterwards with 3 ml of the same buffer and centrifuged for 5 min at 1000 rpm to washout the excess of antibody. The supernatant was removed and the cell pellet was resuspended in 0.5 ml of PBS buffer and used for FACS- measuring on a FACS Calibur (Becton Dickinson).

2.2.5. Regulatory T cells

2.2.5.1. Isolation and purification of CD4⁺ CD25⁺ regulatory T cells from mouse spleen

To isolate CD4⁺ CD25⁺ regulatory T cells from mouse spleen, a respective T cell isolation kit was used (Milteny Biotech Inc). Splenocytes were separated from the mouse spleen and RBCs were lysed to reduce the contamination. To enrich the CD4⁺ CD25⁺ regulatory T cell, in the first step enrichment of CD4⁺ T cells by depletion of non CD4⁺ T cell by using biotin conjugated antibodies were against non CD4⁺ T cells like CD8, CD11b, CD45R, CD49b and Ter-119 and in the second step enrichment of CD4⁺ CD25⁺ T cell from the isolated CD4⁺T cells by using magnetic separation procedure. In each step the enrichment and purity was analyzed by FACS analysis.

The spleen was taken out from 2 mouse and placed into 10 ml MACS buffer (PBS pH 7.2 + 0.5% BSA + 2 mM EDTA), cut it into pieces in 10ml buffer by using scalpel no 21. Cell suspensions were filtered through the 70 µm pore sized filter and the bigger tissue was crushed by using the syringe (10 ml). The cells were collected into the falcon tubes and spun at 4° C 300 g (1350 rpm) for 10 minutes.

After complete removal of supernatant, the pelleted cells were vortexed. 5 ml of lysis buffer (1.55 M NH₄Cl; 0.1 M KHCO₃; 1 mM EDTA, pH 7.4) was added to lyse RBC at 4° C for 3 minutes. After 3 minutes, the cells were diluted with MACS buffer (15 ml) to stop the lysis of RBC and centrifuged at 4° C for 10 minutes at 300 g. The supernatant was removed and the pellet in white color was diluted with 15 ml MACS buffer followed by centrifugation at 4° C 300 g. The supernatant was (completely) removed and the pellet was resuspended with 5 ml MACS buffer. 10 µl of the sample was taken for cell count. Then the remaining cells were centrifuged at 4° C for 10 minutes at 300 g.

Cell pellet was resuspended in 40 µl of MACS buffer per 10⁷ total cells and added 10 µl of biotin-antibody cocktail per 10⁷ total cells. [Cocktail of biotin-conjugated monoclonal anti-mouse antibodies against: CD8 (Ly-2; isotype: rat IgG2a), CD11b (Mac-1; isotype: rat IgG2b), CD45R (B220; isotype: rat IgG2a), CD49b (DX5; isotype: rat IgM), and Ter-119 (isotype: rat IgG2b)]. Mixed well and the cell mixture was kept in rotator for 10 min at 4° C followed by addition of 30 µl of MACS buffer with 20 µl of anti-biotin micro beads and

vortexed. (Microbeads conjugated to monoclonal anti-biotin antibody (isotype: mouse IgG1). Cell suspension was again kept in rotator for 15 min at 4° C in the dark. Cells were washed by adding 10 ml of buffer per 10^7 total cells and centrifuged at 4° C for 10 minutes at 300 g Supernatant was aspirated completely and the cell pellet was resuspended in MACS buffer.

Depletion of non CD4+ T cells was done by using magnetic separation method with LD column. LD column (Miltenyi Biotec) was placed in the magnetic field of a suitable MACS separator and the column was prepared by rinsing with 5 ml of MACS buffer. The cell suspension was applied onto the column and the unlabeled cells which pass through were collected and the column was washed with 3 x 3 ml of buffer. Washing steps were performed by adding buffer successively, once the column reservoir is empty. Total effluent was combined and this was the unlabeled CD4+ T cell fraction.

To enrich CD4+ CD25+ T cells, isolated CD4+ T cells were centrifuged at 300 x g for 10 minutes and the supernatant was aspirated completely. The cell pellet was resuspended in 30 μ l of MACS buffer, 10 μ l of CD25-PE antibody (Monoclonal anti-mouse CD25 antibody conjugated to R-Phycoerythrin (PE) (clone: 7D4; isotype: rat IgM) / 10^7 total cells. The cell suspension was vortexed and kept additionally in rotator for 10 min at 4° C in the dark. Then the cells were washed by adding 2 ml of buffer per 10^7 total cells and centrifuged at 4° C for 10 minutes at 300 g and the supernatant was aspirated completely. The cell pellet was resuspended in 90 μ l of MACS buffer and added with 10 μ l of anti-PE micro beads [Microbeads conjugated to monoclonal anti-PE antibodies (isotype: rat IgG1)]. Again the cell mixture was mixed well and kept additionally in rotator for 10 min at 4° C in the dark. Then the cells were washed by adding 2 ml of buffer/ 10^7 total cells and centrifuged at 4° C for 10 minutes at 300 g and the supernatant was removed completely. Then the pellet was resuspended with MACS buffer (500 μ l for up to 1×10^8 cells) to proceed to magnetic separation method.

Positive selection of CD4+ CD25+ regulatory T cells was done by magnetic separation procedure by using MS column (Miltenyi Biotec). To achieve sufficient purity, always two consecutive column runs were performed. The column was placed in the magnetic field of a suitable MACS separator and the column was prepared by rinsing with 500 μ l of MACS buffer. The cell suspension was applied onto the column and then the column was washed 3 x 500 μ l of MACS buffer. Washing steps were performed by adding buffer three times

(3 x 500 μ l), once the column reservoir is empty. The column was removed from the separator and placed on a suitable collecting tube and then 1 ml of buffer was pipetted onto the column. By firmly pushing the plunger into the column, the magnetically labeled cells (CD4⁺ CD25⁺ cells) were immediately flushed out. In order to increase the purity magnetic separation procedure was repeated as described in above steps by using a new MACS column for second separation. The purity of the magnetically labeled CD4⁺ CD25⁺ cells were analyzed by FACS.

2.2.5.2. FACS-protocol for FOXP3 cells with membrane disintegration

In order to label the intracellular marker FOXP3, which is a characteristic molecule of the T regulatory of (CD4⁺, CD25⁺) cells, we have applied membrane disintegration protocol for labelling of the FOXP3 as given below. FOXP3 is a member of the forkhead or winged helix family of transcription factors and functions as the master regulator in the development and function of regulatory T cells. CD4⁺ CD25⁺ regulatory T cells were isolated from the mouse spleen by using CD4⁺ CD25⁺ regulatory T cells isolation kit and directly analysed the enrichment and purity was analysed by FACS analysis.

To analyze the regulatory T cell purity, cells were resuspended in PBS/ 20%FCS buffer, diluted to a concentration of 2×10^5 / vial and washed with 1 x PBS buffer by centrifugation in FACS tube at 12000 rpm. The supernatant was removed and cell pellet was resuspended in PBS buffer (50 μ l), and then the cells were stored in all steps on crashed ice.

For fixing the cells, the cell suspensions were mixed with 1 ml of 1% formalin in PBS pH 7.4, vortexed, followed by incubated for 10 min on ice. After 10 min, the fixation was stopped with addition of 2 ml PBS/ 20%FCS buffer and centrifuged at 1000 rpm for 5 min. The cells were washed (3 x) with PBS/ 10%FCS buffer. (During each washing step, the supernatant was removed and the cell pellet was resuspended in 50 μ l of PBS buffer). The last washing step contained 0.1 % Triton X-100 or any other detergent (0.1% saponin, etc).

In order to label the intracellular marker FOXP3, FITC labeled FOXP3 (FITC anti-mouse/rat FOXP3 (Clone: FJK-16s) was diluted to a concentration of about 1 μ g/ml (pure IgG-fraction) and used 5-10 μ l/vial (2×10^5 cells) in PBS/FCS 10% + 0.1% detergent was used. Incubated

for 30 min on ice and diluted afterwards with 3 ml of PBS/ 10% FCS + 0.1% detergent. The cells were washed three times by centrifugation at 1000 rpm for 5 min with the same buffer (In the last washing step should be free of detergent). The pellet was resuspended in 0.5 ml of PBS/ 10% FCS (without detergent) and further analysed by FACS Calibur (Becton Dickinson).

2.2.6. Mass spectrometry

2.2.6.1. Preparation of fused silica capillary column

We have used home made fused silica capillary column to separate the membrane peptide mixture. In order to prepare fused silica capillary column, a laser puller (P-2000, Sutter Instruments) was used by using 100 μm I.D. x 365 μm O.D. or 75 μm I.D. x 365 μm O.D (Aligent Technologies) silica capillaries. The program for the machine reproducibly generates apertures of approximately 5 nanometers across from capillaries that have an inner diameter of 100 microns. To ensure good electrospray ionisation performance, the tip was inspected under a low-resolution (5-10 x magnification) microscope to ensure that the tapered tip is blunt and $\sim 2\text{-}3$ μm across.

Stainless steel pressurization bomb was coupled to a helium tank with regulator (at least 1000 psi ~ 70 bar = 7 MPa pressure) with Teflon ferrules (Chromatography Research Supplies, Kentucky). The custom-made "bomb" helps to load packing material and peptides into the self made fused silica capillary columns. In order to pack the materials and peptides, an eppendorf tube was placed inside the bomb, holding the material to be loaded. The bomb is then assembled and the column inserted through the aperture at the top of the bomb into the eppendorf below. Gas pressure forces the material in the tube into the column. By following the above procedure C_{18} reversed phase packing material (3 μm) (Zorbax XDB, Agilent Technologies), Followed by peptides were packed into the columns by using stainless steel pressurization bomb. Ettan microLC (Amersham biosciences) was operated at flow rates of 100-200 microliters/min with pre-column splitting of the flow to produce 100-200 nL/min flow rates at the column.

2.2.6.2. Peptide separation

In order to identify the EC membrane proteins from the mouse heart, purified EC membrane pellets from 10 animals were pooled (totally 10 µg protein), washed with ice-cold deionised water and sedimented by ultra centrifugation at 30,000 rpm for 30 min at 4° C (TH-641, Sorvall). Membranes were resuspended in 60% methanol and 40% of 25 mM ammonium bicarbonate and sonified for 2 x 10 min. Subsequently, trypsin and chymotrypsin (each 1:100 w/w) were added to the membrane pellet (Fischer et al. 444-53). Proteolysis was performed overnight at 37° C. After cleavage, the peptide mixture was centrifuged at 13,000 rpm for 30 min. The membrane peptide containing supernatant was removed and dried in Speed Vac. 20 µl of sample buffer (4% acetonitrile; 0.5% acetic acid) were added to dissolve the peptides for mass spectrometric analysis.

Peptides were separated by C₁₈ reversed phase hydrophobic interaction chromatography on self made fused silica micro capillary columns. A 5 µm tip was pulled on a fused silica micro capillary (75 µm inner diameter) by laser puller (Model P-2000; Sutter Instrument). Initially, the micro column tip was blocked with 11 µm C₁₈ reversed phase chromatographic material (AA12S11, YMC), followed by packing 3 µm C₁₈ reversed phase chromatographic material (Nucleodur C₁₈ Gravity, Macherey-Nagel) for 8 cm by using stainless steel pressurization bomb operated at 500 psi. After equilibrating the micro capillary column with sample buffer, the sample was directly loaded to the column using the helium pressure cell, mounted on to a micro-tee (Upchurch Scientific) and placed in-line with an Ettan microLC system (Amersham Biosciences).

The two buffer solutions used for the chromatography were 4% acetonitrile; 0.012% heptafluorobutyric acid (HFBA); 0.5% acetic acid (Solution A), 80% acetonitrile; 0.012% heptafluorobutyric acid (HFBA); 0.5% acetic acid (Solution B). Peptides were directly eluted into the mass spectrometer with a linear gradient from 0 to 60% solution B for 100 min; 60 - 100% B for 20 min and 100% B for 20 min. The flow rate of 100 µl/min at the HPLC was reduced to 200 nl/min by an integrated flow splitter.

2.2.6.3. Stable isotope dimethyl labeling

For the quantitative proteomic analysis of regulatory T cells from control and CD73 knockout mice, the stable isotope dimethyl labelling method was applied (Hsu et al. 6843-52). This labelling method is very fast (within 5 min), complete (100%) and globally label the N-terminus and ϵ -amino group of lysine through reductive amination. This labelling strategy produces peaks differing by 28 mass units for each d0 (Formaldehyde-d0) derivatized site and 32 mass units for each d2 (Formaldehyde-d2; 20% solution in D₂O) derivatized site relative to its non derivatized counterpart. The mass differences between isotopic pair are 4 mass units.

In order to label the peptides with d0/d2 formaldehyde (Formaldehyde-d0; Formaldehyde-d2-20% solution in D₂O) the regulatory -T cells were lysed with the lysis buffer (25 mM Tris-HCL-pH 7.8, 150 mM NaCL, 1 mM EDTA, Complete protease inhibitor cocktail, 2.5% SDS, DNase) and pipetted up and down for 20 times with out making the foam and incubated for 15 min at room temperature. Once the cells were lysed, the debris was removed by centrifugation at 12000 rpm at RT. The protein concentration was estimated by using BCA assay kit. Proteins were reduced and dealkylated with DTT and IAA respectively and followed by the methanol chloroform precipitation method was performed.

For a 150 μ l sample (~150–300 μ g of protein), 600 μ l of methanol was added and mixed well by vortexing. Again, 150 μ l of chloroform was added and mixed well by vortexing. Then followed by addition of 450 μ l of ultrapure water, it was vortexed, and the sample was centrifuged at ~12,000 rpm for 5 minutes. After, centrifugation, the upper phase was discarded and the white precipitated disc that formed in between the upper and lower phases was sucked and added with 450 μ l of methanol and mixed well by vortexing and then followed by centrifugation at ~12,000 rpm for 5 minutes.

The pellet was resolved in 50mM Ammonium bicarbonate with 0.1% SDS pH 7.8. Trypsin solution (20 μ g trypsin- from Promega resolved in 100 μ l resolving buffer) was added into the protein sample mixture (1:20), containing 50 mM Ammonium bicarbonate, 0.1% SDS, 5 mM CaCl₂ (pH 7.8). Then the sample with enzyme mixture was incubated for 8-16 hrs at 37°C at 400 rpm. The sample was removed from the incubation and adjusted to the pH of 2.5 with HCOOH to stop the enzyme action. Solid phase extraction SPE C18 was done by using varian column for desalting.

The column was conditioned 3 x with 500 μ l MeOH and 5 x with 500 μ l 0.1% TFA. Then the sample was allowed to bind to the column (pH 2.5-3) by adding 0.1% TFA (Same sample were reloaded into the same SEP column for 5 times) and washed with three times 300 μ l 0.1% TFA and two times with 0.1% formic acid. Then the peptides were eluted with 200 μ l - 2 x 20%, 2 x 40%, 2 x 60% ACN containing 0.1% formic acid in steps. (Total volume: 1200 μ l/ each tube). Eluted peptide samples are frozen in liquid N₂ followed by lyophilisation of the sample overnight.

To label the primary amines and ϵ -amino group of lysine residue, the peptide samples were dissolved in 100 mM Na Acetate (pH 5.5) and followed by peptides were labelled with 4% d₀/d₂ formaldehyde (Formaldehyde-d₀; Formaldehyde-d₂- 20% solution in D₂O) and mixed well for 20 sec, immediately 600 mM Sodiumcyanoborohydride was added in to the peptide mixture and vortexed well for 20 sec. In order to label the peptides, the reaction mixture was incubated for 2 hrs at 30° C, 300 rpm in thermo mixture.

After 2 hrs, 4% ammonium hydroxide was added to quench the excess of formaldehyde from the sample. Then the labelled peptides were applied into solid phase extraction by using SPE C18 Varian column for desalting. The same desalting procedure mentioned above was followed and the desalted peptide samples were frozen in liquid N₂ followed by lyophilisation of the sample overnight.

Peptide samples were resolved in 0.1% TFA and d₀ and d₂ formaldehyde labelled peptides were mixed with 1:1 ratio and applied to solid phase extraction SEP C18 varion column for desalting. Once again the desalted samples were frozen in liquid N₂ followed by lyophilisation of the sample overnight. Dimethyl labelled peptide mixtures were fractionated by SCX column and followed by RP column for MS analysis (see below).

2.2.6.4. 2D-LC for peptide separation

In order to reduce the sample complexity, fractionation by HPLC-Ultimate™ 3000 (DIONEX) was performed automated off-line two dimensional separation of peptides. In the first dimension separation was performed 'splitless' on a 1mm I.D. X 15 cm SCX column. The second dimension separation was performed on a 75 µm I.D. X 15 cm RP column using spliteration of 1:1000.

The dimethyl labelled peptide sample was injected into Ultimate 3000 series nano/cap auto sampler for SCX fractionation. The loading pump delivers the salt gradient for the SCX column by buffer B and C with a linear gradient from 0 to 60% solution C for 30 min; 60 - 100% C for 5 min and 100% C for 5 min (Buffer B: 5 mM NaH₂PO₄ -pH 2.7; Buffer C: 5 mM NaH₂PO₄, 20% ACN, 0.5 M NaCl, pH 2.7) through channels A and B for sample loading and fractionation in SCX column. The eluent from the column was directed to the injection needle for the fractionation. After fractionation, a wash program was used to switch from the SCX dimension to the reversed phase dimensions. After the wash program (Pre column washing and sample loading Buffer A: 0, 1% TFA and 0,012% HFBA), an aqueous solution (channel C of loading pump) consisting formic acid was used to load the SCX fractions onto the reversed phase trap column. Desalting of the fraction occurs on the reversed phase trap column. The micro pump delivers the gradient for elution of the peptides by using buffers A and B (Buffer A: 0.1% Formic acid; Buffer B: 0, 09% formic acid and 84% ACN). In this experiment UV detection was applied for both dimensions to monitor the peptide binding and elution from the columns.

2.2.6.5. Protein identification

Mass spectrometric measurements were done on a Finnigan LTQ ion trap mass spectrometer equipped with a nanospray ionisation source (Thermo Finnigan). A spray voltage of 1.8 kV was applied to the column and continuous cycles of one full scan (m/z 200 to 2000) followed by four data dependent MS/MS measurements at 35% normalized collision energy were applied. Operation of the Ettan microLC system and the mass spectrometer was fully automated during the entire procedure using Unicorn (Amersham Biosciences) and Xcalibur 2.0 (Thermo Finnigan) respectively.

The SEQUEST algorithm was used for MS/MS data interpretation. SEQUEST searches were done against a mouse protein database downloaded as FASTA-formatted sequences from Entrez (NCBI, <http://www.ncbi.nlm.nih.gov/entrez>). The peptide mass search tolerance was set to 1.5 Da. In order to obtain reliable protein identification, only the peptides with a minimal cross-correlation score (XCorr) of 1.8, 2.5 and 3.5 for charge states +1, +2 and +3 respectively were taken into account. The DeltaCN had to be > 0.1 .

The molecular weights and functions of each protein were identified by using the Expasy web server (<http://www.expasy.org/sprot>) and the Bioinformatic Marvester (Mouse Harvester) (<http://harvester.embl.de/>) database was used to identify the currently known predominant subcellular localisation. Known or predicted transmembrane-spanning alpha helices were determined through the literature or by using the web-based prediction program TMHMM v2.0 (provided by the Center for Biological Sequence Analysis of the Technical University in Denmark, <http://www.cbs.dtu.dk/services/TMHMM-2.0>) (Durr et al. 985-92).

2.2.7. Statistical analysis

All statistical analyses were performed using the student's paired t test or fisher exact probability test.

3. Results

3.1. Proteomic analysis of endothelial cell membrane

3.1.1. Selective labelling of mouse heart endothelial cell membrane by colloidal silica

In order to specifically label endothelial cell membranes in the mouse heart microvasculature under *in vivo* conditions, we have applied a modified colloidal silica method, which is based on the interaction between positively charged silica beads with the negatively charged endothelial membrane (Chaney and Jacobson 10062-72).

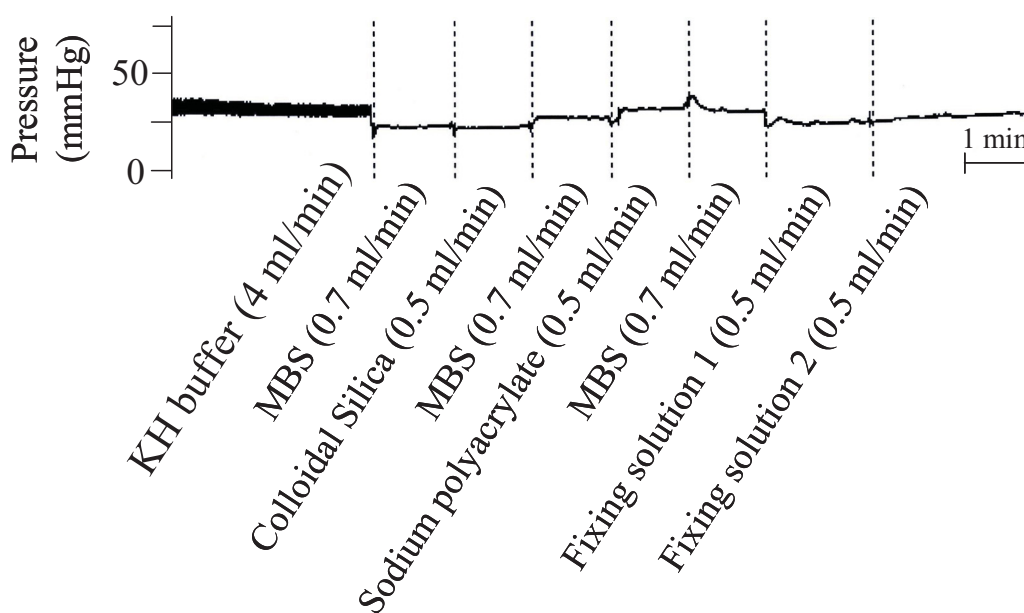


Fig 11: Protocol used to specifically label EC membranes of isolated perfused mouse hearts by colloidal silica: Coronary flow was adjusted during the different interventions to maintain perfusion pressure constant.

As outlined in Fig.11, isolated mouse hearts were perfused at 37° C with a saline medium and coronary flow was adjusted to maintain coronary perfusion pressure constant at the different interventions. Initially the perfusion pressure of the isolated heart was maintained and measured during washing of the coronary blood with Krebs-Henseleit buffer (KH buffer) followed by washing out the KH buffer by MBS buffer (NaCL + MES buffer). The heart

beating was stopped when the calcium was completely washed out after perfusion of MBS buffer. Rate of perfusion was adjusted to keep coronary perfusion pressure constant during the labelling of negatively charged endothelial cell membrane by cationic colloidal silica beads and fixing of endothelial cell membrane by using HEPES/sucrose. (For details please refer method section)

The post fixed and embedded silica coated heart tissue was sectioned (~1 mm), stained in uranyl acetate and lead citrate and micro graphed by transmission electron microscopy (TEM, HITACHI-H600). As shown in figure 12 the coronary endothelial membranes of capillaries, venules and larger conduit arteries were uniformly and selectively labelled with silica beads (20 nm).

3.1.2. Endothelial cell membrane analysis by western blot:

To enrich silica coated endothelial cell membranes, two different methods were systematically evaluated for tissue homogenisation: teflon pestle and ultra blade at two different speed settings followed by nycodenz gradient centrifugation to separate silica coated EC membrane. The recovery of proteins attached to silica beads was generally very low. One isolated perfused mouse heart yielded only about 1 µg protein. Data on western blot analysis are summarized in figure 13. As can be seen, there is a significant enrichment of endothelial membranes with both methods as judged by the endothelial cell marker protein Caveolin 1.

Other mouse specific antibodies were also tested for membrane specific marker proteins, such as eNOS 20/30, VE-cadherin, E-selectin, ICAM-1, VCAM-1, and PECAM-1. However, we were unable to detect any of these markers by western blot, which is most likely due to the low amount of membrane protein available from each heart together with low micro vascular expression. From the western blot results, it is also obvious that the higher speed setting in case of both teflon pestle and ultra blade, resulted in significant enrichment of silica coated EC membrane together with contamination as judged by the appearance of cytochrome C, myoglobin as well as beta-COP, which are markers for mitochondria, myocytes and golgi respectively.

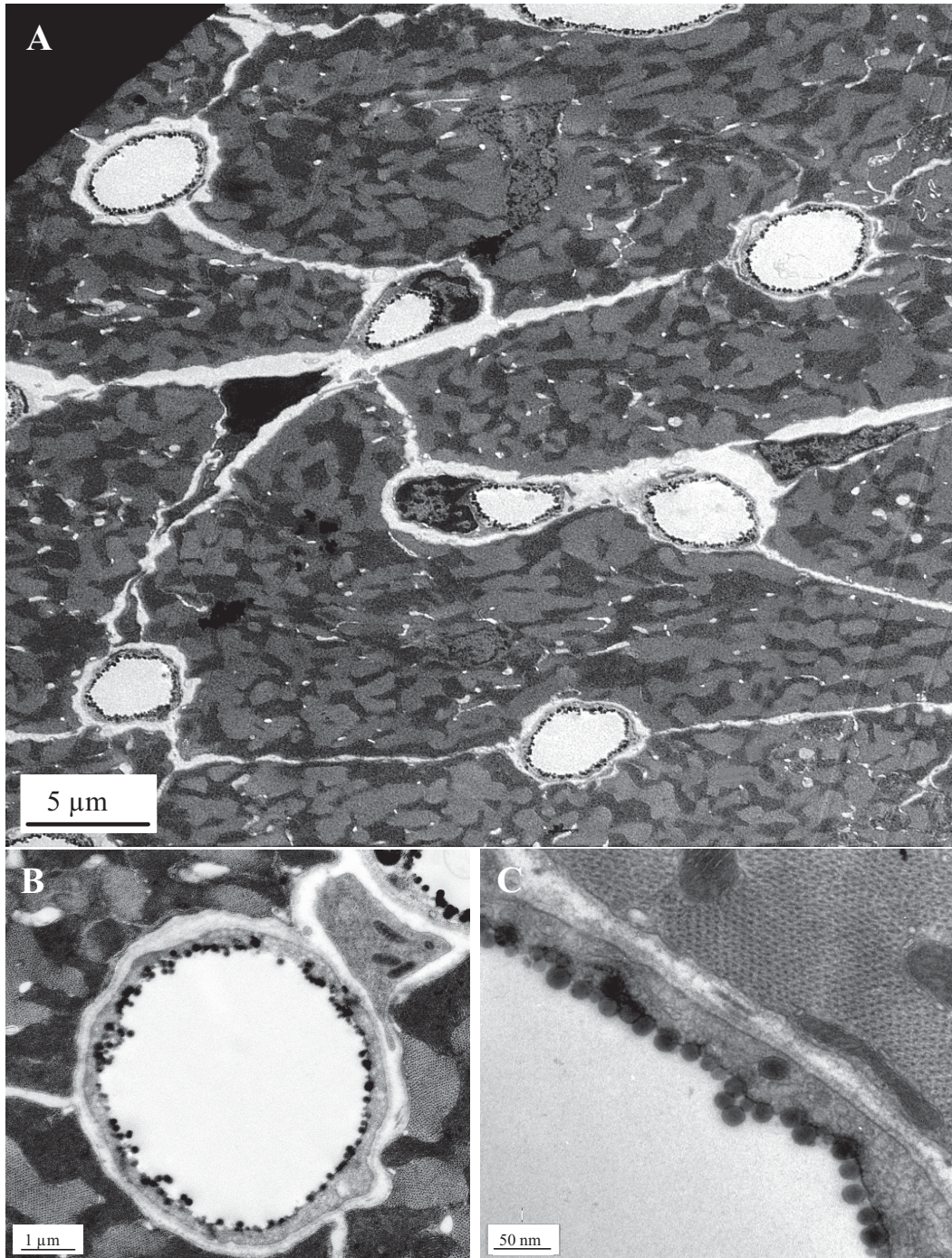


Fig 12: Transmission electron micrograph of a mouse heart perfused with silica beads:
A: Overview showing the silica beads coated microvasculature. B and C: Specificity of the labelling procedure at the level of an individual capillary at different magnifications.

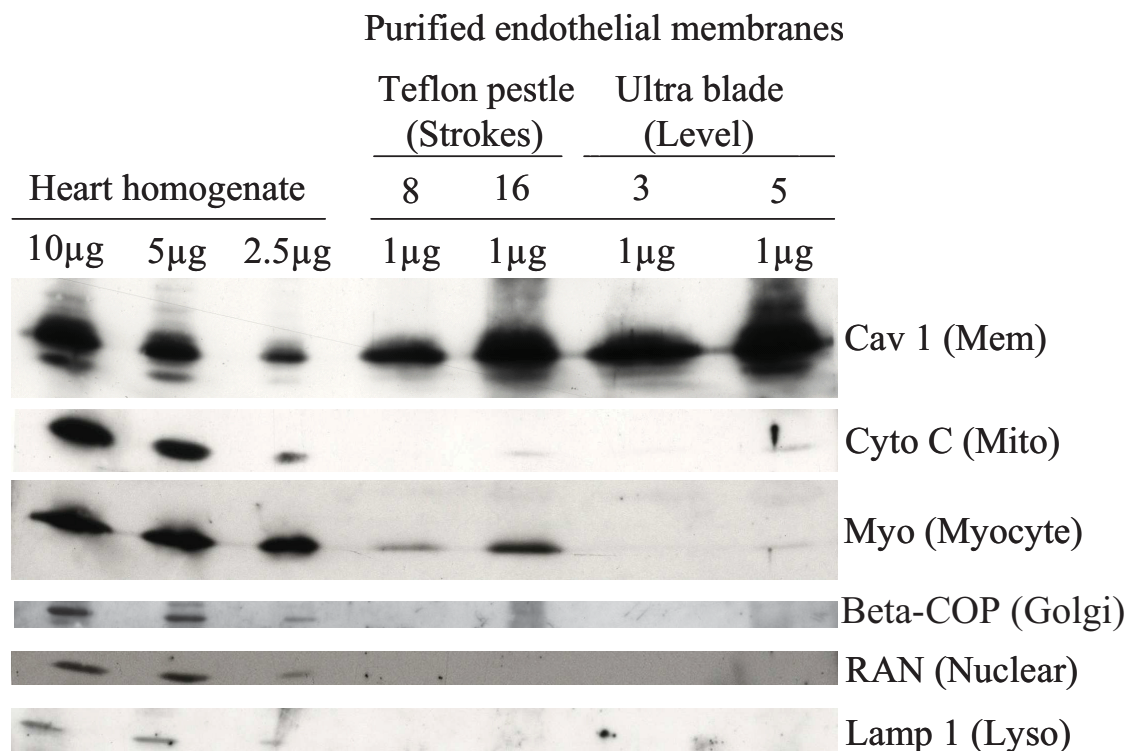


Fig 13: Influence of the homogenization procedure (Teflon pestle vs Ultra blade) on the purity of silica beads enriched EC membrane Proteins: Separated silica coated EC membrane protein enrichment and purity as analyzed by western blot showed that both methods lead to enrichment of membrane protein Caveolin 1 (Cav 1). The degree of contamination with intracellular markers were higher with the Teflon pestle method. (Mitochondria: Cytochrome C (Cyto C); Myocyte: Myoglobin (Myo); Golgi: Beta-COP; Nuclear: Ran; Lysosome: lysosomal-associated membrane protein 1(LAMP1) respectively).

Even at the lower speed setting using the teflon pestle method, a significant contamination with myoglobin was observed. Since the ultra blade method at the lower speed persistently resulted in endothelial membrane enrichment with apparently negligible contamination of other cell compartments (Figure 13), this method (Level 3 at 14,000 rpm for 1 min) was used for purification of silica coated EC membrane and further EC membrane protein analysis was done by mass spectrometry.

3.1.3. Protein identification by LC-MS:

To obtain reliable results by mass spectrometry, pooling of 10 individually colloidal silica perfused and labelled mouse hearts were required, which finally amounted to about 10 µg proteins were obtained by ultra blade method at the lower speed (Level 3 at 14,000 rpm for 1 min) for MS analysis. Then the silica beads were removed from derivatized EC membrane by sonicating and followed by heating of the suspension with 2% SDS. Silica was separated from solubilised proteins by centrifugation at 14,000 x g for 15 minutes. Once again these 10 µg of membrane pellet was washed with ddH₂O and sedimented by ultra centrifugation. Proteolysis was performed overnight at 37° C with trypsin and chymotrypsin in 60% methanol. After cleavage, the peptide mixture was centrifuged, dried and dissolved for mass spectrometric analysis. Peptides mixtures were separated by C₁₈ reversed phase (hydrophobic interaction) chromatography on self made fused silica micro capillary columns.

After equilibrating the micro capillary column with sample buffer, the sample was directly loaded to the column using the helium pressure cell. Peptides were directly eluted into the mass spectrometer with a linear gradient. The SEQUEST algorithm was used for MS/MS data interpretation and the molecular weights and functions of each protein were identified by using the ExPasy web server and the Bioinformatic Marvester (Mouse Harvester) database. The known or predicted transmembrane-spanning alpha helices were determined through the literature or by using the web-based prediction program TMHMM v2.0. As a result, we identified 71 proteins (Table 9) which were obtained in two independent experiments.

Table 9: List of proteins identified from mouse heart endothelial cell membranes

Membrane associated proteins

Protein name	NCBI locus	Nr. of MS/MS spectra	Function	Nr. of TMs*
Adaptor protein complex AP1, gamma 1 subunit	38569409	2	Transport	-
Ancient ubiquitous protein	90403601	1	Others	1
Apolipoprotein-A 1	6753096	3	Others	-
Cadherin 13	9789905	2	Adhesion	-
EBV-induced G protein coupled-receptor 2 variant	62898341	1	Receptor	7
EH-domain containing protein MPAST 2	31981592	3	Others	-
Fimbrial protein precursor	305373	1	Others	-
Glucose receptor protein git3	26394133	1	Receptor	7

GPI-anchored protein P 137	2498734	2	Transport	-
Hypothetical protein LOC 67851	13385904	1	Transport	-
Integrin linked kinase	6754342	4	Signaling	-
Integrin alpha 2b	6754376	2	Adhesion	1
Laminin gamma 1	31791057	1	Others	-
Membrane associated salt inducible-like protein	7268804	1	Others	-
Na ⁺ /K ⁺ -ATPase alpha 1 subunit	21450277	1	Transport	10
NhaP-type Na ⁺ /H ⁺ -and K ⁺ /H ⁺ -antiporters	19484208	1	Transport	12
Nidogen 1	6754854	1	Adhesion	-
Pappalysin 2	51705309	2	Others	-
Peripheral membrane protein B	325194	3	Others	-
Proto cadherin	18087761	1	Adhesion	1
Putative olfactory receptor 494	22129367	3	Receptor	7
Putative protein transport protein	86355992	1	Transport	3
Q7WER6 outer membrane porin protein	33577664	1	Transport	-
Rap guanine nucleotide exchange factor (GEF) 1	16905083	2	Adhesion	-
Ras-related protein rab	26986192	1	Trafficking	-
Serum deprivation response	20270267	2	Signaling	-
Glycosyl hydrolase	51246733	1	Others	-
Tra K lipoprotein precursor	9507814	1	Transport	1
Transglutaminase 1	31982705	1	Others	-
Villin-2	83921618	3	Others	-
Vitellogenin 2	213312	2	Transport	-

Cytoskeletal and/or junction proteins

Aldolase 1	6671539	2	Others	-
AMP deaminase 3	6753048	1	Others	-
Citrate synthase	47523618	1	Others	-
Glutathione-S-transferase GST 2	546199	1	Others	-
Glutamate-cysteine ligase modifier subunit	22653729	1	Others	-
Glyceraldehyde-3-phosphate dehydrogenase (GAPDH)	120702	5	Others	-
Hypothetical protein 44.2 kDa GTP binding	50548785	1	Others	-
Malignant T cell amplified sequence	13384966	1	Others	-
Meosin	6754750	1	Structural	-
Microtubules-associated protein, RB/EB family (2)	31543239	2	Structural	-
Myosin	18859641	19	Structural	-
Peptidyl prolyl isomerase B	410119	2	Others	-
Similar to (segment 1 of 2) neuroblast differentiation associated	55636237	1	Others	-
Succinate-CoA ligase, GDP forming, alpha subunit	9845299	2	Others	-

Mitochondrial proteins

2,4- dienoyl CoA reductase 1	13385680	2	Others	-
AarF domain containing kinase 2	30725855	3	Others	-
Acetyl-coenzyme A acetyltransferase 2	29126205	1	Others	-
ATP synthase, H ⁺ transporting	55638543	3	Receptor	-
Carnitine acetyltransferase	6681009	1	Transport	-
Cytochrome C	6681095	5	Transport	-
Enoyl coenzyme A hydratase	29789289	5	Others	-
Hydroxyacyl-coenzyme-A dehydrogenase/ 3-ketoacyl-coenzyme A thiolase	33859811	5	Others	-
Isocitrate dehydrogenase 3 beta subunit	18700024	2	Others	-

Nuclear proteins

Aristaless 4	6671541	2	Others	-
Eukaryotic translation elongation factor 1 alpha	51829715	3	Others	-
Exonuclease 5	9627460	1	Others	-
High mobility group protein	6754208	1	Others	-
Histones 1, 3	13386452	3	Others	-
Polymerase 1 and transcript release factor	6679567	1	Others	-
SPEN homolog, transcriptional regulator	9790035	5	Others	-
TAF4B RNA polymerase 2, TBP	5032153	1	Others	-
Thymopoietin	6755817	1	Others	-

Others

Albumin 1	33859506	5	Others	-
Conserved hypothetical protein	46361171	1	Others	1
Hypothetical protein ORF314	12515585	1	Others	-
Hypothetical protein DDB0204485	66816357	1	Others	-
Hypothetical protein CHGG- 00688	28829350	1	Others	-
LAMP1	29145014	1	Others	1
Precorrin isomerase	18144888	1	Others	-
Putative secreted antigen	38234735	3	Others	1

*Nr. of TMs: Number of transmembrane-spanning alpha helices.

Among 71 proteins, 31 were membrane proteins such as cadherin, glucose transporter, integrin linked kinase, Na⁺/K⁺-ATPase and Na⁺/H⁺-antiporter. However, also 14 cytoskeletal or junction proteins, 9 mitochondrial proteins and 9 nuclear proteins were identified (Table 9) suggesting significant contamination. These results so far revealed that the purity and yield of the silica coated endothelial membranes were unsatisfactory. Due to this reason the silica beads method does not allow the differential analysis between WT and KO mice such as CD73 knockouts.

3.2. Culturing of endothelial cells from various tissue in the mouse

It was the aim of this experimental series to culture endothelial cells from various organs to see whether it is possible to use a differential proteomic approach between WT and CD73 knockout under *in vitro* condition. To this end the isolation procedure for endothelial cells was optimized using magnetic beads coated with cleavable CD31 and CD102 antibody. In order to obtain sufficient amount of sample (1-2 mg detergent soluble protein/10 million cells), isolated endothelial cells were passaged several times to increase the cell number which is required for MS analysis.

3.2.1. Mouse aortic endothelial cell

Mouse aortic endothelial cells were isolated and purified using cleavable CD-31 dynal beads. In order to achieve sufficient cell number in culture, 8 aortas were prepared from individual animals followed by collagenase enzymatic digestion. Separated total aortic cells were cultured on 1% gelatine coated plate at 37° C in a humidified 5% CO₂ atmosphere with a micro vascular endothelial cell culture medium.

When isolated endothelial cells from the aorta (MAECs) were confluent, cells were applied for positive selection using cleavable CD-31 (PECAM-1) dynal beads which is specific for the positive selection of MAECs. Positively selected MAECs (~56000 cells/ 8 aorta) were counted and further cultured on 1% gelatine coated plate (one 12 well plate). The purity of magnetically separated endothelial cells were analysed by FACS using the endothelial specific marker proteins such as CD31 (PECAM-1), CD102 (ICAM-2) and CD73 (Ecto 5' Nucleotidase) (for details see method section).

Five independent experiments were performed. Mouse aortic endothelial cell number and the degree of purity (FACS analysis) are summarised below in the table 10. Results of FACS analysis for experiment 1 and 2 showed an initial purity above 70%, as judged by the endothelial cell specific marker CD31 (PECAM-1).

The cultured MAECs were trypsinized and the cell number was counted (0.12×10^6) among these counted cells only 20,000 cell were used for FACS analysis, which resulted in 70% of CD31 positive (PECAM-1) (Figure 14) and rest of the MAECs were splitted in a ratio of 1:3 in order to increase the cell number. Cells were cultured to confluence.

During the second splitting 20,000 cells of cultured MAECs (0.24×10^6) were applied for FACS analysis which resulted in 70% of CD31 positive (PECAM-1) and 71% of CD102 positive (ICAM-2) (Figure 15) and rest of the MAECs were splitted into 1:3 ratio for increasing the cell number and cultured until the cells became confluent. During the third splitting of cultured cells (0.436×10^6), only 20,000 cells were applied for FACS analysis which resulted in 73% of CD31 positive (PECAM-1), 79% of CD102 positive (ICAM-2) and 80% of CD73 positive (Ecto 5'-nucleotidase) (Figure 16). These FACS results from the first experiment (Figure 14 - Figure 16) so far revealed that mouse aortic endothelial cell purity remained constant. The cell number was only doubled and the cells in general grew very slowly.

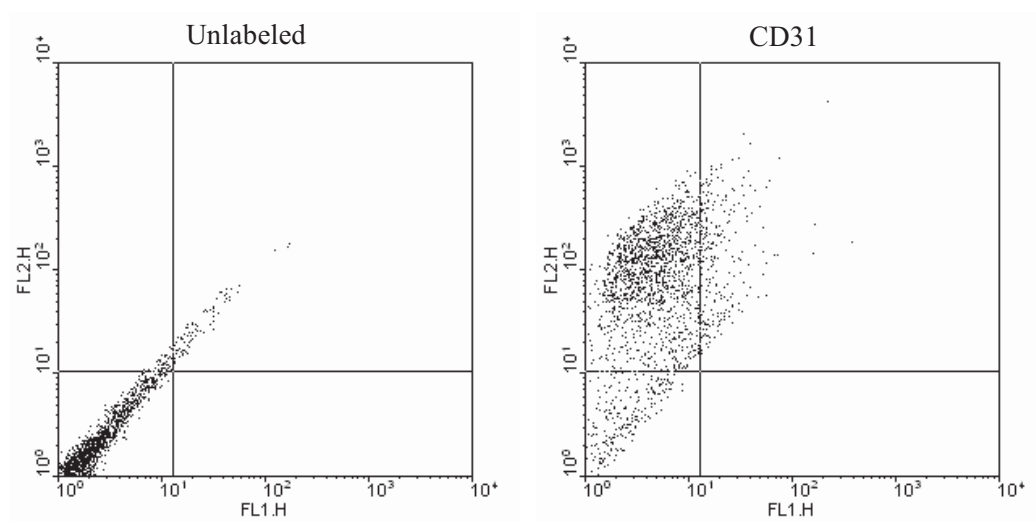


Fig 14: In experiment 1 - 1st Purity analysis of mouse aortic endothelial cells (MAECs): During first splitting the MAECs purity was assessed by FACS analysis by using endothelial cell specific marker protein PE-labeled CD31 (70%) (PECAM-1).

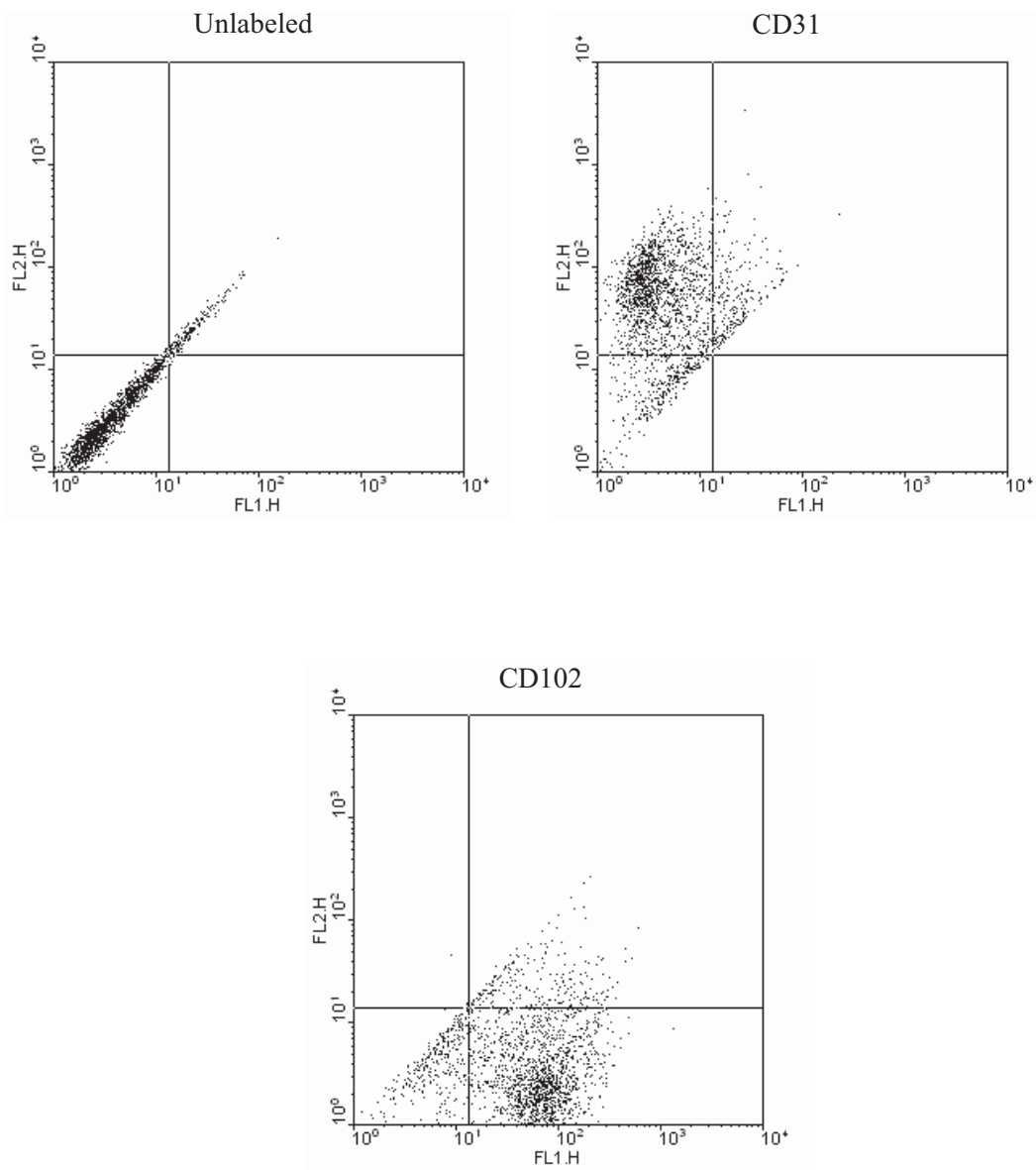


Fig 15: In experiment 1- 2nd Purity analysis of mouse aortic endothelial cells (MAECs):
 During second splitting the MAECs purity was assessed by FACS analysis by using endothelial cell specific marker protein PE-labeled CD31 (70%) (PECAM-1) and FITC-labeled CD102 (71%) (ICAM-2).

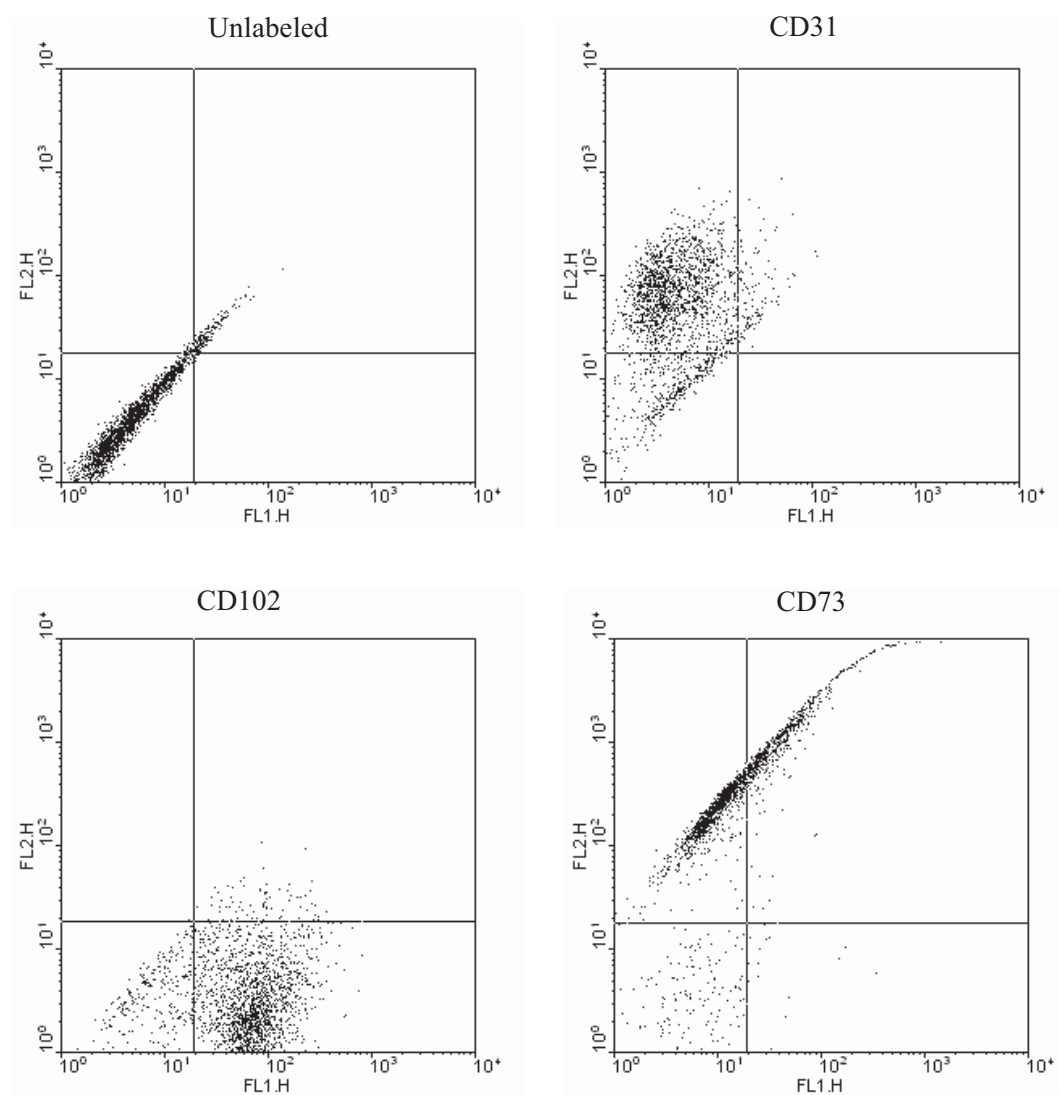


Fig 16: In experiment 1- 3rd Purity analysis of mouse aortic endothelial cells (MAECs): During third splitting the MAECs purity was assessed by FACS analysis by using endothelial cell specific marker protein PE-labeled CD31 (73%) (PECAM-1), FITC-labeled CD102 (79%) (ICAM-2) and PE-labeled CD73 (80%) (ecto 5'-nucleotidase).

In experiment -2, (Figure 17- Figure 19) cultured MAECs were trypsinized and the cell number was counted (0.35×10^6) and only 20,000 cell were used for FACS analysis, which resulted in 71% of CD31 positive (PECAM-1) (Figure 17) and rest of the MAECs were splitted into 1:3 ratio for increasing the cell number.

During the second splitting 20,000 cells were from cultured MAECs (0.69×10^6) were applied for FACS analysis which, resulted in 32% of CD31 positive (PECAM-1) and 45% of CD102 positive (ICAM-2) (Figure 18) and rest of the MAECs were splitted into 1:3 ratio for increasing the cell number and cultured until the cells were become confluent. During the third splitting of those cultured cells (10.5×10^6), 20,000 cells were applied for FACS analysis, which resulted in 18% of CD31 positive (PECAM-1), and 18% of CD102 positive (ICAM-2) (Figure 19).

These results so far revealed that the purity of MAECs from the second set of experiment was unsatisfactory. Cell number more than doubled within 4-5 days (Figure 17 - Figure 19). Cells which more than doubled within 4-5 days showed a strong loss of purity over the time of growth (Figure 18 & Figure 19) due to dedifferentiation or overgrowth by non endothelial cells like SMC and fibroblasts.

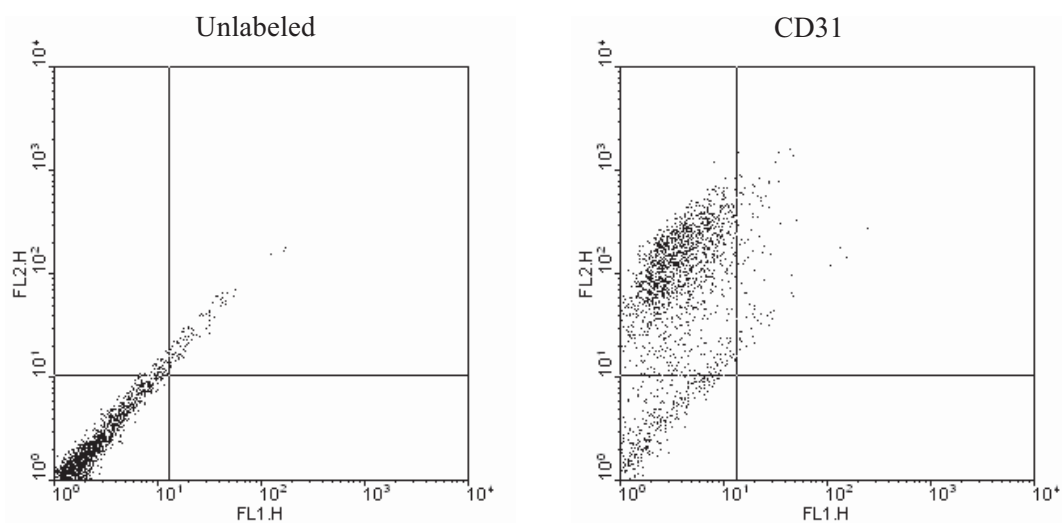


Fig 17: In experiment 2- 1st Purity analysis of mouse aortic endothelial cells (MAECs): During first splitting the MAECs purity was assessed by FACS analysis by using endothelial cell specific marker protein PE-labeled CD31 (71%) (PECAM-1).

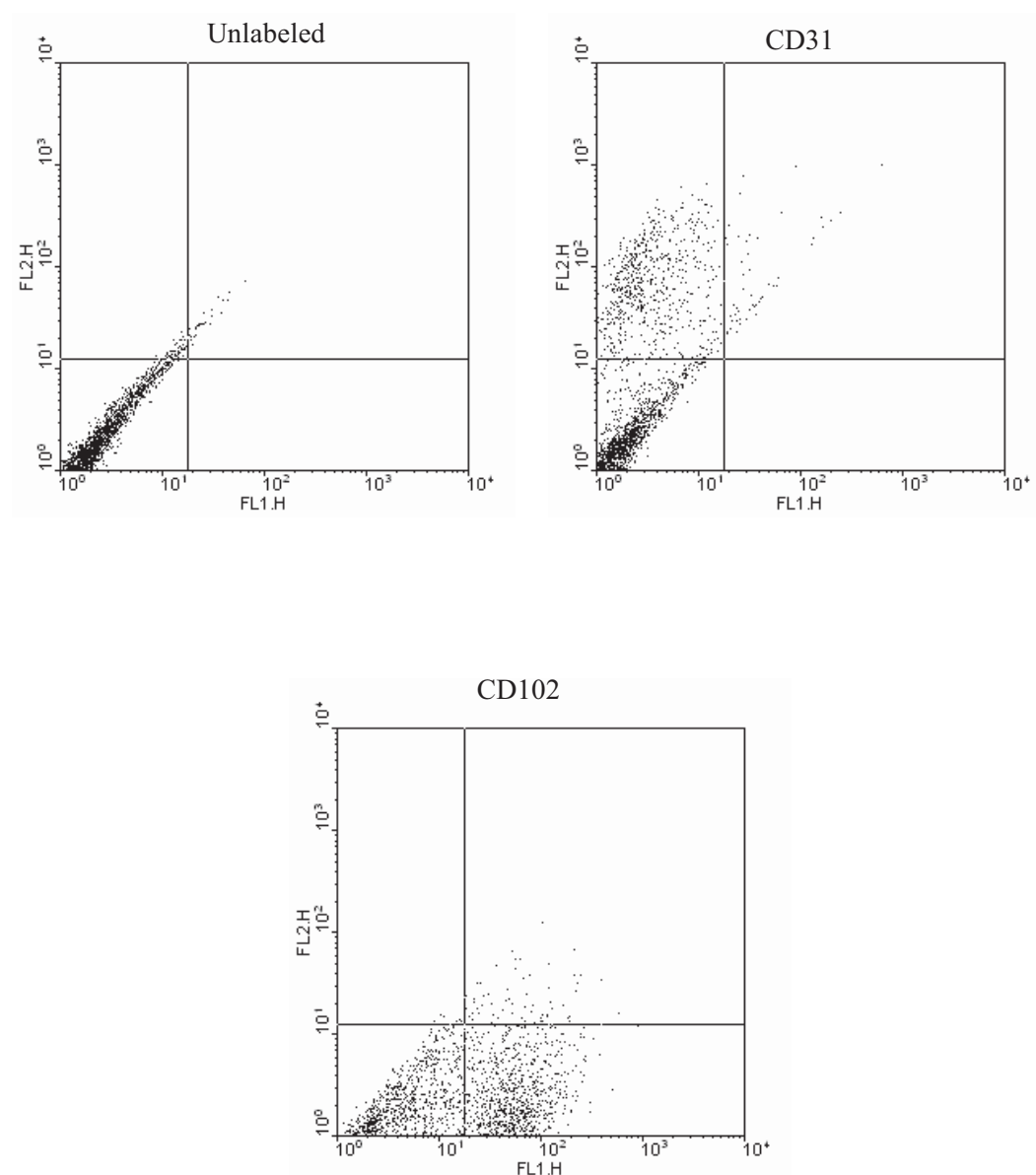


Fig 18: In experiment 2- 2nd Purity analysis of mouse aortic endothelial cells:

During second splitting the MAECs purity was assessed by FACS analysis by using endothelial cell specific marker protein PE-labeled CD31 (32%) (PECAM-1) and FITC-labeled CD102 (45%) (ICAM-2).

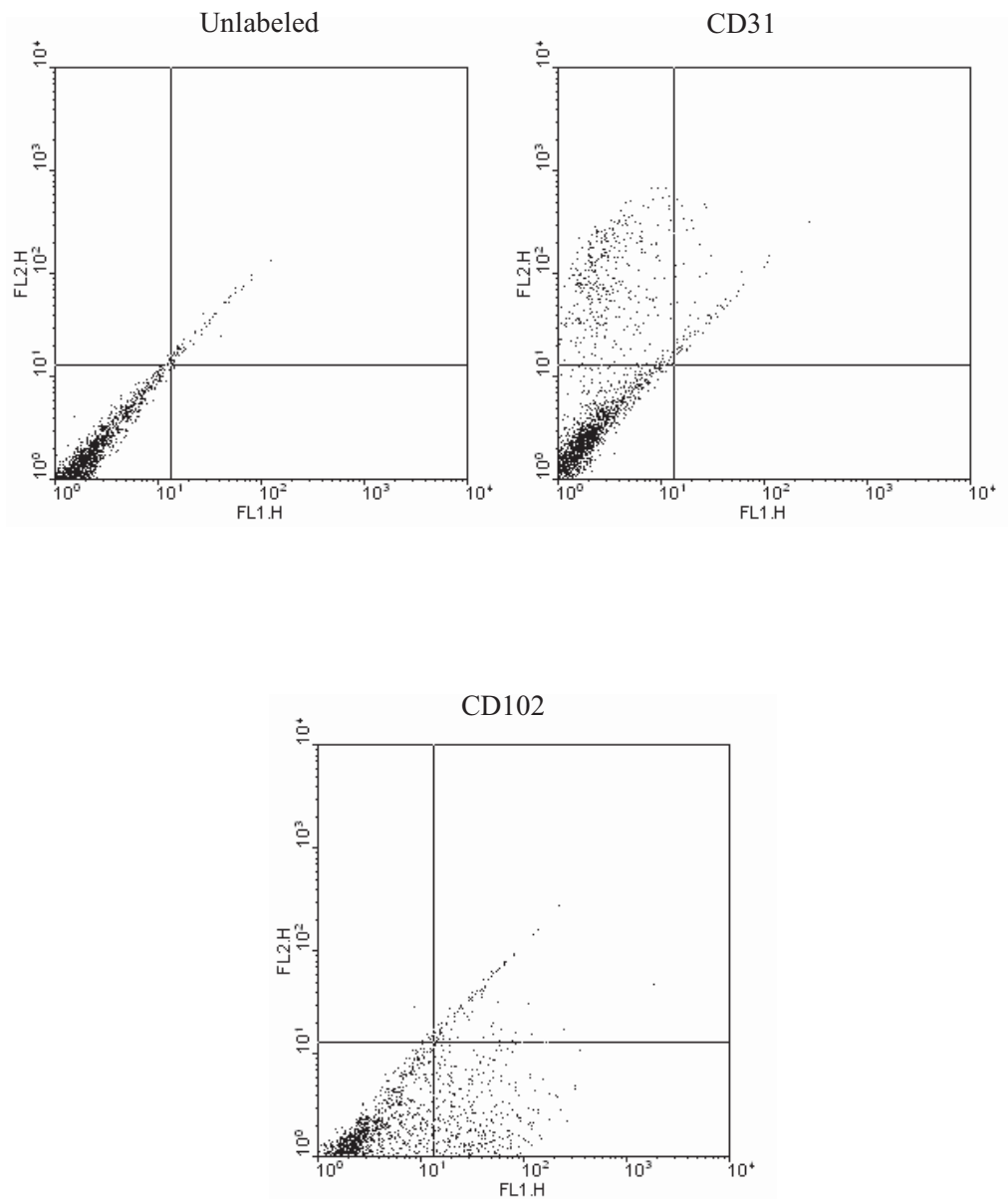


Fig 19: In experiment 2- 3rd Purity analysis of mouse aortic endothelial cells:

During third splitting the MAECs purity was assessed by FACS analysis by using endothelial cell specific marker protein PE-labeled CD31 (18%) (PECAM-1), FITC-labeled CD102 (18%) (ICAM-2).

Table 10: Mouse aortic endothelial cell purity analysis after magnetic bead separation

Experiments	Mouse Aortic Endothelial Cells (MAECs)	CD31 (PECAM-1)	CD102 (ICAM-2)	CD73 (Ecto 5'-nucleotidase)
Experiment 1	Initial cell number: 0.056 x 10 ⁶ / 8 aorta			
1 st purity analysis	Total cell number: 0.12 x 10 ⁶	70%		
2 nd purity analysis	Total cell number: 0.24 x 10 ⁶	70%	71%	
3 rd purity analysis	Total cell number: 0.436 x 10 ⁶	73%	79%	80%
Experiment 2	Initial cell number: 0.12 x 10 ⁶ / 16 aorta			
1 st purity analysis	Total cell number: 0.35 x 10 ⁶	71%		
2 nd purity analysis	Total cell number: 0.69 x 10 ⁶	32%	45%	
3 rd purity analysis	Total cell number: 10.5 x 10 ⁶	18%	18%	
Experiment 3	Initial cell number: 0.09 x 10 ⁶ / 8 aorta			
1 st purity analysis	Total cell number: 0.45 x 10 ⁶	20%	20%	
Experiment 4	Initial cell number: 0.06 x 10 ⁶ / 8 aorta			
1 st purity analysis	Total cell number: 0.16 x 10 ⁶	23%	25%	
Experiment 5	Initial cell number: 0.062 x 10 ⁶ / 8 aorta			
1 st purity analysis	Total cell number: 0.21 x 10 ⁶	23%	27%	

From the data summarized in table 10 it is evident that, it was not possible to maintain a sufficiently high purity while increasing cell number by additional passages. In most of the experiments the initial purity averaged only between 20-23%. Due to this reason this isolation procedure was not further pursued, because differential proteomic analysis required higher cell purity.

3.2.2. Mouse lung endothelial cell

Mouse lung endothelial cells were isolated and purified by the same magnetic beads method as used before [cleavable CD102-dynal beads (ICAM-2)]. In order to achieve sufficient cell number in culture, lung samples were prepared from two animals and lung cells were separated by collagenase enzymatic digestion. Combined lung cells were cultured on 1% gelatine coated plate at 37° C in a humidified 5% CO₂ atmosphere with 50% DMEM with 50% F12 medium according to Kuhlencordt et al., (Kuhlencordt et al. C1195-C1202).

When isolated total lung cells were confluent in the culture, positive selection for mouse lung endothelial cells (MLECs) was performed using cleavable CD102-dynal beads (ICAM-2). Positively selected MLECs were counted and cultured on 1% gelatine coated plates. Cells exhibited “cobblestone” morphology typical for endothelial cells (Figure 22).

The purity of endothelial cells was analysed by FACS using endothelial specific marker proteins like CD31 (PECAM-1), CD102 (ICAM-2) and CD73 (Ecto 5' Nucleotidase). (Figure 20- Figure 21). Two independent experiments were performed and the results are summarized in table 11.

Table 11: MLECs purity analysis after first and second magnetic bead sorting

	CD31 (PECAM-1)	CD102 (ICAM-2)	CD73 (Ecto 5'-nucleotidase)
Experiment 1			
After first magnetic bead sorting	76%	62%	17%
After second magnetic bead sorting	84%	93%	3%
Experiment 2			
After first magnetic bead sorting	91%	88%	16%
After second magnetic bead sorting	98%	99%	1%

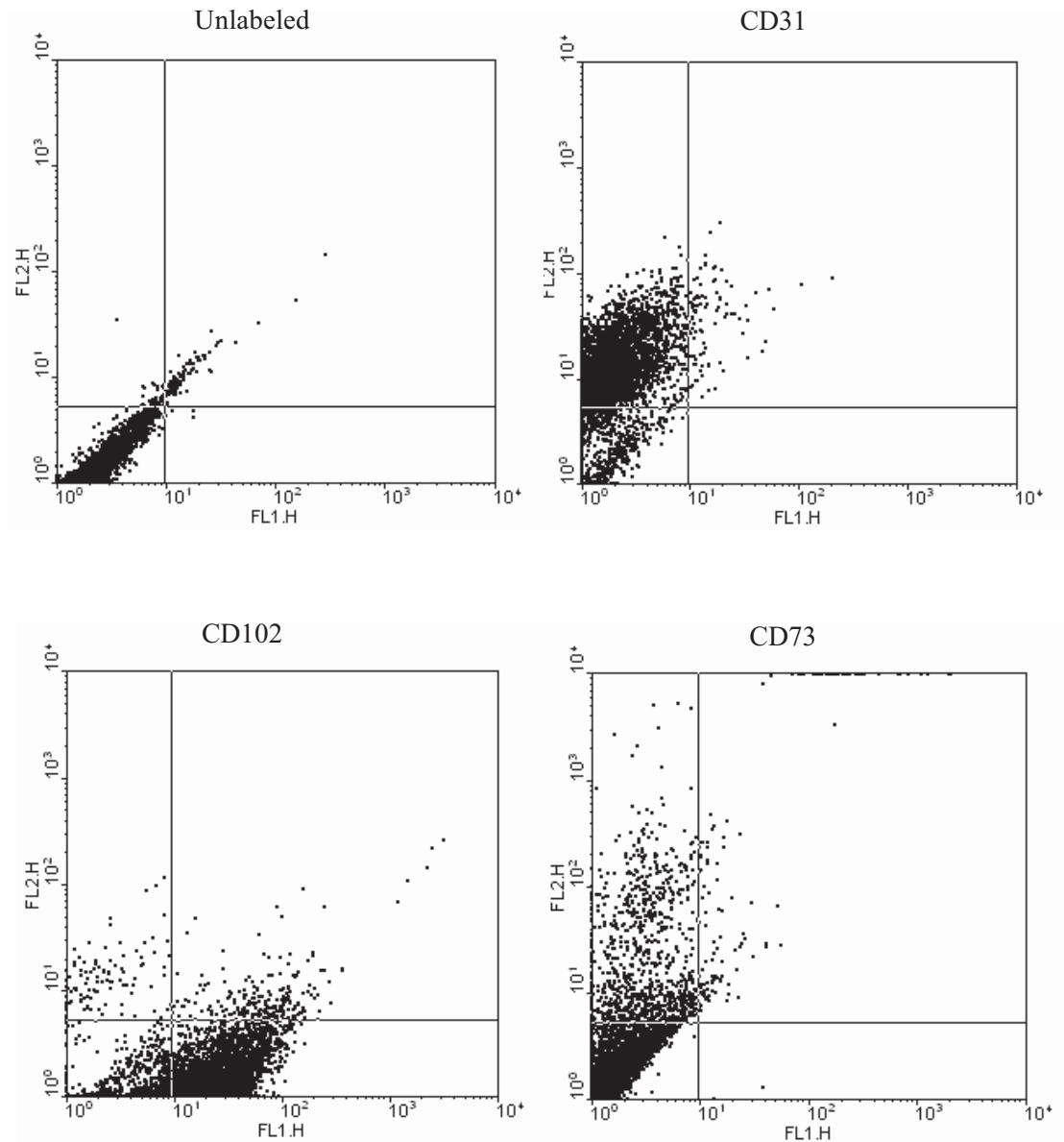


Fig 20: Experiment 1 - Purity analysis of mouse lung endothelial cells (MLECs) after first positive selection with CD102-dynal beads: Purity of mouse lung endothelial cells (after first magnetic bead sorting) was analyzed by FACS analysis using endothelial cell specific marker proteins such as PE-labeled CD31 (76%) (PECAM-1), FITC-labeled CD102 (62%) (ICAM-2) and PE-labeled CD 73(17%)(Ecto 5' nucleotidase).

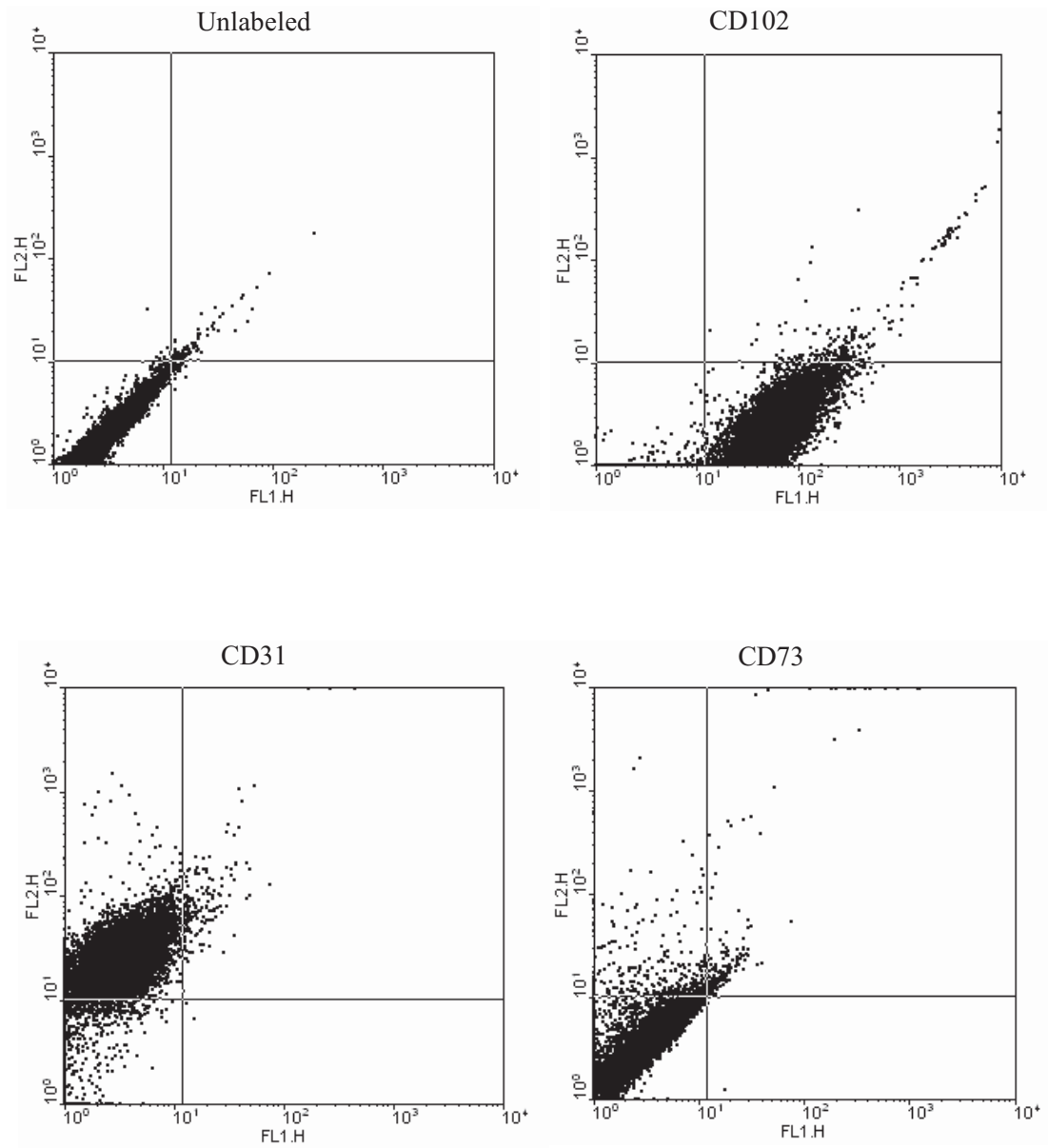


Fig 21: Experiment 1 - Purity analysis of mouse lung endothelial cells (MLECs) after second positive selection with CD102-dynal beads: Purity of mouse lung endothelial cells (after second magnetic bead sorting) was analyzed by FACS analysis using endothelial cell specific marker proteins such as PE-labeled CD31 (76%) (PECAM-1), FITC-labeled CD102 (62%) (ICAM-2) and PE-labeled CD 73(17%) (Ecto 5' nucleotidase).

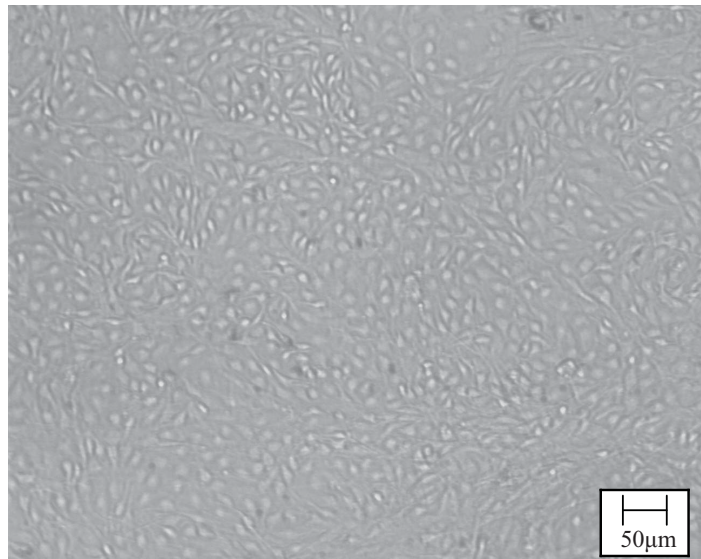


Fig 22: Mouse lung endothelial cells (MLECs): Cells which exhibited “cobblestone” morphology showed higher purity.

Experiment 1 and experiment 2 showed a similar percentage of purity when analysed with the endothelial cell specific markers CD31 (PECAM-1), CD102 (ICAM-2) and CD73 (Ecto 5' nucleotidase). In experiment 1, after purification with CD102-dynal beads, MLECs were cultured until cells became confluent (4-5 days). Confluent MLECs were then trypsinised and applied for FACS analysis. 40,000 cells revealed 76% of CD31 positive (PECAM-1), 62% of CD102 positive (ICAM-2) and 17% of CD73 positive (Ecto 5' nucleotidase) (Figure 20). Purified cells were splitted in a 1:3 ratio for further culture to expand MLECs. For the second sorting, once again CD102-dynal beads were applied to confluent MLECs. After the second expansion the FACS analysis of 40,000 cells revealed 84% of CD31 positive (PECAM-1), 93% of CD102 positive (ICAM-2) and 1% of CD73 positive (Ecto 5' nucleotidase) (Figure 21).

Isolated MLECs were doubled within 4-5 days and the cells maintained a constant purity as judged by CD31 and CD102 expression (Table 11). These results demonstrate that endothelial cell enrichment can be achieved from the total mouse lung. However the expression of CD73 was already low after the first magnetic bead sorting and further decreased to 1-3% after the second sorting.

3.2.3. Expression of CD73 (Ecto 5' nucleotidase) in mouse kidney and spleen by immunohistochemistry (IHC)

In order to further explore the distribution of CD73, immunohistochemistry (IHC) of this enzyme was performed in mouse kidney and spleen. In order to assay the expression of CD73, thin tissue sections were from the different organs (for details see method section) were treated with the IHC using mouse endothelial cell specific marker proteins CD73 and vWF. [Monoclonal rat CD73–rhodamine (Red-fluorescent) labelled and polyclonal rabbit vWF-FITC (Green fluorescent) labelled antibody].

Mouse kidney tissue sections (Figure 23) stained with the endothelial specific marker protein CD73 and vWF showed a high activity of CD73 (Ecto 5' nucleotidase) within the glomerulus (Mesangium) (Figure 23B & D) and tubular luminal membranes. Additionally, there was expression of vWF on the endothelium of the capillaries (Figure 23C & D), whereas CD73 expression on capillary endothelial cells was negative.

Figure 24 shows that typical morphology of the spleen consisting of red pulp, white pulp, splenic cords, splenic sinuses and central arteriole. In order to assay the CD73 expression in the spleen, tissue sections were stained with rhodamine conjugated-CD73 (Red-fluorescent) and FITC labeled vWF (Green fluorescent). Figure 25A and B, show that there is a strong expression of both markers preferentially in the red pulp. As shown in the figure 25C, high activity of CD73 (Ecto 5' nucleotidase) are associated with individual cells of the red pulp.

These histochemical data revealed that in mesangial cells of the kidney there is a high expression of CD73. Similarly, high expression of CD73 was found to be associated with cells of the red pulp which are most likely T reg cells since CD73 has recently been reported to be a specific marker for T reg cells (Kobie et al. 6780-86). Since T reg cells can be conveniently be isolated from the spleen with commercially available purification kits. I have concentrated on this cell type for further quantitative and differential proteomic analysis.

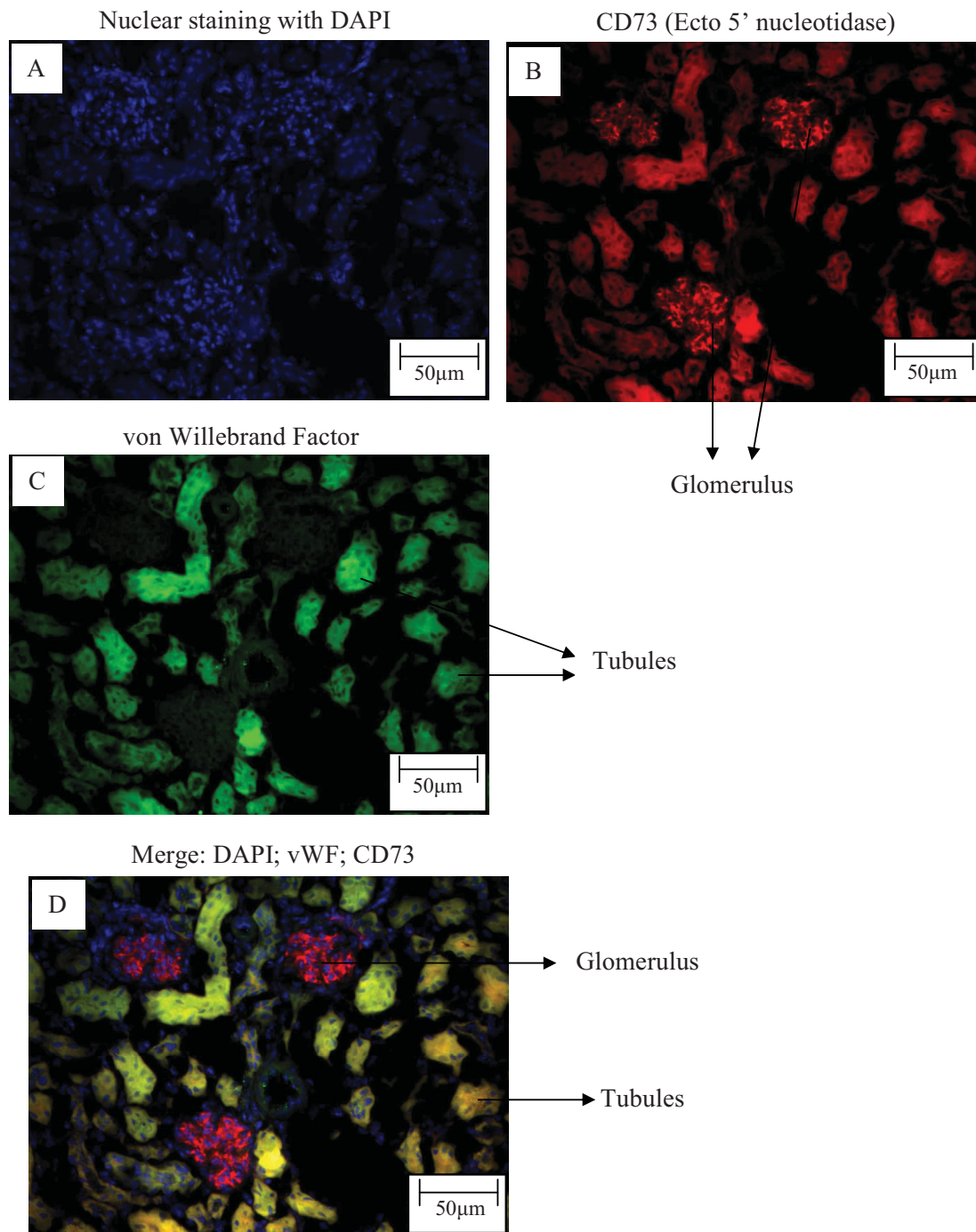


Fig 23: Expression of CD73 in mouse kidney by immunohistochemistry (IHC): Mouse kidney tissue sections were stained with DAPI, monoclonal rat CD73–rhodamine (Red-fluorescent) labelled and polyclonal rabbit vWF- FITC (Green fluorescent) labelled antibody.

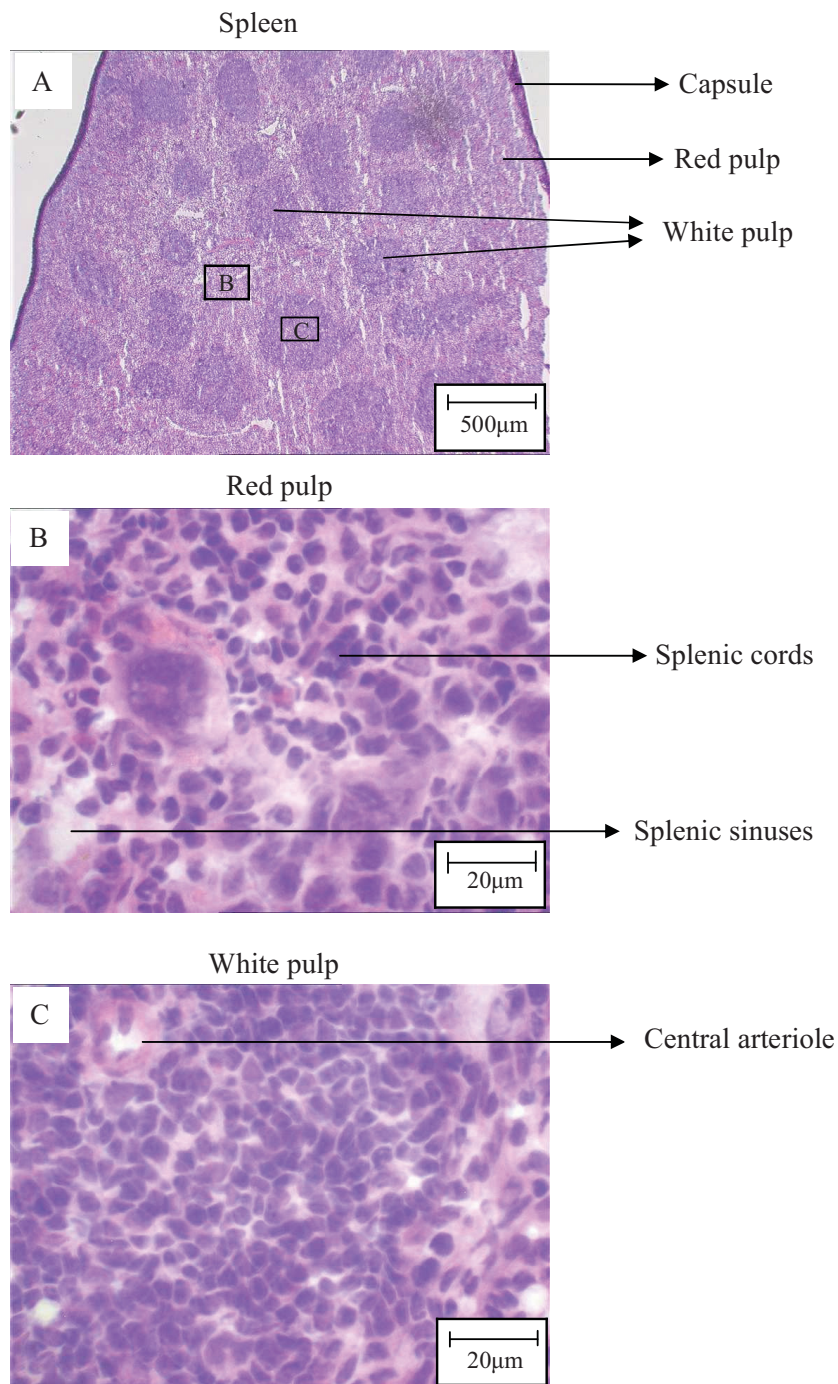


Fig 24: Sections from mouse spleen were stained with Hemalaun-eosin: The typical morphology of the spleen can be seen which consist of red and white pulp.

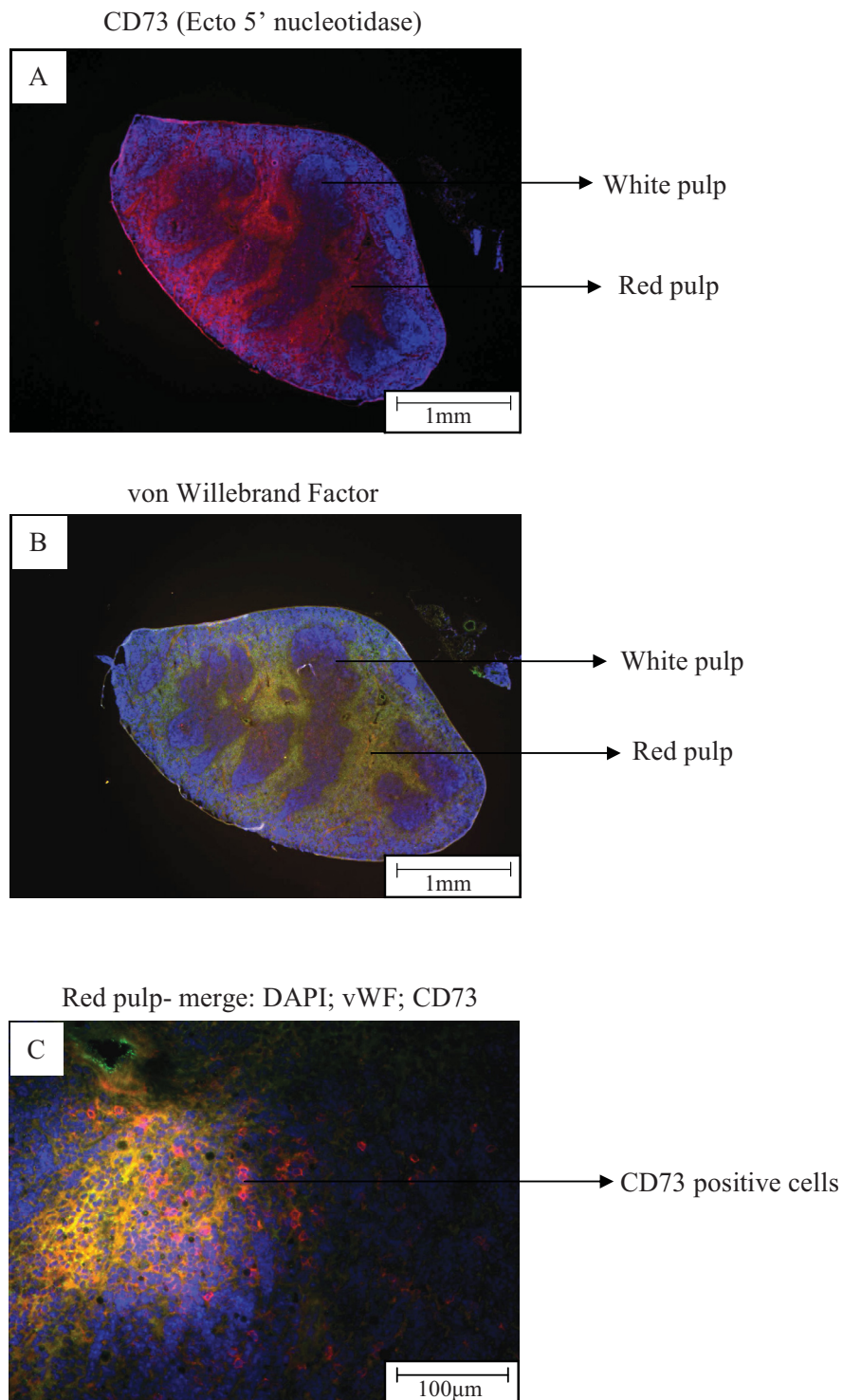


Fig 25: Expression of CD73 in mouse spleen by immunohistochemistry (IHC): Mouse spleen sections were stained with a Monoclonal rat CD73–rhodamine (Red-fluorescent) labelled and vWF (Polyclonal rabbit vWF- FITC (Green fluorescent) labelled antibody.

3.3. Proteomic study on regulatory T cells

3.3.1. Analysis of CD73 expression on isolated regulatory T cell by FACS analysis:

Regulatory T cells (T reg cells) were isolated from mouse spleen by using CD4⁺CD25⁺ regulatory T cells isolation kit (Milteny Biotech Inc). In order to isolate the T reg cells, the first step was the depletion of non-CD4⁺ T cells and enrichment of the CD4⁺ T cells. The purity of CD4⁺ T cells (78%) (Figure 26B) was achieved after excluding non CD4⁺ T cells by using biotin-conjugated monoclonal anti mouse antibodies against CD8a, CD11b, CD45R, CD49b and Ter-119. The positive selection of CD4⁺CD25⁺ T cells from the isolated CD4⁺ T cells by using monoclonal anti mouse CD25⁺ antibody conjugated to R-Phycoerythrin (PE), resulted in 80% of CD4⁺CD25⁺ T cells (Figure 26C) (for details see method section).

T-reg cells purity was analysed by FACS analysis using T-reg cell marker proteins FOXP3, CD73 (Ecto 5' Nucleotidase). Isolated T-reg cells were further applied for double staining with mouse specific antibodies for T-reg cells specific marker proteins, such as PE-CD25⁺ & FITC-CD4⁺ resulted in 53% enrichment (Figure 26D), PE-CD25⁺ & FITC-FOXP3 resulted in 63% (Figure 26E) and PE-CD25⁺ & FITC-CD73 resulted in 54% enrichment respectively (Figure 26F). Data on FACS analysis are summarized in figure 26 and it can be seen, that there is a significant enrichment of CD4⁺CD25⁺ T cells after the two step procedure.

In addition, regulatory T cells isolated from CD73 knockout mice were applied for double staining of CD25⁺ & CD73 and those cells resulted in only 3% of PE-CD25⁺ & FITC-CD73 (Figure 27). Thus, 3% of PE-CD25⁺ & FITC-CD73⁺ is due to non specific staining. This clearly indicates that there is no expression of CD73 on CD73- knockout mice.

These FACS results so far revealed that the purity of the T -reg cells was satisfactory and also showed that the isolated cells express the T-reg cell specific marker proteins FOXP3, and CD73 (Ecto 5' Nucleotidase). These regulatory T cells isolated from mouse spleen were used for differential proteome analysis between WT and CD73 KO mice.

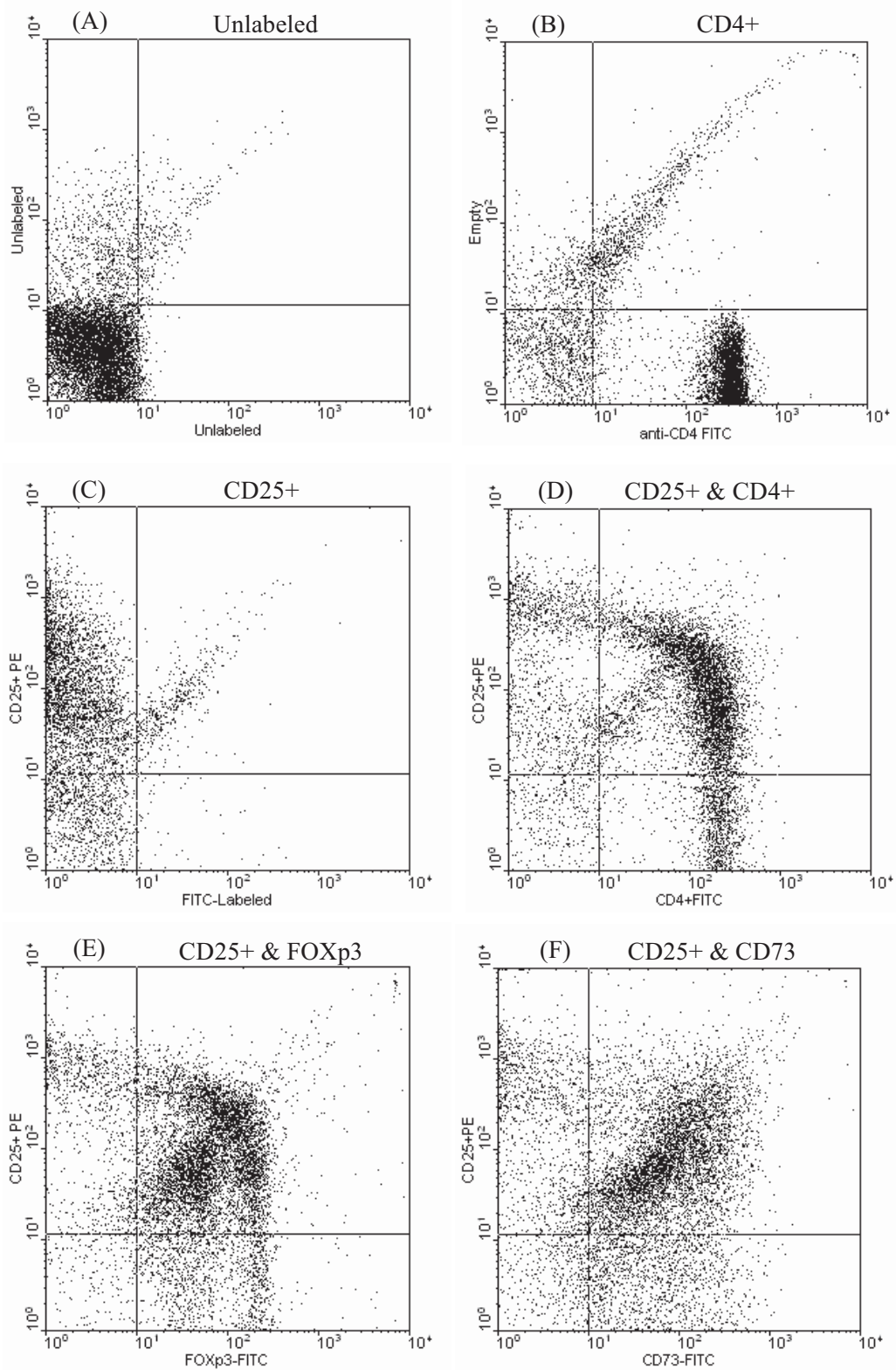


Fig 26: Purity analysis of regulatory T cells: Regulatory T cells purity was achieved by using CD4+CD25+ regulatory T cells isolation kit. In first step, CD4+ T cells (Figure 26B) was enriched then followed by positive selection of CD4+CD25+ T cells (Figure 26D).

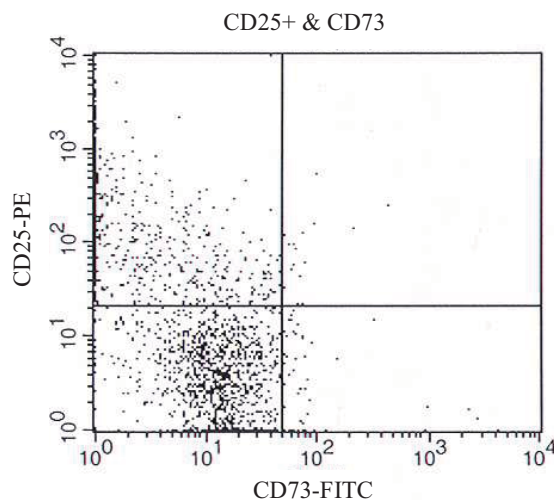


Fig 27: Analysis of CD73 expression on regulatory T cells from CD73 knockout: Purity was achieved by using CD4+CD25+ regulatory T cells isolation kit. Positively selected regulatory T cells from knockout mice (Figure 27) were applied for double staining with PE labeled-CD25+ & FITC labeled CD73 and resulted in 3% (Figure 27).

3.3.2. Proteomic study of regulatory T cells in Control Vs CD73 knockout mice.

In order to explore the significance of CD73 (Ecto 5' Nucleotidase) on regulatory T cells, quantitative proteomic study was applied on regulatory T cells isolated from mouse spleen. CD4+ CD25+ regulatory- T cells were isolated from the individual control and knockout mice (Figure 27) (for details see method section). The isolated cells were lysed and equal amount of proteins (100 μ g) were digested with trypsin followed by stable isotope dimethyl labeling (Peptides from the control mice were deuterium labeled with d0-formaldehyde and the peptides from the knockout mice were labeled with d2-formaldehyde). The stable isotope dimethyl labelling method globally labels the N-terminus and ϵ -amino group of lysine through reductive amination of the peptide. This labelling strategy produces peaks differing by 28 mass units for each d0 (Formaldehyde-d0) derivatized site and 32 mass units for each d2 (Formaldehyde-d2; 20% solution in D₂O) derivatized site relative to its non derivatized counterpart. The mass differences between isotopic pairs therefore are 4 mass units.

Labeled peptide mixtures (d0 and d2) were combined (ratio 1:1) and the samples were injected into ultimate 3000 series nano/cap auto sampler for SCX fractionation. Fractions were collected by each minute and each fraction was further applied to reversed phase chromatography. Peptides were directly eluted into the mass spectrometer (Finnigan LTQ ion trap mass spectrometer) with a linear gradient (For details see method section). In order to identify the proteins, fragmentation spectra were searched against the Mouse International Protein Index database by using MASCOT (Matrix Science, London). The search parameters were used in all MASCOT was maximum of one missed trypsin cleavage, cysteine carbamidomethylation, methionine oxidation. Protein hits with ions score >43 were considered for identification without manual inspection.

The MSQuant (MSQuant: 1.5a22) algorithm was used for the quantitative proteomic analysis of regulatory T cells. The ratios of the 'heavy' and 'light' forms of the peptide were calculated over the respective MS peaks in the total ion chromatogram. The quantification is based on the average of a number of independently determined ratios for each peptide as the peak elutes from the chromatography column. These d0-labeled and d2-labeled peptide pairs were identified by their charge state and mass difference. Each ratio of these peptide pair was subsequently calculated from the extracted ion chromatograms after manually verifying that the MS spectra containing the respective peaks were at a sufficient level above background and separated from interfering peaks of other peptides.

The results of quantitative proteomic analysis by MSQuants, revealed that there are significant differences between the proteins identified from regulatory-T cells of control and CD73 knockouts. In order to quantify, the ratio for each protein is given in the table 14. A protein ratio exceeding factor of 1.5 indicates upregulation. Conversely, a ratio of lower than 0.5 indicates downregulation. In addition the asteric (*) indicates that the protein can not be quantified due to peptide pair overlapping. As a result, I was able to identify 355 proteins. Among the 355 proteins, 25 proteins showed significant changes. Among 25 proteins, 17 proteins (as shown in table 12) were upregulated and 8 protein (shown in the table 13) were downregulated. The identified 355 proteins and the number of peptides and ratio of the individual peptide pair of the proteins are summarized in the table 14.

Table 12: List of upregulated proteins

Nr	Name of the proteins	Peptides	Ratio
1	Coactosin-like protein	1	1.53
2	Dynein, axonemal, heavy chain 12	1	1.95
3	Glutaminyl-tRNA synthetase, full insert sequence	1	1.82
4	Hydroxyacyl-coenzyme A dehydrogenase, mitochondrial precursor	1	1.81
5	Importin subunit beta-1	1	4.48
6	Isoform 1 of JmjC domain-containing histone demethylation protein 2A	1	2.09
7	Isoform 1 of THO complex subunit 4	1	1.50
8	Isoform 2 of Core histone macro-H2A.1	1	1.79
9	Isoform 2 of 60 kDa heat shock protein, mitochondrial precursor	1	1.65
10	LOC665032 60S ribosomal protein L29	1	1.60
11	Nucleolar RNA helicase 2	1	1.92
12	Protein flightless-1 homolog	1	1.67
13	Proteasome subunit beta type-9 precursor	1	1.58
14	Proteasome subunit alpha type-3	1	2.43
15	Sept7 cell division cycle 10 homolog	1	2.93
16	Stress-induced-phosphoprotein 1	1	2.09
17	Thioredoxin-dependent peroxide reductase, mitochondrial precursor	1	1.66

Table 13: List of downregulated proteins

Nr	Name of the proteins	Peptides	Ratio
1	Calreticulin precursor	1	0.45
2	Clone:9830118D19 -Product:lactotransferrin, full insert sequence	1	0.16
3	Fructose-bisphosphate aldolase A	1	0.03
4	Igh-6 protein	2	0.33
5	Mast cell protease-11	1	0.13
6	Myeloperoxidase precursor	1	0.18
7	Protein disulfide isomerase associated 4	1	0.32
8	T-cell specific GTPase, full insert sequence	2	0.30

Table 14: List of identified proteins from regulatory T cells (control versus CD73 knockout)

Nr	Name of the proteins	Peptides	Ratio
1	6-phosphogluconate dehydrogenase, decarboxylating	1	0.72
2	40S ribosomal protein S3	1	1.06
3	40S ribosomal protein S3a	2	1.22
4	40S ribosomal protein S7	1	0.92
5	40S ribosomal protein S19	1	1.0
6	60S ribosomal protein L6	1	1.09
7	60S ribosomal protein L22	1	0.93
8	60S ribosomal protein L17	1	1.52
9	Aconitate hydratase, mitochondrial precursor	1	0.66

10	Actin-related protein 2/3 complex subunit 2	1	0.92
11	Actin, cytoplasmic 1	4	1.15
12	Actin, alpha skeletal muscle	2	1.12
13	Actin-related protein 2/3 complex subunit 2	1	1.01
14	Activated RNA polymerase II transcriptional coactivator p15	1	1.24
15	Adenosylhomocysteinase	1	1.16
16	Adenylyl cyclase-associated protein 1	1	1.62
17	Adenylate kinase isoenzyme 2, mitochondrial	1	0.90
18	ADP/ATP translocase 1	2	1.19
19	Ahnak Desmoyokin (Fragment)	1	*
20	Alcohol dehydrogenase	1	0.88
21	Aldose reductase	1	1.22
22	Aldoa 21 kDa protein	1	0.87
23	Annexin A6 isoform b	1	1.01
24	Annexin A1	1	0.19
25	Annexin A11	1	1.16
26	Arpc1b protein	1	0.63
27	Atp5a1 55 kDa protein	3	0.81
28	ATP synthase subunit alpha, mitochondrial precursor	1	1.08
29	ATP synthase subunit beta, mitochondrial precursor	3	0.77
30	Beta-catenin-like protein 1	1	1.46
31	Bifunctional purine biosynthesis protein PURH	1	1.07
32	Biliverdin reductase A precursor	1	1.18
33	Calcium-binding mitochondrial carrier protein Aralar1	1	1.09
34	Calpain-2 catalytic subunit precursor	1	*
35	Calreticulin precursor	1	0.45
36	CAP, adenylyl cyclase-associated protein 1	1	1.02
37	Capping protein	1	1.14
38	Calnexin precursor	1	0.95
39	Cell cycle control protein 50A	1	1.18
40	Cell division cycle 5-related protein	1	1.29
41	Chitinase-3-like protein 3 precursor	1	0.27
42	Chromodomain helicase DNA binding protein 5	1	*
43	Chromobox protein homolog 1	1	1.29
44	Chromobox protein homolog 3	1	1.33
45	Citrate synthase, mitochondrial precursor	1	1.03
46	Clone:A730099C22-Coatomer alpha subunit	1	1.18
47	Clone:2410026P17 -Product: ribosomal protein L14, cytosolic homolog	1	1.46
48	Clone:I730048B17 -Product: capping protein (actin filament) muscle Z- line, alpha 1, full insert sequence	1	0.58
49	Clone:9830118D19 -Product:lactotransferrin, full insert sequence	1	0.16
50	Clone:7120411E18 -Product: hypothetical protein	1	1.06
51	CPN10-like protein	1	*
52	Coactosin-like protein	1	1.53
53	Coronin-7	1	0.78
54	Coronin-1A	3	0.86
55	Cytochrome c oxidase subunit 2	1	0.96

56	Cytoskeleton-associated protein 4	1	0.42
57	D-3-phosphoglycerate dehydrogenase	1	*
58	DEAD box polypeptide 17 isoform 3	1	1.15
59	Dolichyl-diphosphooligosaccharide--protein glycosyltransferase 63 kDa subunit precursor	1	0.60
60	Dolichyl-diphosphooligosaccharide--protein glycosyltransferase 67 kDa subunit precursor	1	0.66
61	DNA-(apurinic or apyrimidinic site) lyase	1	1.09
62	DNA topoisomerase 1	1	0.86
63	DNA topoisomerase 2-beta	2	0.93
64	Dynein heavy chain, cytosolic	1	1.20
65	Dynein, axonemal, heavy chain 12	1	1.95
66	EG386551 Try10-like trypsinogen	1	1.24
67	EG433182 Alpha-enolase	2	1.15
68	EG432798 similar to ribosomal protein L27A	1	1.23
69	Electron transfer flavoprotein subunit alpha, mitochondrial precursor	1	0.88
70	Elongation factor 2	2	1.30
71	Elongation factor 1-alpha 1	3	1.02
72	Elongation factor 1-gamma	1	1.04
73	Enolase	2	0.81
74	Eno1;EG433182 Alpha-enolase	1	0.87
75	Eukaryotic initiation factor 4A-I	1	0.81
76	Eukaryotic translation initiation factor 2 subunit 1	1	1.10
77	Ewing sarcoma homolog	1	1.27
78	Ezrin	1	1.14
79	F-actin-capping protein subunit alpha-1	1	1.12
80	Far upstream element-binding protein 2	1	0.99
81	Fructose-bisphosphate aldolase A	1	0.03
82	Gamma actin-like protein	3	0.96
83	Glutamate dehydrogenase 1, mitochondrial precursor	1	1.32
84	Glutamyl-tRNA synthetase, full insert sequence	1	1.82
85	Guanine nucleotide binding protein, alpha inhibiting 2, full insert sequence	1	0.87
86	GTPase-activating protein rhoGAP homolog	1	1.26
87	GTP-binding nuclear protein Ran, testis-specific isoform	1	0.60
88	H/ACA ribonucleoprotein complex subunit 4	1	1.28
89	Hemoglobin, beta adult major chain, full insert sequence	1	1.25
90	Heterogeneous nuclear ribonucleoprotein A0 (hnRNP A0)	1	1.39
91	High mobility group protein B2	1	1.20
92	High-mobility group (nonhistone chromosomal) protein 1-like 1	1	0.90
93	Histone protein Hist1h2aa	1	*
94	Histone cluster 1, H1t	1	1.01
95	Histone H2A.x	1	1.24
96	Heat shock protein 84b	3	0.92
97	Heat shock cognate 71 kDa protein	3	0.99
98	Heat shock 70 kDa protein 1L	1	1.00
99	Hsp90b1 Endoplasmic precursor	1	0.63

100	Hsp90 co-chaperone Cdc37	1	1.04
101	Hspa9 Stress-70 protein, mitochondrial precursor	1	1.09
102	Heat shock protein HSP 90-alpha	2	1.10
103	Heat shock cognate 71 kDa protein	2	1.08
104	Hepatoma-derived growth factor	1	1.15
105	Heterochromatin protein 1, binding protein 3	1	*
106	Heterochromatin protein 1, binding protein 3, full insert sequence	1	0.85
107	Heterogeneous nuclear ribonucleoprotein A/B	1	1.26
108	Heterogeneous nuclear ribonucleoprotein R, full insert sequence	1	*
109	Heterogeneous nuclear ribonucleoprotein D-like	1	0.99
110	Heterogeneous nuclear ribonucleoprotein H	1	1.22
111	Heterogeneous nuclear ribonucleoprotein U, full insert sequence	1	1.08
112	Heterogeneous nuclear ribonucleoprotein U-like protein 2	2	1.19
113	Hsp90b1 Endoplasmic precursor	1	0.50
114	Histidine triad nucleotide-binding protein 1	1	1.27
115	Histone H1.1	1	0.56
116	Histone H1.2	4	1.23
117	Histone H1.3	1	1.04
118	Histone H1.4	1	0.63
119	Histone H1.5	2	1.00
120	Histone H3	2	1.14
121	Histone H3.2	2	1.28
122	H2A histone family, member J	3	1.15
123	Histone H2A.Z	2	1.02
124	Histone H2B	!	1.17
125	Histone H2B type 1-A	2	0.91
126	Histone H2B type 1-F/J/L	5	0.96
127	Histone H4	3	0.91
128	Histone-binding protein RBBP4	1	1.34
129	Hnrpl protein	1	0.94
130	Hydroxyacyl-coenzyme A dehydrogenase, mitochondrial	1	1.81
131	Hypothetical P-loop containing nucleotide triphosphate hydrolases structure containing protein, full insert sequence	1	0.96
132	Hypothetical protein LOC666586	2	1.00
133	IFN-response element binding factor 2 (Fragment)	1	1.14
134	Igh-6 protein	2	0.29
135	Importin subunit beta-1	1	4.48
136	Inorganic pyrophosphatase	1	1.10
137	Integrin alpha-L precursor	1	1.10
138	Interferon gamma inducible protein, full insert sequence	1	1.18
139	Isoform Long of Poly [ADP-ribose] polymerase 1	2	0.80
140	Isoform Long of Splicing factor, arginine/serine-rich 3	1	1.21
141	Isoform Long of Delta-1-pyrroline-5-carboxylate synthetase	1	1.33
142	Isoform Mitochondrial of Fumarate hydratase, mitochondrial precursor	1	1.32
143	Isoform C2 of Lamin-A/C	1	1.01

144	Isoform M2 of Pyruvate kinase isozymes M1/M2	1	1.05
145	Isoform SCP2 of Non-specific lipid-transfer protein	1	1.19
146	Isoform V of Septin-6	1	1.22
147	Isoform Smooth muscle of Myosin light polypeptide 6	1	1.22
148	Isoform Long of 14-3-3 protein beta/alpha	1	0.80
149	Isoform 1 of 60 kDa heat shock protein, mitochondrial precursor	1	1.40
150	Isoform 1 of JmjC domain-containing histone demethylation protein 2A	1	2.09
151	Isoform 1 of Heterogeneous nuclear ribonucleoprotein A3	1	1.08
152	Isoform 1 of Heterogeneous nuclear ribonucleoprotein K	2	1.16
153	Isoform 1 of Heterogeneous nuclear ribonucleoprotein M	1	*
154	Isoform 1 of Regulator of differentiation 1	1	1.12
155	Isoform 1 of Splicing factor, arginine/serine-rich 1	1	1.29
156	Isoform 1 of Splicing factor, arginine/serine-rich 10	1	1.32
157	Isoform 1 of Sister chromatid cohesion protein PDS5 homolog B	1	1.05
158	Isoform 1 of Core histone macro-H2A.1	2	1.15
159	Isoform 1 of Core-binding factor subunit beta	1	0.92
160	Isoform 1 of Smu-1 suppressor of mec-8 and unc-52 protein homolog	1	1.33
161	Isoform 1 of Ezrin-radixin-moesin-binding phosphoprotein 50	1	1.10
162	Isoform 1 of Eukaryotic translation initiation factor 4 gamma 2	1	0.99
163	Isoform 1 of Plasminogen activator inhibitor 1 RNA-binding protein	1	0.82
164	Isoform 1 of SUMO-activating enzyme subunit 1	1	1.10
165	Isoform 1 of T-complex protein 1 subunit alpha B	1	1.01
166	Isoform 1 of Transcription intermediary factor 1-beta	1	0.96
167	Isoform 1 of THO complex subunit 4	1	1.50
168	Isoform 1 of Pre-mRNA-processing factor 6	1	*
169	Isoform 1 of Myosin-14	1	1.26
170	Isoform 1 of Splicing factor 3B subunit 3	1	1.03
171	Isoform 1 of Negative elongation factor E	1	0.85
172	Isoform 1 of Ubiquitin-conjugating enzyme E2 variant 1	1	1.28
173	Isoform 2 of Drebrin-like protein	1	1.06
174	Isoform 2 of Core histone macro-H2A.1	1	1.79
175	Isoform 2 of Heterogeneous nuclear ribonucleoprotein K	1	1.32
176	Isoform 2 of Apoptotic chromatin condensation inducer in the nucleus	1	*
177	Isoform 2 of Leukocyte common antigen precursor	1	1.33
178	Isoform 2 of Splicing factor, arginine/serine-rich 1	1	*
179	Isoform 2 of Tropomyosin alpha-3 chain	2	0.98
180	Isoform 2 of ATP-dependent RNA helicase A	1	1.43
181	Isoform 2 of Cell division control protein 42 homolog precursor	1	1.02
182	Isoform 2 of Pre-mRNA-processing factor 6	1	1.05
183	Isoform 2 of Protein SET	1	1.27

184	Isoform 2 of 60 kDa heat shock protein, mitochondrial precursor	1	1.65
185	Isoform 3 of Heterogeneous nuclear ribonucleoproteins A2/B1	2	0.96
186	Isoform 3 of Transcription elongation regulator 1	1	*
187	Isoform 3 of Programmed cell death 6-interacting protein	1	0.99
188	Isoform 4 of 2-oxoglutarate dehydrogenase E1 component, mitochondrial precursor	1	0.83
189	Keratin complex 1, acidic, gene 10	1	0.76
190	Lactotransferrin, full insert sequence	2	1.03
191	L-lactate dehydrogenase A chain	2	2.01
192	Lamin-B1	1	1.15
193	Lamin-B receptor	1	0.98
194	LIM domain-containing protein 2	1	1.96
195	LOC100044829 similar to Fibrillarin isoform 2	1	0.93
196	LOC632401 H2A histone family, member J	2	1.01
197	LOC100047613 Thymosin beta-10	1	1.14
198	LOC671392 Isoform 1 of Protein SET	1	1.49
199	LOC100041307 High mobility group protein B1	1	1.30
200	LOC100043755 60S ribosomal protein L23a	1	1.10
201	LOC100047349 60S ribosomal protein L28	1	1.27
202	LOC100048119 Prostaglandin E synthase 3	1	1.31
203	LOC100044516 60S ribosomal protein L35a	1	0.98
204	LOC675192 hypothetical protein	1	1.32
205	LOC665032 60S ribosomal protein L29	1	1.60
206	LOC100044829 rRNA 2'-O-methyltransferase fibrillarin	1	1.13
207	LOC100043129 similar to hCG2040565	1	0.85
208	LOC100043295 60S ribosomal protein L5	1	0.67
209	Leucine-rich PPR motif-containing protein, mitochondrial precursor	1	1.13
210	Leukotriene A-4 hydrolase	1	0.93
211	Leukocyte elastase inhibitor A	1	1.02
212	MAP kinase-activated protein kinase 2	1	0.64
213	Mast cell protease-11	1	0.13
214	Malate dehydrogenase, cytoplasmic	1	0.49
215	Malate dehydrogenase, mitochondrial precursor	5	0.77
216	Matrin-3	1	1.09
217	Moesin	1	1.28
218	Myosin heavy chain IX, full insert sequence	12	1.31
219	Myosin, heavy polypeptide 10, non-muscle	2	1.47
220	Myosin light polypeptide 6B	1	1.06
221	Myosin light chain, regulatory B-like	1	1.06
222	Myosin-9	5	1.02
223	Myeloid bactericidin	3	0.12
224	Myeloperoxidase precursor	1	0.18
225	Multifunctional protein ADE2	1	1.13
226	NADH dehydrogenase [ubiquinone] iron-sulfur protein 6, mitochondrial precursor	1	0.66
227	NADP-dependent malic enzyme, mitochondrial precursor	1	0.96

228	N-acetylneuraminic acid synthase	1	1.09
229	Novel histone H2A family member	1	1.99
230	Non-histone chromosomal protein HMG-17	1	0.96
231	Nuclear mitotic apparatus protein 1	1	1.11
232	Nuclear migration protein nudC	1	1.16
233	Nucleolar RNA helicase 2	1	1.92
234	Nucleolin	2	1.05
235	Nucleosome assembly protein 1-like 4, full insert sequence	1	0.97
236	Nucleophosmin	1	1.05
237	Nuclease sensitive element-binding protein 1	1	1.11
238	Peptidyl-prolyl cis-trans isomerase	2	1.08
239	PEST proteolytic signal-containing nuclear protein	1	*
240	Peroxiredoxin 5, full insert sequence	1	1.23
241	Peroxiredoxin-1	1	0.94
242	Peroxiredoxin-4	1	1.10
243	Peroxiredoxin-2	1	1.22
244	Phb2 Protein	1	1.09
245	Phosphoglycerate mutase 2	1	1.07
246	Phosphoglycerate kinase 1	1	0.88
247	Phosphatidylethanolamine-binding protein 1	1	0.83
248	Platelet-activating factor acetylhydrolase IB subunit beta	1	1.05
249	Plastin-2	3	1.41
250	Pinin	1	1.38
251	Polypyrimidine tract binding protein 1, full insert sequence	1	1.16
252	Predicted gene, EG433923	1	0.84
253	Predicted gene, EG622339	1	1.21
254	Pre-mRNA-splicing factor RBM22	1	1.18
255	Probable ATP-dependent RNA helicase DDX5	1	1.17
256	Protein disulfide-isomerase A3 precursor	3	1.09
257	Peptidyl-prolyl cis-trans isomerase	1	1.00
258	Protein disulfide-isomerase A3 precursor	1	1.17
259	Profilin-1	1	1.12
260	Prohibitin-2	1	1.01
261	Proline-serine-threonine phosphatase-interacting protein 1	1	0.96
262	Prolyl 4-hydroxylase, beta polypeptide, full insert sequence	1	0.98
263	Prothymosin alpha	1	1.98
264	Protein KIAA1967 homolog	1	1.20
265	Protein DJ-1	1	1.45
266	Protein S100-A9	1	0.62
267	protein disulfide isomerase associated 4	1	0.32
268	Protein flightless-1 homolog	1	1.67
269	Proteasome subunit beta type-9 precursor	1	1.58
270	Proteasome subunit beta type-10 precursor	1	0.98
271	Proteasome subunit alpha type-1	1	1.20
272	Proteasome subunit alpha type-3	1	2.43
273	Proteasome activator complex subunit 1	1	1.42
274	Proto-oncogene tyrosine-protein kinase LCK	1	0.96
275	Prolyl 4-hydroxylase, beta polypeptide, full insert sequence	1	0.65
276	Ptms protein	1	1.12

277	Putative pre-mRNA-splicing factor ATP-dependent RNA helicase DHX15	1	1.15
278	Pyrin and HIN domain family, member 1	1	1.35
279	Pyruvate kinase isozymes R/L	1	0.99
280	Pyruvate dehydrogenase E1 component subunit beta, mitochondrial precursor	2	1.45
281	rRNA 2'-O-methyltransferase fibrillarin	1	1.35
282	Ras-related C3 botulinum toxin substrate 2 precursor	2	0.98
283	RAS-related C3 botulinum substrate 1, full insert sequence	1	0.96
284	Ras-related protein Rap-1A precursor	1	1.02
285	Ras-related protein Rab-11B	1	0.69
286	Ras GTPase-activating protein-binding protein 1	1	0.82
287	Ras GTPase-activating-like protein IQGAP1	1	0.92
288	Regulator of chromosome condensation 2	1	0.77
289	Rho GDP-dissociation inhibitor 2	1	1.10
290	Rho-related GTP-binding protein RhoC precursor	1	1.01
291	RIKEN cDNA 1700009N14 gene	2	1.09
292	Ribosomal protein L14, cytosolic homolog	2	1.07
293	Rps5 20 kDa protein	1	*
294	Rps16 protein	1	1.00
295	Rpl8 60S ribosomal protein L8	1	1.26
296	Rpl31 protein	1	0.74
297	RP23-24J10.5 hypothetical protein LOC666586	1	0.60
298	RNA-binding protein 28	1	*
299	RNA-binding protein FUS	1	0.93
300	SAM domain and HD domain-containing protein 1	1	0.91
301	Scavenger mRNA-decapping enzyme DcpS	1	1.35
302	SH3 domain-binding glutamic acid-rich-like protein	1	1.09
303	Sept7 cell division cycle 10 homolog	1	2.93
304	Serotransferrin precursor	1	1.16
305	Serum albumin precursor	2	1.07
306	Similar to calmodulin	1	1.42
307	Similar to ribosomal protein L19	1	1.03
308	Similar to ribosomal protein L26	1	1.04
309	Similar to Myoblast KIAA0223 (Putative uncharacterized protein)	1	1.15
310	Similar to adenine nucleotide translocase isoform 1	1	0.98
311	Similar to SMT3B protein isoform 2	1	1.00
312	Similar to Aspartyl-transsynthetasehomolog	1	1.13
313	Similar to thymosin beta-4	1	0.53
314	Similar to Major urinary proteins 11 and 8	1	0.64
315	Similar to telomeric and tetraplex DNA binding protein qTBP42 V	1	1.32
316	Similar to heterogeneous nuclear ribonucleoprotein R homolog	1	1.18
317	Small nuclear ribonucleoprotein polypeptide F	1	1.12
318	Sodium/potassium-transporting ATPase subunit alpha-1 precursor	1	1.28
319	Sodium/potassium-transporting ATPase subunit alpha-3	1	1.39

320	Splicing factor 3a, subunit 2	1	1.42
321	Splicing factor, arginine/serine-rich 2	1	1.26
322	Splicing factor, arginine/serine-rich 5	1	0.98
323	Stress-induced-phosphoprotein 1	1	2.09
324	Structural maintenance of chromosomes protein 3	1	1.01
325	Superoxide dismutase	2	1.39
326	SWI/SNF-related matrix-associated actin-dependent regulator of chromatin subfamily A member 5	1	*
327	TAR DNA-binding protein 43	1	*
328	Talin 1 (Fragment)	1	0.95
329	T-cell specific GTPase, full insert sequence	1	0.30
330	T-complex protein 1 subunit alpha A	1	1.10
331	T-complex protein 1 subunit theta	1	1.35
332	T-complex protein 1 subunit delta	1	1.15
333	T-complex protein 1 subunit zeta	1	1.05
334	T-complex protein 1 subunit gamma	1	1.43
335	Thioredoxin-dependent peroxide reductase, mitochondrial precursor	1	1.66
336	Tpr protein	1	1.07
337	Tpm3 29 kDa protein	1	1.13
338	Triosephosphate isomerase	1	0.55
339	Transketolase	1	1.01
340	Transitional endoplasmic reticulum ATPase	3	0.91
341	Transgelin-2	1	1.40
342	Trafficking protein particle complex subunit 3	1	*
343	Tropomyosin 3, gamma	1	0.96
344	Tubulin alpha-1A chain	3	0.98
345	Tubulin beta-5 chain	2	1.19
346	Tubulin beta-2B chain	1	1.18
347	Tubulin beta-2C chain	1	*
348	U1 small nuclear ribonucleoprotein A	1	1.41
349	Ubiquitin-conjugating enzyme E2 N	1	1.01
350	Ubiquitin-like modifier-activating enzyme 1 X	1	*
351	Uncharacterized protein C17orf62 homolog	1	1.10
352	UV excision repair protein RAD23 homolog B	1	1.05
353	Vimentin	4	1.67
354	WD repeat-containing protein 1	1	1.0
355	Ywhaz 14-3-3 protein zeta/delta	1	1.22

(* - Not quantifiable)

4. Discussion

The aim of this study was to investigate whether loss of the ecto-enzyme CD73 results in compensatory changes in the protein expression of other membrane proteins. To this end I have first carried out a proteomic analysis of coronary endothelial cell membranes isolated under *in vivo* conditions. Since purity and yield of membrane proteins precluded a differential proteomic analysis between wild type and CD73 knockouts, I have next aimed to cultivate endothelial cells from the aorta and the lung to be able to carry out the differential proteomic approach under *in vitro* condition. This, however, proved to be not feasible since *in vitro* expansion of endothelial cells necessary to obtain sufficient material for proteomic analysis, either resulted in a loss of cell purity or loss of CD73. Finally regulatory T cells (T reg) were analysed in which CD73 was recently reported to be a novel marker enzyme (Kobie et al. 6780-86; Resta and Thompson 131-39). Differential proteomic analysis of wild type and CD73 deficient regulatory T cells yielded 17 proteins which were upregulated and 8 proteins which were downregulated.

4.1. Isolation and proteomic analysis of endothelial membranes under *in vivo* conditions

The present study reports that the coronary endothelial membranes can be conveniently labeled *in vivo* after perfusion of isolated hearts with colloidal silica beads. Following tissue homogenization I have obtained significant enrichment of endothelial membrane proteins. However, the shear forces necessary to disintegrate contractile tissue such as the heart resulted in significant contamination with non-endothelial proteins. This together with only a low overall protein yield shows the limitations of the labeling procedure to obtain a full and selective coverage of endothelial membrane proteins from the *in vivo* mouse heart.

Direct proteomic mapping of the endothelial cell surface was pioneered by Schnitzer (Durr et al. 985-92) who similar to the present study applied the colloidal silica method to selectively label endothelial membranes. He isolated luminal endothelial cell plasma membranes from rat lung and identified 450 proteins by mass spectrometry. Interestingly, about 19% of total proteins identified were located primarily in endoplasmic reticulum, mitochondria, golgi, ribosomes and nuclei. Consistent with these findings, I have also identified intracellular proteins in the “endothelial cell membrane fraction” (Table 9). The presence of plasma

protein albumin in the EC membrane fraction of our present study, could be due to the presence of the albumin-binding glycoprotein expressed in the endothelium (Schnitzer and Oh 6072-82; Schnitzer H246-H254). Furthermore, it is possible that proteins reside in more than one sub cellular location. The eukaryotic translation elongation factor-1, which is a cytosolic protein and has a less well known function in cytoskeletal reorganization (Negrutskii and El'skaya 47-78), was found in the EC membrane fraction of the present study. This is an accordance with finding of Durr et al (Durr et al. 985-92) who also described endothelial membrane location of translation elongation factor-1. Contamination with histones and other polycationic proteins could be interpreted in that way, that they were released by tissue homogenization and adsorbed electrostatically to the polyanionic polyacrylic acid cross linker of the silica-coated beads (Durr et al. 985-92). Protein-protein interaction could as well contribute to some of the proteins identified. Another likely interpretation could be that due to the reversible interaction of cationic colloidal silica with positively charged endothelial membranes, this technique is highly sensitive to the mechanical shear rate required for tissue homogenization. In fact, the present study clearly demonstrates that the method used for tissue homogenization profoundly alters the degree of contamination with proteins from other cell compartments. By comparing two different techniques for tissue homogenization at two different speed settings (Figure 13), found for cardiac tissue that the ultra blade homogenization at low speed is superior to the commonly used teflon pestle method. Clearly, lung used in all previous studies is a rather soft tissue so that the low mechanical shear forces necessary for homogenization only slightly altered purity of the membrane fraction obtained.

Lung tissue is also advantageous for proteomic analysis of endothelial cells because endothelial cells comprise about 30% of all cells present in the lung (Zhou et al. C950-C956; Danilov et al. L1335-L1347). Although the heart is also highly vascularized, endothelial cells comprise only about 3% of all cells present in cardiac tissue on a volume basis (Kroll, Deussen, and Sweet 590-604; Anversa et al. 57-64). Given a coronary endothelial surface area of approximately 500 cm²/g (Bassingthwaighe, Yipintsoi, and Harvey 229-49), the endothelial surface area of the mouse heart (~120 mg wet weight) can be calculated to be about 60 cm². Using the colloidal silica method, found the recovery of endothelial cell membrane proteins from one mouse heart to be rather low (about 1 µg) which is only 0.005% of the total heart homogenate (about 20 mg). Thus, proteomic analysis in the present study required the pooling of 10 individually prepared hearts. This low recovery further limits a broad application of the cationic colloidal silica method for the purification of endothelial cell

membrane *in vivo* such as muscle and other organs showing a similar degree of vascularisation.

Aside from reversible ionic interactions such as with colloidal silica, membranes can be covalently and selectively labeled with the biotin derivative sulfo-NHS-LC-biotin (Zhou et al. C950-C956; Zhang et al. 15-19). Due to the charged sulfonate group, this molecule cannot penetrate the cell membrane. Furthermore, the covalent nature of the bond should endure tissue homogenization and solubilisation of the proteins with detergents. However, the drawback of this method is that due to the low molecular weight and size of the biotin derivative, it readily can reach the interstitial space and thereby causes labeling of other cells in addition to the luminal endothelial surface. This does not appear to be a major problem in the lung because of the large fraction of endothelial cells. However, perfusion of the coronary vasculature of the heart with sulfo-NHS-LC-biotin unselectively labeled membranes both of endothelial cells and cardiomyocytes equally well (M. Reinartz, unpublished observation). Provided the biotin derivative could be chemically modified e.g. by increasing its size so that it can no longer permeate the endothelial barrier, this would constitute a promising procedure for the covalent *in vivo* labeling of solely luminal endothelial cell membrane proteins of all organs.

4.2. Functional role of endothelial CD73 (ecto- 5'-nucleotidase)

CD73 (ecto-5'-nucleotidase), a 70-kDa glycosylphosphatidylinositol (GPI)-anchored cell surface molecule, is expressed on the vascular endothelium and catalyzes the extracellular conversion of 5'-AMP to adenosine (Zimmermann 345-65; Deussen et al. H692-H700). Adenosine, is known to be implicated in many physiological and pathophysiological functions (Deussen et al. H692-H700; Shryock and Belardinelli 2-10). In endothelial cells (ECs), adenosine has been shown to inhibit the release of cytokines and the expression of adhesion molecules (Bouma, van den Wildenberg, and Buurman C522-C529; Bouma, van den Wildenberg, and Buurman C522-C529; Morandini et al. H807-H816). Recent studies revealed that the genetic deletion of CD73 associated with an impaired extracellular generation of adenosine demonstrated its importance in modulating vascular tone and barrier function and in limiting inflammatory and prothrombotic responses by attenuating leukocyte adhesion and platelet function. (Koszalka et al. 814-21; Thompson et al. 1395-405).

Stimulation of endothelial cells by cytokines or endotoxin results in *de novo* expression or upregulation of different classes of adhesion molecules, such as E-selectin, intercellular adhesion molecule 1 (ICAM-1) and vascular cell adhesion molecule 1 (VCAM-1), on their cell surface (Stad and Buurman 261-68). Similarly, a study by Zerneck et al., showed that luminal expression and mRNA of the endothelial adhesion molecule VCAM-1 is constitutively upregulated in carotid arteries of CD73^{-/-} mice versus wild-type mice. Moreover, the upregulation of luminal VCAM-1 in CD73^{-/-} carotid arteries was even more pronounced after wire injury than in uninjured CD73^{-/-} arteries. Additionally, aortic endothelial cells (ECs) from CD73^{-/-} mice display an upregulation of mRNA and protein expression of VCAM-1, associated with increased nuclear factor (NF)κB activity, as determined by chromatin cross-linking and immunoprecipitation or quantitative p65 binding assays. These findings revealed the crucial role of CD73 in the constitutive regulation of endothelial adhesion molecules and inflammatory homeostasis (Zerneck et al. 2120-27).

Adenosine binding to the A_{2A} receptor can counteract the stimulation of very late antigen - 4 (VLA-4) expression which in turn bind to VCAM-1 in neutrophils suppress inflammation via a cAMP/protein kinase A mediated pathway (Sullivan et al. 127-34). VLA-4 binding to VCAM-1 is also known to mediate mononuclear cell adhesion to early atherosclerotic endothelium in apolipoprotein E-deficient mice (Huo, Hafezi-Moghadam, and Ley 153-59). Study by Zerneck et al. identified VLA-4/VCAM-1 as the primary receptor-ligand pair crucial for proinflammatory monocyte recruitment in CD73^{-/-} carotid arteries.

The pivotal role of NF-κB is in the transcription of multiple proinflammatory and antiapoptotic genes (Collins et al. 899-909; Collins et al. 899-909; de Martin et al. E83-E88). Indeed, NF-κB activity was increased in CD73^{-/-} ECs *in vitro*, as evident by ChIP analysis of NF-κB and acetylated histone H3 binding to the VCAM-1 promoter and quantitative p65-DNA binding assays. This implies that the absence of adenosine, which would usually limit NF-κB activation, leads to constitutive NF-κB activity and transcriptional upregulation of VCAM-1 (Zerneck et al. 2120-27).

An increase in luminal thrombin causing platelet activation may support a proinflammatory phenotype in CD73^{-/-} arteries with deficient adenosine synthesis. Moreover, treatment with the adenosine receptor agonist ATL-146e attenuated neointima formation in wild-type mice

and completely prevented neointimal plaque formation in CD73^{-/-} mice. This indicates that adenosine synthesis and subsequent activation of A2A receptors in CD73^{-/-} mice constitutes an underlying mechanism by which CD73 protects against inflammation (Zernecke et al. 2120-27). Additionally, a study by Hasko et al, revealed that the adenosine receptor activation on activated macrophages has been shown to inhibit the release of tumor necrosis factor- α , which can act directly on ECs to increase leukocyte adhesion (Hasko et al. 4634-40).

The study by Zernecke et al., suggests that CD73 is crucially involved in the finely tuned constitutive balancing of proinflammatory and antiinflammatory mechanisms in the macrovasculature (Zernecke et al. 2120-27). These findings give an approach elevating or mimicking CD73 activity or substituting its metabolites to reduce vascular inflammation and lesion formation. In order to further understand the molecular mechanisms of adenosine mediated suppression of cytokines production and the expression of adhesion molecules on endothelial cells and regulatory T cells, I have used WT and CD73 knockouts in a differential proteomic approach.

4.3. Limitations of proteomic analysis of endothelial cells

The present study found that proteomic analysis of coronary endothelial cell membranes isolated under *in vivo* conditions from the mouse heart by cationic colloidal silica beads method was not feasible due to partial loss of ionic interaction between the endothelial cell membrane and cationic silica during tissue homogenization. In addition using the silica bead methods yielded only about 1 μ g protein from one heart. To perform the proteomic approach reported therefore required the pooling of 10 individually prepared hearts. In summary 71 proteins were identified by this procedure. Among the 71 proteins, 31 were membrane proteins, 14 cytoskeletal or junction proteins, 9 mitochondrial proteins and 9 nuclear proteins (Table 9) suggesting significant contamination. The low yield and purity therefore limits the differential proteomic analysis of EC membranes isolated by the cationic colloidal silica method under *in vivo* condition and precluded further analysis of CD73 knockout mice.

Since the in-vivo isolation of coronary endothelial membranes proved to be not feasible. Endothelial cells were isolated from mouse aorta and lung to see whether it is possible to use

a differential proteomic approach between WT and CD73 knockout under *in vitro* condition. To this end respective tissue was disintegrated by collagenase and followed by purification of endothelial cells by magnetic beads coated with cleavable CD31 and CD102 antibody. In order to obtain a sufficient amount of sample (1-2 mg detergent soluble protein/ 10 million cells), positively selected endothelial cells were cultured and further passaged several times in order to increase the cell number which is required for proteomic analysis by mass spectrometry.

Culturing of isolated endothelial cells resulted in significant contamination with non-endothelial cells, so that an additional purification step was included. To this end I have adapted the method of Hewett and Murray et al 1993, who similar to the present study made a positive selection of endothelial cells from the isolated total cells mixture (from aorta and lung) using super paramagnetic beads which is coupled to the endothelial specific marker proteins (CD31 and CD102) on the surface. CD31 is a 130KDa integral membrane protein which exhibits a 10-fold higher expression level on ECs as compared to other cell type like platelets and leukocytes (Dong et al. 1599-604). However, during each passage of aortic endothelial cells, FACS analysis (CD31, CD102 and CD73) showed a loss of purity over the time of growth. Finally only 18% of the cells were positive for the endothelial specific markers CD31 and CD102. This low purity might be due to overgrowth with non endothelial cells like smooth muscle cells and fibroblast. In addition dedifferentiation also can lead to loss of phenotypic characteristic features of the endothelial cells (Madri and Williams 153-65).

In contrast the purity of isolated mouse lung endothelial cells could be maintained in culture. However, expression of CD73 on mouse lung endothelial cells significantly decreased after the second magnetic bead sorting (for details see result section). Therefore loss of CD73 in cultured lung endothelial cells again precluded the use of cultured lung endothelial cells for the differential proteomic approach using WT and CD73 knockouts.

4.4. Functional role of CD73 in regulatory T cells (T reg)

In human lymphocyte subsets, it has been shown that 10% of CD4⁺ T cells express CD73 (Thompson et al. 9-19). More recently, CD73 has been shown to be expressed by CD25⁺FoxP3⁺ T reg cells and CD25⁻ uncommitted primed precursor T helper cells (Thpp cells) which, through the generation of adenosine, dampen the inflammatory response (Kobie et al. 6780-86). Although CD73 is expressed by both Thpp and Treg populations, each has distinct characteristics; only the Thpp cells secrete IL-2, and only the Treg population is capable of controlling immune responses *in vivo* and *in vitro* including the suppressive cytokines TGF-beta and IL-10 (von Boehmer 338-44).

Although both Treg and Thpp cells have the potential to suppress inflammatory responses by the CD73/adenosine mechanism, these two cell types may be important in different pathologies. Thpp cells temporarily suppress acute antipathogen responses and, in addition, the Thpp cells retain the potential to differentiate later into strong effector (e.g., Th1 or Th2) phenotypes (Sad and Mosmann 3514-22; Divekar et al. 1465-73). In contrast, Treg cells are more suitable for long-term suppression of autoimmune anti-inflammatory responses, without the risk of future differentiation into effector cells.

During immune responses, hypoxia, proinflammatory soluble factors, and cell-mediated cytotoxicity, causes the destruction of healthy cells within the tissue microenvironment (Sitkovsky et al. 657-82; Sitkovsky and Ohta 299-304). Given the high intracellular concentration of ATP leads to cell damage and also, increase in the extracellular ATP concentration. Upon binding to purinergic receptors of the P2 type, extracellular ATP itself can further enhance local inflammation, for instance by triggering proinflammatory cytokine secretion by mononuclear phagocytes or by promoting dendritic cell chemotaxis.

CD73⁺Foxp3⁺CD4⁺ T cells are potentially very important for the control of inflammation *in situ*. Firstly, it is their ability to mediate extracellular ATP catabolism to attenuate local inflammation by reducing the pool of extracellular ATP and neutralizing its direct proinflammatory effects. Secondly, these cells efficiently enhance CD39 and CD73 ecto nucleotidase activity to generate pericellular adenosine, which inhibits various activated immune cell types through A2a receptors. A study by Ohta et al. has shown that adenosine is

a potent inhibitor of T cell responses and the A2a receptor has been identified as the major anti-inflammatory adenosine receptor associated with T cells (Ohta and Sitkovsky 916-20).

Hypoxia associated with is known to enhance CD73 expression through hypoxia-inducible factors (HIFs) (Synnestvedt et al. 993-1002), possibly reinforcing the 5'-AMP hydrolysis activity of CD73+Foxp3+CD4+ T cells within inflamed tissues. It has been known for some time that CD73 is expressed on subsets of T lymphocytes, but it was only recently detected at high levels on the regulatory T cell (Treg) subset of naturally occurring suppressor T cells (Kobie et al. 6780-86).

Hypoxia is known to inhibit the intracellular adenosine kinase which normally rephosphorylates adenosine into AMP (Sitkovsky et al. 657-82). This effect limit the equilibrative transporter-mediated entry of pericellular adenosine generated by Foxp3+CD4+ T cells and, consequently, helps to maintain its pericellular concentration. Hence, extracellular adenosine generation by CD73+Foxp3+CD4+ T lymphocytes, is likely to contributes to the protection of tissues from excessive inflammatory damage and therefore to the control of immunopathologies.

Previous reports, which showed lack of Treg-mediated suppression of IFN- γ synthesis in the absence of 5'-AMP, indicated that stimulation through CD28 can block Treg-mediated suppression (Takahashi et al. 1969-80;Thornton and Shevach 287-96). However, the presence of 5'-AMP at concentrations as low as 0.5 μ M resulted in the inhibition of Th1 IFN- γ synthesis in cultures containing CD73+ Thpp or Treg cells, but not CD73- naïve cells. The role of CD73 in inhibiting IFN- γ production was confirmed by showing that suppression was prevented by a specific inhibitor of CD73 enzymatic activity, APCP (Synnestvedt et al. 993-1002). An A2A receptor antagonist (SCH58261) also prevented suppression, confirming that the effect was mediated through adenosine.

4.5. Differentially expressed proteins in regulatory T cells lacking CD73

From the previous studies it is known that, CD73 (ecto 5' nucleotidase) is expressed on subsets of T lymphocytes, but it was only recently found that CD73 is a novel marker enzyme on the regulatory T cell (T reg) (Kobie et al. 6780-86). I have also found an expression of CD73 on regulatory T cells as evidenced in figure 26. The regulatory T cells were isolated by commercially available CD4⁺ CD25⁺ regulatory T cells isolation kit. For differential proteomic analysis peptides from isolated T reg cells were applied for dimethyl labeling method (Hsu et al. 6843-52). An advantage of this method is that labeling is fast (within 5 min), complete (100%) and globally labels the N-terminus and ϵ -amino group of lysine through reductive amination. This labeling strategy produces peaks differing by 28 mass units for each d0 (Formaldehyde-d0) derivatized site (control) and 32 mass units for each d2 (Formaldehyde-d2; 20% solution in D₂O) derivatized site (CD73 knockout) relative to its non derivatized counterpart. The mass differences between isotopic pair are 4 mass units. These d0-labeled (control) and d2-labeled (CD73 knockout) peptide pairs were identified by their charge state and mass difference by the MSQuant (MSQuant: 1.5a22) algorithm. As a result, 355 proteins were identified. Among the 355 proteins, interestingly 25 proteins were shown significant changes. Among 25 proteins, 17 proteins were upregulated and 8 proteins were downregulated. Molecular weight, localization and functions of each protein were identified by using the Uniprot web server, ExPasy web server and the Bioinformatic Marvester (Mouse Harvester) database. Among the differentially expressed proteins the following deserve particular attentions.

1. Coactosin-like protein (CLP)

Coactosin-like protein (CLP), which is 50% upregulated in CD73 knockouts. Is a filamentous (F)-actin binding protein, which interacts with 5-lipoxygenase (5LO) and F-actin. CLP can up-regulate and modulate 5LO activity in a calcium-independent manner. Regulation of 5-lipoxygenase (5LO) activity is a key determinant for the biosynthesis of proinflammatory leukotrienes (Rakonjac et al. 13150-55). The actions of leukotrienes (LTs) as inflammatory mediators is relevant in relation to asthma, but several findings now imply a role for 5-lipoxygenase (5LO) and LTs also in another chronic inflammatory disorder, i.e.,

atherosclerosis (Funk 664-72; Lotzer, Funk, and Habenicht 30-37). Recent studies also support a role for 5LO metabolites in cancer cell survival (Ghosh 624-35; Catalano et al. 1740-42).

Additionally a study by Ochi et al., revealed that ATP is another factor stimulating 5LO activity. ATP was shown to stimulate 5LO (Ochi et al. 5754-58; Werz and Steinhilber 327-33). Giving maximum activation at 0.1mM (Werz and Steinhilber 327-33; Noguchi, Miyano, and Matsumoto 367-71). Taken together, lack of CD73 causes upregulation of CLP, which may indirectly participate in the modulation of the inflammatory response. CLP may therefore participate in the adenosine mediated immunosuppression.

2. Isoform 2 of 60 kDa heat shock protein

Heat shock proteins (HSPs), also called stress proteins, are a group of proteins that are present in all cells in all life forms. They are induced when a cell undergoes various types of environmental stresses like heat, cold and oxygen deprivation. They act like ‘chaperones,’ making sure that the cell’s proteins are in the right shape and in the right place at the right time. Heat shock proteins are also believed to play a role in the presentation of pieces of proteins (or peptides) on the cell surface to help the immune system recognize diseased cells.

Isoform 2 of 60 kDa heat shock protein, a mitochondrial precursor, is 65% upregulated in CD73 knockouts. An accordance with the finding of Alexandra Zanin-Zhorov et al., (Zanin-Zhorov et al. 1567-69; Zanin-Zhorov et al. 2022-32) HSP60 upregulated in CD4+CD25+ T cells (regulatory T cells), amplifies their response to TCR-dependent (anti-CD3) stimulation, via innate TLR2 signaling which leads to upregulation of AKT, Pyk2, and p38 and downregulation of ERK. These innate effects of HSP60 signaling amplify IL-10, TGF- β , and by contact-dependent Treg suppressor mechanisms have an effect on TCR-activated effector T cells to downregulate ERK, NF- κ B. Which leads to downregulated proliferation and secretion of the other proinflammatory cytokines (Zanin-Zhorov et al. 1567-69; Zanin-Zhorov et al. 2022-32).

In order to test whether the CD4+CD25+ T cells were essential for the effects of HSP60 on T cell cytokine secretion Alexandra Zanin-Zhorov et al., depleted CD25+ T cells (T reg cells) by magnetic beads. They found that removal of the CD4+CD25+ T cells from the CD4+

population completely prevented the inhibition of IFN- γ and TNF- α secretion by HSP60 treatment of the residual CD4+CD25⁻ T cells. This experiment revealed that the depletion of CD4+CD25⁺ T cells abrogates inhibitory effects of proinflammatory cytokine production by HSP60. Recent studies also found that the human 60-kDa heat shock (HSP60) molecule, via innate TLR2 signaling, can downregulate T cell migration (Zanin-Zhorov et al. 1567-69) and inhibit the secretion of proinflammatory cytokines by activated T cells (Zanin-Zhorov et al. 2022-32). Thus the upregulation of HSP60 in the CD73 knockout mice in the present study suggests that HSP60 via CD73 participates in the anti-inflammatory action of the adenosine (Kobie et al. 6780-86).

3. Proteasome subunit beta type-9 precursor; Proteasome subunit alpha type-3

The proteasome is a multicatalytic proteinase complex which is characterized by its ability to cleave peptides with Arg, Phe, Tyr, Leu, and Glu adjacent to the leaving group at neutral or slightly basic pH. The proteasome has an ATP-dependent proteolytic activity. This subunit is involved in antigen processing to generate class I binding peptides. The 26S proteasome consists of a 20S proteasome core and two 19S regulatory subunits. The 20S proteasome core is composed of 28 subunits that are arranged in four stacked rings, resulting in a barrel-shaped structure. The two end rings are each formed by seven alpha subunits, and the two central rings are each formed by seven beta subunits. The catalytic chamber with the active sites is on the inside of the barrel [for review see (Tanahashi et al. 241-51)].

Proteasomal degradation has been shown to be highly regulated, tightly controlled, system that is central to normal cellular homeostasis including cell cycle regulation, DNA repair, sodium channel function, regulation of immune and inflammatory responses and cellular response to stress (Ciechanover 7151-60;Ciechanover S7-19;Malik et al. F1285-F1294). In the present study it was found that the proteasome subunit beta type-9 precursor and proteasome subunit alpha type-3 by 58% and 243% respectively upregulated in the CD73 lacking T cells.

In a previous study, it was shown that NF- κ B is upregulated in endothelial cells lacking CD73 (Zernecke et al. 2120-27). In T cells NF- κ B is a master regulator of many inflammatory cytokine genes, and its activation is mediated through the ubiquitin proteome system. NF- κ B

is actively inhibited when bound to I κ B (inhibitor of kappa B). NF- κ B activation follows the degradation of I κ B, which is dependent on ubiquitination of I κ B followed by proteasomal degradation. Qureshi et al., showed that alterations in the UPS may have profound effects on the immune response including the regulation of an array of inflammatory cytokines (Qureshi et al. 243-60). Proteasomal activity may also been linked to inflammatory and autoimmune diseases (Wang and Maldonado 255-61). Thus, the upregulation of two proteasome subunit (alpha type 3 and beta type-9) observed in the present study in regulatory T cell lacking CD73 is likely to relate to the enhanced production of the pro inflammatory cytokines IFN- γ (M.Romio- unpublished observation).

4. T-cell specific GTPase

GTPases are a large family of hydrolase enzymes that can bind and hydrolyze guanosine triphosphate (GTP). The GTP binding and hydrolysis takes place in the highly conserved G domain common to all GTPases. Ras also called small GTPases. Small GTPases have a molecular weight of about 21 kilo-Dalton (kDa) and generally serve as molecular switches for a variety of cellular signaling events.

A study by Mor et al., indicates that Ras inhibition not only increased Treg cell numbers and their Foxp3 content, but also enhanced their suppressive capacity (Mor et al. 1493-502). Thus the inhibition of Ras results in the development of anti-inflammatory responses (Marks et al. 1982-88) and attenuation of experimental autoimmune disorders (Karussis et al. 1-9;Katzav et al. 570-77). These findings are interesting since the present study found a 70% downregulation of T-cell specific GTPase, in CD73 deficient regulatory T cells. Thus, CD73 derived adenosine may signal through GTPase in T reg cells. Thus the significant changes of expression of 25 proteins (both upregulated and downregulated) showed the important contribution of CD73 mediated function under physiological condition.

5. Summary

The surface located enzyme ecto-5' nucleotidase (CD73) is a glycosylphosphatidylinositol (GPI)-linked membrane-bound glycoprotein which hydrolyzes extracellular nucleoside monophosphates (AMP) into bioactive nucleoside intermediates (adenosine). Adenosine is an activator of one of the four types of G-protein coupled, seven transmembrane spanning adenosine receptors (AdoR). Recent studies indicated that ecto-5' nucleotidase from endothelial cells and regulatory T cells play an integral role in adenosine mediated suppression of inflammation. However, the mechanism of suppression of inflammation not fully known. Modulation of cytokines production, regulation of the expression of adhesion molecules on the cell surface of endothelial cells and regulatory T cells have recently been reported to be influenced by CD73. In the present study an attempt was made to study the molecular consequences of CD73 deletion at the level of the plasma membrane proteome using different approaches.

Initially the cationic colloidal silica bead method was applied to enrich the endothelial cell membrane from the mouse heart under *in vivo* condition. In summary, 71 proteins were identified from endothelial cell (EC) membrane fraction separated by colloidal silica bead method. Among 71 proteins, 31 were membrane proteins. However, 14 cytoskeletal or junction proteins, 9 mitochondrial proteins and 9 nuclear proteins were also identified, suggesting a significant contamination. These results of EC membranes obtained by the colloidal silica beads method revealed that the coronary endothelial membranes can be conveniently labelled with colloidal silica. However, due to the ionic nature of interaction of colloidal silica with the EC membrane, cardiac homogenisation resulted in the partial loss of specificity. Furthermore, the amount of protein recovered from one mouse heart is rather low and despite pooling precluded a more detailed analysis of the coronary endothelial membrane proteome under *in vivo* conditions.

Since the *in-vivo* isolation of coronary endothelial membranes proved to be not feasible, additional experiments were carried out. Endothelial cells were isolated from mouse aorta and lung to see whether it is possible to use a differential proteomic approach between WT and CD73 knockout under *in vitro* condition. Mouse aortic and lung endothelial cells were conveniently isolated by magnetic bead method (using CD31 and CD102-dynal beads respectively). However, during each passage of aortic endothelial cells, there was a loss of

purity over the time of growth. Finally only 18% of the cells were positive for the endothelial specific markers CD31 and CD102. This low purity might be due to overgrowth with non endothelial cells like smooth muscle cells and fibroblast. In addition, dedifferentiation also can lead to loss of phenotypic characteristic features of the endothelial cells.

In contrast the purity of isolated mouse lung endothelial cells could be maintained in culture, as judged by the expression of CD31 and CD102. However, expression of CD73 on mouse lung endothelial cells significantly decreased after the second magnetic bead sorting. Therefore these experiments proved to be not feasible since *in vitro* expansion of endothelial cells necessary to obtain sufficient material for differential proteomic analysis using WT and CD73 knockouts, either resulted in a loss of cell purity or loss of CD73.

In a final step the expression of ecto-5' nucleotidase (CD73) on mouse kidney and spleen was studied by immunohistochemistry. Staining on mouse kidney revealed that there is a high expression of CD73 (ecto 5' nucleotidase) within the glomerulus (Mesangium) and tubular luminal membranes. Immunohistochemical staining of mouse spleen revealed that there is a high expression of CD73 to be associated with cells of the red pulp which are most likely regulatory T cells. Regulatory T cells have recently been shown to possess an ecto nucleotidase cascade involving production of adenosine. Thus, regulatory T cells were isolated by using a commercially available kit (Miltenyi Biotech) to be finally able to carry out a differential proteomic analysis.

To analyze the potential changes in membrane protein composition the stable isotope dimethyl labeling method was applied to regulatory T cells isolated from WT and CD73 knockouts mice. In summary, 355 proteins were identified. Among 355 proteins, interestingly 25 proteins showed significant changes. Among 25 proteins, 17 proteins were upregulated proteins and 8 proteins were downregulated proteins. Among the differentially expressed proteins the following deserve particular attentions.

1. Coactosin-like protein (CLP), which is 50% upregulated in CD73 knockouts, may indirectly participate in the adenosine mediated immunosuppression.

2. Isoform 2 of 60 kDa heat shock protein is 65% upregulated in CD73 knockouts. Upregulation of HSP60 in the CD73 knockout mice suggests that HSP60 via CD73 participates in the anti-inflammatory action of the adenosine.

3. Proteasome subunit beta type-9 precursor and proteasome subunit alpha type-3 by 58% and 243% respectively upregulated in the CD73 lacking T cells. Thus, the upregulation of two proteasome subunit observed in the present study is likely to relate to the known enhanced production of the pro inflammatory cytokines IFN- γ .

4. There was a 70% downregulation of T-cell specific GTPase in CD73 deficient regulatory T cells. Thus, CD73 derived adenosine may signal through GTPase in T reg cells.

In summary the changes in the expression of 25 proteins (both upregulated and downregulated) due to the lack of CD73 on Treg cells, suggest a role in the suppression of inflammation through adenosine. Future studies must delineated details of the signaling pathway of adenosine

6. References

Reference List

- Aird, W. C. "Vascular bed-specific hemostasis: role of endothelium in sepsis pathogenesis." Crit Care Med. 29.7 Suppl (2001): S28-S34.
- Aird, W. C. "Endothelial cell heterogeneity." Crit Care Med. 31.4 Suppl (2003): S221-S230.
- Aird, W. C. "Spatial and temporal dynamics of the endothelium." J.Thromb.Haemost. 3.7 (2005): 1392-406.
- Aird, W. C. "Phenotypic heterogeneity of the endothelium: I. Structure, function, and mechanisms." Circ.Res. 100.2 (2007): 158-73.
- Aird, W. C. "Phenotypic heterogeneity of the endothelium: II. Representative vascular beds." Circ.Res. 100.2 (2007): 174-90.
- Anderson, N. L. and N. G. Anderson. "Proteome and proteomics: new technologies, new concepts, and new words." Electrophoresis 19.11 (1998): 1853-61.
- Andries, L. J., D. L. Brutsaert, and S. U. Sys. "Nonuniformity of endothelial constitutive nitric oxide synthase distribution in cardiac endothelium." Circ.Res. 82.2 (1998): 195-203.
- Anversa, P. et al. "Morphometry of exercise-induced right ventricular hypertrophy in the rat." Circ.Res. 52.1 (1983): 57-64.
- Arap, W. et al. "Steps toward mapping the human vasculature by phage display." Nat.Med. 8.2 (2002): 121-27.
- Au, W. W. L. "Application of the reverberation-limited form of the sonar equation to dolphin echolocation." Journal Of The Acoustical Society Of America 92 (1992): 1822-26.

- Bassingthwaighte, J. B., T. Yipintsoi, and R. B. Harvey. "Microvasculature of the dog left ventricular myocardium." Microvasc.Res. 7.2 (1974): 229-49.
- Bechard, D. et al. "Characterization of the secreted form of endothelial-cell-specific molecule 1 by specific monoclonal antibodies." J.Vasc.Res. 37.5 (2000): 417-25.
- Belloni, P. N. and G. L. Nicolson. "Differential expression of cell surface glycoproteins on various organ-derived microvascular endothelia and endothelial cell cultures." J.Cell Physiol 136.3 (1988): 398-410.
- Bevilacqua, M. P. et al. "Identification of an inducible endothelial-leukocyte adhesion molecule." Proc.Natl.Acad.Sci.U.S.A 84.24 (1987): 9238-42.
- Bianchi, C. et al. "Receptor-type protein-tyrosine phosphatase mu is expressed in specific vascular endothelial beds in vivo." Exp.Cell Res. 248.1 (1999): 329-38.
- Blackstock, W. P. and M. P. Weir. "Proteomics: quantitative and physical mapping of cellular proteins." Trends Biotechnol. 17.3 (1999): 121-27.
- Bouma, M. G. et al. "Adenosine inhibits neutrophil degranulation in activated human whole blood: involvement of adenosine A2 and A3 receptors." J.Immunol. 158.11 (1997): 5400-08.
- Bouma, M. G., F. A. van den Wildenberg, and W. A. Buurman. "Adenosine inhibits cytokine release and expression of adhesion molecules by activated human endothelial cells." Am.J.Physiol 270.2 Pt 1 (1996): C522-C529.
- Carmeliet, P. "Mechanisms of angiogenesis and arteriogenesis." Nat.Med. 6.4 (2000): 389-95.
- Carmeliet, P. and R. K. Jain. "Angiogenesis in cancer and other diseases." Nature 407.6801 (2000): 249-57.

- Castrop, H. et al. "Impairment of tubuloglomerular feedback regulation of GFR in ecto-5'-nucleotidase/CD73-deficient mice." J.Clin.Invest 114.5 (2004): 634-42.
- Catalano, A. et al. "5-lipoxygenase antagonizes genotoxic stress-induced apoptosis by altering p53 nuclear trafficking." FASEB J. 18.14 (2004): 1740-42.
- Chaney, L. K. and B. S. Jacobson. "Coating cells with colloidal silica for high yield isolation of plasma membrane sheets and identification of transmembrane proteins." J.Biol.Chem. 258.16 (1983): 10062-72.
- Ciechanover, A. "The ubiquitin-proteasome pathway: on protein death and cell life." EMBO J. 17.24 (1998): 7151-60.
- Ciechanover, A. "The ubiquitin proteolytic system: from a vague idea, through basic mechanisms, and onto human diseases and drug targeting." Neurology 66.2 Suppl 1 (2006): S7-19.
- Collins, T. et al. "Transcriptional regulation of endothelial cell adhesion molecules: NF-kappa B and cytokine-inducible enhancers." FASEB J. 9.10 (1995): 899-909.
- Cordon-Cardo, C. et al. "Multidrug-resistance gene (P-glycoprotein) is expressed by endothelial cells at blood-brain barrier sites." Proc.Natl.Acad.Sci.U.S.A 86.2 (1989): 695-98.
- Danilov, S. M. et al. "Lung uptake of antibodies to endothelial antigens: key determinants of vascular immunotargeting." Am.J.Physiol Lung Cell Mol.Physiol 280.6 (2001): L1335-L1347.
- de Martin, R. et al. "The transcription factor NF-kappa B and the regulation of vascular cell function." Arterioscler.Thromb.Vasc.Biol. 20.11 (2000): E83-E88.

- Deaglio, S. et al. "Adenosine generation catalyzed by CD39 and CD73 expressed on regulatory T cells mediates immune suppression." J.Exp.Med. 204.6 (2007): 1257-65.
- DeFouw, D. O. "Structural heterogeneity within the pulmonary microcirculation of the normal rat." Anat.Rec. 221.2 (1988): 645-54.
- Deussen, A. et al. "Formation and salvage of adenosine by macrovascular endothelial cells." Am.J.Physiol 264.3 Pt 2 (1993): H692-H700.
- Di Virgilio, F. et al. "Nucleotide receptors: an emerging family of regulatory molecules in blood cells." Blood 97.3 (2001): 587-600.
- Divekar, A. A. et al. "Protein vaccines induce uncommitted IL-2-secreting human and mouse CD4 T cells, whereas infections induce more IFN-gamma-secreting cells." J.Immunol. 176.3 (2006): 1465-73.
- Dong, Q. G. et al. "A general strategy for isolation of endothelial cells from murine tissues. Characterization of two endothelial cell lines from the murine lung and subcutaneous sponge implants." Arterioscler.Thromb.Vasc.Biol. 17.8 (1997): 1599-604.
- Drake, T. A. et al. "Expression of tissue factor, thrombomodulin, and E-selectin in baboons with lethal Escherichia coli sepsis." Am.J.Pathol. 142.5 (1993): 1458-70.
- Durr, E. et al. "Direct proteomic mapping of the lung microvascular endothelial cell surface in vivo and in cell culture." Nat.Biotechnol. 22.8 (2004): 985-92.
- Elble, R. C. et al. "Cloning and characterization of lung-endothelial cell adhesion molecule-1 suggest it is an endothelial chloride channel." J.Biol.Chem. 272.44 (1997): 27853-61.

- Eltzschig, H. K. et al. "Coordinated adenine nucleotide phosphohydrolysis and nucleoside signaling in posthypoxic endothelium: role of ectonucleotidases and adenosine A2B receptors." J.Exp.Med. 198.5 (2003): 783-96.
- Eppihimer, M. J. et al. "Heterogeneity of expression of E- and P-selectins in vivo." Circ.Res. 79.3 (1996): 560-69.
- Esmon, C. T. "Protein C anticoagulant pathway and its role in controlling microvascular thrombosis and inflammation." Crit Care Med. 29.7 Suppl (2001): S48-S51.
- Fatehi, M. I. et al. "Characterization of the blood-brain barrier: glycoconjugate receptors of 14 lectins in canine brain, cultured endothelial cells, and blotted membrane proteins." Brain Res. 415.1 (1987): 30-39.
- Fischer, F. et al. "Toward the complete membrane proteome: high coverage of integral membrane proteins through transmembrane peptide detection." Mol.Cell Proteomics. 5.3 (2006): 444-53.
- Funk, C. D. "Leukotriene modifiers as potential therapeutics for cardiovascular disease." Nat.Rev.Drug Discov. 4.8 (2005): 664-72.
- Gamba, G. "Molecular physiology and pathophysiology of electroneutral cation-chloride cotransporters." Physiol Rev. 85.2 (2005): 423-93.
- Gerritsen, M. E. et al. "In silico data filtering to identify new angiogenesis targets from a large in vitro gene profiling data set." Physiol Genomics 10.1 (2002): 13-20.
- Ghandour, S. et al. "A surface marker for murine vascular endothelial cells defined by monoclonal antibody." J.Histochem.Cytochem. 30.2 (1982): 165-70.

- Ghosh, J. "Rapid induction of apoptosis in prostate cancer cells by selenium: reversal by metabolites of arachidonate 5-lipoxygenase." Biochem.Biophys.Res.Comm. 315.3 (2004): 624-35.
- Greenwalt, D. E., S. H. Scheck, and T. Rhinehart-Jones. "Heart CD36 expression is increased in murine models of diabetes and in mice fed a high fat diet." J.Clin.Invest 96.3 (1995): 1382-88.
- Gygi, S. P. et al. "Quantitative analysis of complex protein mixtures using isotope-coded affinity tags." Nat.Biotechnol. 17.10 (1999): 994-99.
- Hajra, L. et al. "The NF-kappa B signal transduction pathway in aortic endothelial cells is primed for activation in regions predisposed to atherosclerotic lesion formation." Proc.Natl.Acad.Sci.U.S.A 97.16 (2000): 9052-57.
- Han, B. et al. "Gamma-glutamyl leukotrienase, a novel endothelial membrane protein, is specifically responsible for leukotriene D(4) formation in vivo." Am.J.Pathol. 161.2 (2002): 481-90.
- Han, D. K. et al. "Quantitative profiling of differentiation-induced microsomal proteins using isotope-coded affinity tags and mass spectrometry." Nat.Biotechnol. 19.10 (2001): 946-51.
- Hasko, G. et al. "Adenosine receptor agonists differentially regulate IL-10, TNF-alpha, and nitric oxide production in RAW 264.7 macrophages and in endotoxemic mice." J.Immunol. 157.10 (1996): 4634-40.
- Henninger, D. D. et al. "Cytokine-induced VCAM-1 and ICAM-1 expression in different organs of the mouse." J.Immunol. 158.4 (1997): 1825-32.

- Hsu, J. L., S. Y. Huang, and S. H. Chen. "Dimethyl multiplexed labeling combined with microcolumn separation and MS analysis for time course study in proteomics." Electrophoresis 27.18 (2006): 3652-60.
- Hsu, J. L. et al. "Stable-isotope dimethyl labeling for quantitative proteomics." Anal.Chem. 75.24 (2003): 6843-52.
- Hsu, J. L. et al. "Beyond quantitative proteomics: signal enhancement of the a1 ion as a mass tag for peptide sequencing using dimethyl labeling." J.Proteome.Res. 4.1 (2005): 101-08.
- Huo, Y., A. Hafezi-Moghadam, and K. Ley. "Role of vascular cell adhesion molecule-1 and fibronectin connecting segment-1 in monocyte rolling and adhesion on early atherosclerotic lesions." Circ.Res. 87.2 (2000): 153-59.
- Ishii, H. et al. "Thrombomodulin, an endothelial anticoagulant protein, is absent from the human brain." Blood 67.2 (1986): 362-65.
- Jacobson, B. S. et al. "Isolation and partial characterization of the luminal plasmalemma of microvascular endothelium from rat lungs." Eur.J.Cell Biol. 58.2 (1992): 296-306.
- Jean, J. C. et al. "DANCE in developing and injured lung." Am.J.Physiol Lung Cell Mol.Physiol 282.1 (2002): L75-L82.
- Karhausen, J. et al. "Epithelial hypoxia-inducible factor-1 is protective in murine experimental colitis." J.Clin.Invest 114.8 (2004): 1098-106.
- Karussis, D. et al. "The Ras-pathway inhibitor, S-trans-trans-farnesylthiosalicylic acid, suppresses experimental allergic encephalomyelitis." J.Neuroimmunol. 120.1-2 (2001): 1-9.

- Katzav, A. et al. "Treatment of MRL/lpr mice, a genetic autoimmune model, with the Ras inhibitor, farnesylthiosalicylate (FTS)." Clin.Exp.Immunol. 126.3 (2001): 570-77.
- Kedzierski, R. M. and M. Yanagisawa. "Endothelin system: the double-edged sword in health and disease." Annu.Rev.Pharmacol.Toxicol. 41 (2001): 851-76.
- Kim, J. et al. "Endothelial cell apoptotic genes associated with the pathogenesis of thrombotic microangiopathies: an application of oligonucleotide genechip technology." Microvasc.Res. 62.2 (2001): 83-93.
- Klein, C. L. et al. "Effects of cytokines on the expression of cell adhesion molecules by cultured human omental mesothelial cells." Pathobiology 63.4 (1995): 204-12.
- Kobie, J. J. et al. "T regulatory and primed uncommitted CD4 T cells express CD73, which suppresses effector CD4 T cells by converting 5'-adenosine monophosphate to adenosine." J.Immunol. 177.10 (2006): 6780-86.
- Koszalka, P. et al. "Targeted disruption of cd73/ecto-5'-nucleotidase alters thromboregulation and augments vascular inflammatory response." Circ.Res. 95.8 (2004): 814-21.
- Kroll, K., A. Deussen, and I. R. Sweet. "Comprehensive model of transport and metabolism of adenosine and S-adenosylhomocysteine in the guinea pig heart." Circ.Res. 71.3 (1992): 590-604.
- Kruger, M. et al. "SILAC mouse for quantitative proteomics uncovers kindlin-3 as an essential factor for red blood cell function." Cell 134.2 (2008): 353-64.
- Kuhlenordt, P. J. et al. "Role of endothelial nitric oxide synthase in endothelial activation: insights from eNOS knockout endothelial cells." Am.J.Physiol Cell Physiol 286.5 (2004): C1195-C1202.

- Lassalle, P. et al. "ESM-1 is a novel human endothelial cell-specific molecule expressed in lung and regulated by cytokines." J.Biol.Chem. 271.34 (1996): 20458-64.
- Laszik, Z. et al. "Human protein C receptor is present primarily on endothelium of large blood vessels: implications for the control of the protein C pathway." Circulation 96.10 (1997): 3633-40.
- Lennon, P. F. et al. "Neutrophil-derived 5'-adenosine monophosphate promotes endothelial barrier function via CD73-mediated conversion to adenosine and endothelial A2B receptor activation." J.Exp.Med. 188.8 (1998): 1433-43.
- Levin, E. G., L. Santell, and K. G. Osborn. "The expression of endothelial tissue plasminogen activator in vivo: a function defined by vessel size and anatomic location." J.Cell Sci. 110 (Pt 2) (1997): 139-48.
- Ley, K. "Plugging the leaks." Nat.Med. 7.10 (2001): 1105-06.
- Lotzer, K., C. D. Funk, and A. J. Habenicht. "The 5-lipoxygenase pathway in arterial wall biology and atherosclerosis." Biochim.Biophys.Acta 1736.1 (2005): 30-37.
- Lupu, C. et al. "Tissue factor-dependent coagulation is preferentially up-regulated within arterial branching areas in a baboon model of Escherichia coli sepsis." Am.J.Pathol. 167.4 (2005): 1161-72.
- Madara, J. L. et al. "5'-adenosine monophosphate is the neutrophil-derived paracrine factor that elicits chloride secretion from T84 intestinal epithelial cell monolayers." J.Clin.Invest 91.5 (1993): 2320-25.
- Madri, J. A. and S. K. Williams. "Capillary endothelial cell cultures: phenotypic modulation by matrix components." J.Cell Biol. 97.1 (1983): 153-65.

- Malik, B. et al. "Regulation of epithelial sodium channels by the ubiquitin-proteasome proteolytic pathway." Am.J.Physiol Renal Physiol 290.6 (2006): F1285-F1294.
- Mann, M. "Quantitative proteomics?" Nat.Biotechnol. 17.10 (1999): 954-55.
- Marks, R. E. et al. "Farnesyltransferase inhibitors inhibit T-cell cytokine production at the posttranscriptional level." Blood 110.6 (2007): 1982-88.
- McIntosh, D. P. et al. "Targeting endothelium and its dynamic caveolae for tissue-specific transcytosis in vivo: a pathway to overcome cell barriers to drug and gene delivery." Proc.Natl.Acad.Sci.U.S.A 99.4 (2002): 1996-2001.
- Mitulovic, G. and K. Mechtler. "HPLC techniques for proteomics analysis--a short overview of latest developments." Brief Funct.Genomic.Proteomic. 5.4 (2006): 249-60.
- Mitulovic, G. et al. "Automated, on-line two-dimensional nano liquid chromatography tandem mass spectrometry for rapid analysis of complex protein digests." Proteomics 4.9 (2004): 2545-57.
- Mo, F. M. and H. J. Ballard. "The effect of systemic hypoxia on interstitial and blood adenosine, AMP, ADP and ATP in dog skeletal muscle." J.Physiol 536.Pt 2 (2001): 593-603.
- Moncada, S. et al. "An enzyme isolated from arteries transforms prostaglandin endoperoxides to an unstable substance that inhibits platelet aggregation." Nature 263.5579 (1976): 663-65.
- Mor, A. et al. "N-Ras or K-Ras inhibition increases the number and enhances the function of Foxp3 regulatory T cells." Eur.J.Immunol. 38.6 (2008): 1493-502.

- Morandini, R. et al. "Action of cAMP on expression and release of adhesion molecules in human endothelial cells." Am.J.Physiol 270.3 Pt 2 (1996): H807-H816.
- Negrutskii, B. S. and A. V. El'skaya. "Eukaryotic translation elongation factor 1 alpha: structure, expression, functions, and possible role in aminoacyl-tRNA channeling." Prog.Nucleic Acid Res.Mol.Biol. 60 (1998): 47-78.
- Noguchi, M., M. Miyano, and T. Matsumoto. "Physiochemical characterization of ATP binding to human 5-lipoxygenase." Lipids 31.4 (1996): 367-71.
- Obermeyer, N. et al. "Proteome analysis of migrating versus nonmigrating rat heart endothelial cells reveals distinct expression patterns." Endothelium 10.3 (2003): 167-78.
- Ochi, K. et al. "Arachidonate 5-lipoxygenase of guinea pig peritoneal polymorphonuclear leukocytes. Activation by adenosine 5'-triphosphate." J.Biol.Chem. 258.9 (1983): 5754-58.
- Ohta, A. and M. Sitkovsky. "Role of G-protein-coupled adenosine receptors in downregulation of inflammation and protection from tissue damage." Nature 414.6866 (2001): 916-20.
- Ong, S. E. et al. "Stable isotope labeling by amino acids in cell culture, SILAC, as a simple and accurate approach to expression proteomics." Mol.Cell Proteomics. 1.5 (2002): 376-86.
- Ong, S. E., L. J. Foster, and M. Mann. "Mass spectrometric-based approaches in quantitative proteomics." Methods 29.2 (2003): 124-30.

- Ong, S. E., I. Kratchmarova, and M. Mann. "Properties of ¹³C-substituted arginine in stable isotope labeling by amino acids in cell culture (SILAC)." J.Proteome.Res. 2.2 (2003): 173-81.
- Ong, S. E., G. Mittler, and M. Mann. "Identifying and quantifying in vivo methylation sites by heavy methyl SILAC." Nat.Methods 1.2 (2004): 119-26.
- Osterud, B., M. S. Bajaj, and S. P. Bajaj. "Sites of tissue factor pathway inhibitor (TFPI) and tissue factor expression under physiologic and pathologic conditions. On behalf of the Subcommittee on Tissue factor Pathway Inhibitor (TFPI) of the Scientific and Standardization Committee of the ISTH." Thromb.Haemost. 73.5 (1995): 873-75.
- Page, C. et al. "Antigenic heterogeneity of vascular endothelium." Am.J.Pathol. 141.3 (1992): 673-83.
- Pasqualini, R. and E. Ruoslahti. "Organ targeting in vivo using phage display peptide libraries." Nature 380.6572 (1996): 364-66.
- Pollock, J. S. et al. "Characterization and localization of endothelial nitric oxide synthase using specific monoclonal antibodies." Am.J.Physiol 265.5 Pt 1 (1993): C1379-C1387.
- Ponder, B. A. and M. M. Wilkinson. "Organ-related differences in binding of Dolichos biflorus agglutinin to vascular endothelium." Dev.Biol. 96.2 (1983): 535-41.
- Porter, G. A., G. E. Palade, and A. J. Milici. "Differential binding of the lectins Griffonia simplicifolia I and Lycopersicon esculentum to microvascular endothelium: organ-specific localization and partial glycoprotein characterization." Eur.J.Cell Biol. 51.1 (1990): 85-95.

- Qureshi, N. et al. "The proteasome: a central regulator of inflammation and macrophage function." Immunol.Res. 31.3 (2005): 243-60.
- Rajotte, D. et al. "Molecular heterogeneity of the vascular endothelium revealed by in vivo phage display." J.Clin.Invest 102.2 (1998): 430-37.
- Rajotte, D. and E. Ruoslahti. "Membrane dipeptidase is the receptor for a lung-targeting peptide identified by in vivo phage display." J.Biol.Chem. 274.17 (1999): 11593-98.
- Rakonjac, M. et al. "Coactosin-like protein supports 5-lipoxygenase enzyme activity and up-regulates leukotriene A(4) production." Proceedings Of The National Academy Of Sciences Of The United States Of America 103.35 (2006): 13150-55.
- Resta, R. and L. F. Thompson. "T cell signalling through CD73." Cell Signal. 9.2 (1997): 131-39.
- Rosengren, S., K. E. Arfors, and K. G. Proctor. "Potentiation of leukotriene B4-mediated inflammatory response by the adenosine antagonist, 8-phenyl theophylline." Int.J.Microcirc.Clin.Exp. 10.4 (1991): 345-57.
- Sad, S. and T. R. Mosmann. "Single IL-2-secreting precursor CD4 T cell can develop into either Th1 or Th2 cytokine secretion phenotype." J.Immunol. 153.8 (1994): 3514-22.
- Saito, H. et al. "Plasma concentration of adenosine during normoxia and moderate hypoxia in humans." Am.J.Respir.Crit Care Med. 159.3 (1999): 1014-18.
- Schnitzer, J. E. "gp60 is an albumin-binding glycoprotein expressed by continuous endothelium involved in albumin transcytosis." Am.J.Physiol 262.1 Pt 2 (1992): H246-H254.

- Schnitzer, J. E. and P. Oh. "Albondin-mediated capillary permeability to albumin. Differential role of receptors in endothelial transcytosis and endocytosis of native and modified albumins." J.Biol.Chem. 269.8 (1994): 6072-82.
- Schnitzer, J. E. et al. "Caveolae from luminal plasmalemma of rat lung endothelium: microdomains enriched in caveolin, Ca(2+)-ATPase, and inositol trisphosphate receptor." Proc.Natl.Acad.Sci.U.S.A 92.5 (1995): 1759-63.
- Schnitzer, J. E., C. P. Shen, and G. E. Palade. "Lectin analysis of common glycoproteins detected on the surface of continuous microvascular endothelium in situ and in culture: identification of sialoglycoproteins." Eur.J.Cell Biol. 52.2 (1990): 241-51.
- Semenza, G. L. et al. "Hypoxia, HIF-1, and the pathophysiology of common human diseases." Adv.Exp.Med.Biol. 475 (2000): 123-30.
- Shadforth, I. P. et al. "i-Tracker: for quantitative proteomics using iTRAQ." BMC.Genomics 6 (2005): 145.
- Shryock, J. C. and L. Belardinelli. "Adenosine and adenosine receptors in the cardiovascular system: biochemistry, physiology, and pharmacology." Am.J.Cardiol. 79.12A (1997): 2-10.
- Sitkovsky, M. V. et al. "Physiological control of immune response and inflammatory tissue damage by hypoxia-inducible factors and adenosine A2A receptors." Annu.Rev.Immunol. 22 (2004): 657-82.
- Sitkovsky, M. V. and A. Ohta. "The 'danger' sensors that STOP the immune response: the A2 adenosine receptors?" Trends Immunol. 26.6 (2005): 299-304.

- Smith, U. et al. "Endothelial projections as revealed by scanning electron microscopy."
Science 173.4000 (1971): 925-27.
- Smolka, M. B. et al. "Optimization of the isotope-coded affinity tag-labeling procedure for quantitative proteome analysis." Anal.Biochem. 297.1 (2001): 25-31.
- Stad, R. K. and W. A. Buurman. "Current views on structure and function of endothelial adhesion molecules." Cell Adhes.Commun. 2.3 (1994): 261-68.
- Stolz, D. B. and B. S. Jacobson. "Macro- and microvascular endothelial cells in vitro: maintenance of biochemical heterogeneity despite loss of ultrastructural characteristics." In Vitro Cell Dev.Biol. 27A.2 (1991): 169-82.
- Stolz, D. B. and B. S. Jacobson. "Examination of transcellular membrane protein polarity of bovine aortic endothelial cells in vitro using the cationic colloidal silica microbead membrane-isolation procedure." J.Cell Sci. 103 (Pt 1) (1992): 39-51.
- Streeter, P. R. et al. "A tissue-specific endothelial cell molecule involved in lymphocyte homing." Nature 331.6151 (1988): 41-46.
- Sullivan, G. W. et al. "Activation of A2A adenosine receptors inhibits expression of alpha 4/beta 1 integrin (very late antigen-4) on stimulated human neutrophils."
J.Leukoc.Biol. 75.1 (2004): 127-34.
- Synnestvedt, K. et al. "Ecto-5'-nucleotidase (CD73) regulation by hypoxia-inducible factor-1 mediates permeability changes in intestinal epithelia." J.Clin.Invest 110.7 (2002): 993-1002.

- Takahashi, T. et al. "Immunologic self-tolerance maintained by CD25+CD4+ naturally anergic and suppressive T cells: induction of autoimmune disease by breaking their anergic/suppressive state." Int.Immunol. 10.12 (1998): 1969-80.
- Takano, T. et al. "Neutrophil-mediated changes in vascular permeability are inhibited by topical application of aspirin-triggered 15-epi-lipoxin A4 and novel lipoxin B4 stable analogues." J.Clin.Invest 101.4 (1998): 819-26.
- Tanahashi, N. et al. "Molecular structure of 20S and 26S proteasomes." Enzyme Protein 47.4-6 (1993): 241-51.
- Thompson, L. F. et al. "Crucial role for ecto-5'-nucleotidase (CD73) in vascular leakage during hypoxia." J.Exp.Med. 200.11 (2004): 1395-405.
- Thornton, A. M. and E. M. Shevach. "CD4+CD25+ immunoregulatory T cells suppress polyclonal T cell activation in vitro by inhibiting interleukin 2 production." J.Exp.Med. 188.2 (1998): 287-96.
- Tsai, J. C. et al. "The Egr-1 promoter contains information for constitutive and inducible expression in transgenic mice." FASEB J. 14.13 (2000): 1870-72.
- Turner, R. R. et al. "Endothelial cell phenotypic diversity. In situ demonstration of immunologic and enzymatic heterogeneity that correlates with specific morphologic subtypes." Am.J.Clin.Pathol. 87.5 (1987): 569-75.
- von Boehmer, H. "Mechanisms of suppression by suppressor T cells." Nat.Immunol. 6.4 (2005): 338-44.

- Wagner, K. et al. "An automated on-line multidimensional HPLC system for protein and peptide mapping with integrated sample preparation." Anal.Chem. 74.4 (2002): 809-20.
- Wagner, K. et al. "Protein mapping by two-dimensional high performance liquid chromatography." J.Chromatogr.A 893.2 (2000): 293-305.
- Wang, H. U., Z. F. Chen, and D. J. Anderson. "Molecular distinction and angiogenic interaction between embryonic arteries and veins revealed by ephrin-B2 and its receptor Eph-B4." Cell 93.5 (1998): 741-53.
- Wang, J. and M. A. Maldonado. "The ubiquitin-proteasome system and its role in inflammatory and autoimmune diseases." Cell Mol.Immunol. 3.4 (2006): 255-61.
- Weissmuller, T., H. K. Eltzschig, and S. P. Colgan. "Dynamic purine signaling and metabolism during neutrophil-endothelial interactions." Purinergic.Signal. 1.3 (2005): 229-39.
- Werz, O. and D. Steinhilber. "Development of 5-lipoxygenase inhibitors - lessons from cellular enzyme regulation." Biochemical Pharmacology 70.3 (2005): 327-33.
- Whitehouse, C. M. et al. "Electrospray interface for liquid chromatographs and mass spectrometers." Anal.Chem. 57.3 (1985): 675-79.
- Wolters, D. A., M. P. Washburn, and J. R. Yates, III. "An automated multidimensional protein identification technology for shotgun proteomics." Anal.Chem. 73.23 (2001): 5683-90.
- Yamamoto, K. et al. "Tissue distribution and regulation of murine von Willebrand factor gene expression in vivo." Blood 92.8 (1998): 2791-801.

- Yamamoto, K. and D. J. Loskutoff. "Fibrin deposition in tissues from endotoxin-treated mice correlates with decreases in the expression of urokinase-type but not tissue-type plasminogen activator." J.Clin.Invest 97.11 (1996): 2440-51.
- Yates, J. R., III et al. "Method to correlate tandem mass spectra of modified peptides to amino acid sequences in the protein database." Anal.Chem. 67.8 (1995): 1426-36.
- Yegutkin, G., P. Bodin, and G. Burnstock. "Effect of shear stress on the release of soluble ecto-enzymes ATPase and 5'-nucleotidase along with endogenous ATP from vascular endothelial cells." Br.J.Pharmacol. 129.5 (2000): 921-26.
- Zanin-Zhorov, A. et al. "Heat shock protein 60 enhances CD4+ CD25+ regulatory T cell function via innate TLR2 signaling." J.Clin.Invest 116.7 (2006): 2022-32.
- Zanin-Zhorov, A. et al. "T cells respond to heat shock protein 60 via TLR2: activation of adhesion and inhibition of chemokine receptors." FASEB J. 17.11 (2003): 1567-69.
- Zernecke, A. et al. "CD73/ecto-5'-nucleotidase protects against vascular inflammation and neointima formation." Circulation 113.17 (2006): 2120-27.
- Zhang, W. et al. "Preparation of tissue-specific monoclonal antibodies using purified endothelial membrane proteins from biotinylated pulmonary vasculature of rhesus monkey." Hybridoma (Larchmt.) 25.1 (2006): 15-19.
- Zhou, Y. J. et al. "A novel method to isolate and map endothelial membrane proteins from pulmonary vasculature." Am.J.Physiol Cell Physiol 288.4 (2005): C950-C956.
- Zieske, L. R. "A perspective on the use of iTRAQ reagent technology for protein complex and profiling studies." J.Exp.Bot. 57.7 (2006): 1501-08.

Zimmermann, H. "5'-Nucleotidase: molecular structure and functional aspects." Biochem.J.
285 (Pt 2) (1992): 345-65.

7. Curriculum vitae

Persönliche Angaben:

Selvam Arjunan

geboren am 21. Juli 1977 in Avalurpettai, Indien

Bildungsweg:

- | | |
|-----------|---|
| 1982-1992 | Secondary School, PS Annai BHS, Pavitram, Indien |
| 1992-1994 | Higher Secondary School, ST Joseph's HSS, Athipet, Indien |
| 1994-1997 | Bachelor of Science (Biochemie), Madras Universität, Indien |
| 1997-1999 | Master of Science (Biochemie), Madras Universität, Indien |

Tätigkeiten:

- | | |
|----------------|---|
| 2000-2002 | Junior Research Fellow in der Abteilung für Biochemie, National Center for Biological Sciences, TIFR, India.(Expression und Aufreinigung von Green Fluorescence Protein [GFP] in E.coli und Steigerung des monoklonalen Antikörpers gegen die GFP in der Maus) |
| 2002-2003 | Projekt-Assistent in der Abteilung für Biochemie, Indian Institute Science, India (Änderungen in Leydig-Zell-Gen-Expression während der Entwicklung in der Ratte Charakterisierung von Luteinisierendes hormon a/s |
| Seit 2003-2008 | Wissenschaftlicher Mitarbeiter am Institut für Kardiovaskuläre Physiologie, Heinrich-Heine-Universität Düsseldorf, Germany |

Düsseldorf, den

(Selvam Arjunan)

Erklärung

Ich versichere, daß ich die von mir vorgelegte Dissertation selbstständig angefertigt, die benutzten Quellen und Hilfsmittel vollständig angegeben und die Stellen der Arbeit – einschließlich Tabellen, Karten und Abbildungen –, die anderen Werken im Wortlaut oder dem Sinn nach entnommen sind, in jedem Einzelfall als Entlehnung kenntlich gemacht habe; daß die Dissertation noch keiner anderen Fakultät oder Universität zur Prüfung vorgelegen hat; daß sie noch nicht veröffentlicht worden ist sowie, daß ich eine solche Veröffentlichung vor Abschluß des Promotionsverfahrens nicht vornehmen werde. Die Bestimmungen dieser Promotionsordnung sind mir bekannt.

Düsseldorf, den 8. Dezember 2008

(Selvam Arjunan)